A Study on Advanced Technologies Inspired by Nature for Wireless LAN

Ryo Hamamoto

A dissertation submitted in partial fulfillment of
the requirements for the degree of
Doctor of Computer Engineering

Graduate School of Information Sciences,
Hiroshima City University

March 2016

List of Publications

Journal Articles

1. R. Hamamoto, H. Obata, C. Takano, and K. Ishida, "A study on applicability of media access control mechanism based on synchronization of coupled oscillators SP-MAC over wireless LAN," *IEICE Trans. Commun.* (Japanese Edition), J99-B, 2, pp.31–44, Feb. 2016. (in Japanese)

2. H. Obata, R. Hamamoto, C. Takano, and K. Ishida, "SP-MAC: A media access control method based on the synchronization phenomena of coupled oscillators over WLAN," *IEICE Trans. Inf. & Syst.*, E98-D, 12, pp.2060–2070, Dec. 2015.

3. R. Hamamoto, T. Murase, C. Takano, H. Obata, and K. Ishida, "A proposal of access point selection method based on cooperative movement of both access points and users," *IEICE Trans. Inf. & Syst.*, E98-D, 12, pp.2048–2059, Dec. 2015.

4. R. Hamamoto, C. Takano, K. Ishida, and M. Aida, "Guaranteeing method for the stability of cluster structure formed by autonomous decentralized clustering mechanism," *Journal of Communications*, 10, 8, pp.562–571, Aug. 2015.

5. R. Hamamoto, C. Takano, H. Obata, and K. Ishida, "An acceleration of throughput prediction method for access point in multi-rate wireless LAN considering terminal distribution," *IEICE Trans. Fundamentals* (Japanese Edition), J98-A, 2, pp.209–220, Feb. 2015. (in Japanese)

6. R. Hamamoto, C. Takano, K. Ishida, and M. Aida, "Power consumption characteristics of autonomous decentralized clustering based on local interaction," *IEICE Trans. Inf. & Syst.*, E97-D, 12, pp.2984–2994, Dec. 2014.

International Conference Proceedings

1. R. Ando, R. Hamamoto, H. Obata, C. Takano, and K. Ishida, "Characterization of priority control based on media access control method SP-MAC over WLAN," *Proc. the 19th Innovations in Cloud, Internet and Networks* (*ICIN 2016*), pp.149–156, Paris, France, Mar. 2016.

2. Y. Yamamoto, R. Hamamoto, H. Obata, C. Takano, and K. Ishida, "Control method to guarantee throughput based on media access control method SP-MAC

over WLAN," *Proc. the 13th Annual IEEE Consumer Communications and Networking Conference* (*CCNC 2016*), pp.657–662, Las Vegas, USA, Jan. 2016.

3. F. Teshima, H. Obata, R. Hamamoto, and K. Ishida, "Redundancy setting method for TCP congestion control based on FEC over wireless LAN," *Proc. the 8th International Workshop on Autonomous Self-Organizing Networks* (*ASON 2015*), pp.259–264, Sapporo, Japan, Dec. 2015.

4. Y. Yamamoto, R. Hamamoto, H. Obata, C. Takano, and K. Ishida, "Performance evaluation of control method to guarantee throughput based on media access control SP-MAC over WLAN," *Proc. the 8th International Workshop on Autonomous Self-Organizing Networks* (*ASON 2015*), pp.265–270, Sapporo, Japan, Dec. 2015.

5. R. Ando, R. Hamamoto, H. Obata, C. Takano, and K. Ishida, "An adaptive control parameter setting method for priority control based on media access control SP-MAC over WLAN," *Proc. the 8th International Workshop on Autonomous Self-Organizing Networks* (*ASON 2015*), pp.220–226, Sapporo, Japan, Dec. 2015.

6. R. Hamamoto, C. Takano, H. Obata, and K. Ishida, "Improvement of throughput prediction method for access point in multi-rate WLANs considering media access control and frame collision," *Proc. the 8th International Workshop on Autonomous Self-Organizing Networks* (*ASON 2015*), pp.227–233, Sapporo, Japan, Dec. 2015.

7. R. Hamamoto, H. Obata, Y. Yamamoto, R. Ando, C. Takano, and K. Ishida, "Performance evaluation of media access control method based on synchronization phenomena of coupled oscillators over multi-rate WLAN," *Proc. 2015 International Symposium on Nonlinear Theory and its Applications* (*NOLTA 2015*), pp.415–418, Hong Kong, China, Dec. 2015.

8. R. Hamamoto, C. Takano, H. Obata, M. Aida, and K. Ishida, "Setting radio transmission range using target problem to improve communication reachability and power saving," *Proc. the 7th EAI International Conference on Ad Hoc Networks* (*ADHOCNETS 2015*), San Remo, Italy / *Lecture Notes of the Institute for Computer Sciences, Social Informatics and Telecommunications Engineering*, 155, pp.15–28, Springer, Sep. 2015.

9. R. Hamamoto, C. Takano, H. Obata, K. Ishida, and T. Murase, "An access point selection mechanism based on cooperation of access points and users movement," *Proc. the 14th IFIP/IEEE Symposium on Integrated Network and Service Management* (*IM 2015*), pp.926–929, Ottawa, Canada, May 2015.

10. R. Hamamoto, C. Takano, H. Obata, K. Ishida, and T. Murase, "Characteristics analysis of an AP selection method based on coordination moving both users and APs," *Proc. the 7th International Workshop on Autonomous Self-Organizing Networks* (*ASON 2014*), pp.243–248, Shizuoka, Japan, Dec. 2014.

11. H. Obata, R. Hamamoto, C. Takano, and K. Ishida, "Throughput characteristics evaluation of media access control method based on synchronization phenomena of coupled oscillators over WLAN coexisting of CSMA/CA terminals," *Proc. the 7th International Workshop on Autonomous Self-Organizing Networks* (*ASON 2014*), pp.254–259, Shizuoka, Japan, Dec. 2014.

12. H. Tsushima, R. Hamamoto, H. Obata, and K. Ishida, "Performance evaluation of flow QoS guarantee method based on TCP congestion control and MAC frame priority control over multi-rate WLAN environment," *Proc. the 7th International Workshop on Autonomous Self-Organizing Networks* (*ASON 2014*), pp.266–271, Shizuoka, Japan, Dec. 2014.

13. R. Hamamoto, C. Takano, K. Ishida, and M. Aida, "Characteristics of autonomously configured structure formation based on power consumption and data transfer efficiency," *Proc. the 6th International Workshop on Autonomous Self-Organizing Networks* (*ASON 2013*), pp.409–414, Matsuyama, Japan, Dec. 2013.

14. R. Hamamoto, C. Takano, Kenji, Ishida, and M. Aida, "Guaranteeing asymptotic stability of clustering for MANET by autonomous decentralized structure formation mechanism based on local Interaction," *Proc. the 12th IEEE International Workshop on Assurance in Distributed Systems and Networks* (*ADSN 2013*), pp.345–350, Philadelphia, USA, Jul. 2013.

15. R. Hamamoto, C. Takano, K. Ishida, and M. Aida, "Power consumption characteristics by autonomous decentralized structure formation technology," *Proc. the 9th Asia-Pacific Symposium on Information and Telecommunication Technologies* (*APSITT 2012*), pp.1–5, Santiago and Valparaiso, Chile, Nov. 2012.

16. R. Hamamoto, C. Takano, K. Ishida, and M. Aida, "Guaranteeing asymptotic stability of clustering by autonomous decentralized structure formation," *Proc. the 9th IEEE International Conference on Autonomic and Trusted Computing* (*ATC 2012*), pp.408–414, Fukuoka, Japan, Sep. 2012.

Domestic Conference Proceedings

1. K. Izui, H. Obata, R. Hamamoto, C. Takano, and K. Ishida, "A study on transmission rate modeling of multi-rate wireless LAN," *The 2016 IEICE general conference*, B-7-45, Mar. 2016. (in Japanese)

2. R. Hamamoto, H. Obata, R. Ando, Y. Yamamoto, C. Takano, and K. Ishida, "Power consumption characteristics of media access control method based on synchronization phenomena of coupled oscillators," *The 2016 IEICE general conference*, B-7-46, Mar. 2016. (in Japanese)

3. R. Ando, R. Hamamoto, H. Obata, C. Takano, and K. Ishida, "Throughput characteristics of WLAN media access control method SP-MAC considering capture effect," *The 2016 IEICE general conference*, B-7-47, Mar. 2016. (in Japanese)

4. R. Ando, R. Hamamoto, H. Obata, C. Takano, and K. Ishida, “Performance evaluation of media access control method SP-MAC over multi-hop WLAN,” *IEICE technical report*, IN2015-106, 115, 405, pp.63–68, Jan. 2016. (in Japanese)

5. R. Hamamoto, R. Ando, Y. Yamamoto, H. Obata, C. Takano, and K. Ishida, “Solution of hidden terminal problem for media access control method based on synchronization of coupled oscillators SP-MAC,” *IEICE technical report*, IN2015-77, 115, 370, pp.37–42, Dec. 2015. (in Japanese)

6. R. Ando, R. Hamamoto, H. Obata, C. Takano, and K. Ishida, “The control parameter setting method for the priority control based on media access control SP-MAC over WLAN,” *The 4th IEICE technical committee on NetSci/CCS workshop*, CCS2015-36, 115, 178, pp.39–44, Aug. 2015. (in Japanese)

7. Y. Yamamoto, R. Hamamoto, H. Obata, C. Takano, and K. Ishida, “Characteristic evaluation of throughput guarantee control based on media access control method SP-MAC,” *The 4th IEICE technical committee on NetSci/CCS workshop*, CCS2015-35, 115, 178, pp.33–38, Aug. 2015. (in Japanese)

8. R. Hamamoto, C. Takano, H. Obata, and K. Ishida, “A performance study on throughput prediction method for access point over multi-rate wireless LAN environment,” *IEICE technical report*, IN2015-35, 115, 140, pp.73–78, Jul. 2015. (in Japanese)

9. H. Obata, R. Hamamoto, C. Takano, and K. Ishida, “A study on applicability of media access control method SP-MAC based on synchronization phenomena of coupled oscillators for real-time communication over WLAN,” *IEICE technical report* (Invited Lecture), IN2015-7, 115, 42, pp.33–38, May 2015.

10. H. Obata, R. Hamamoto, C. Takano, and K. Ishida, “Throughput evaluation of media access control method SP-MAC considering the number of communication terminals over WLAN,” *The 2015 IEICE general conference*, BS-8-10, Mar. 2015. (in Japanese)

11. R. Hamamoto, Y. Yamamoto, H. Obata, C. Takano, and K. Ishida, “Performance evaluation of media access control method based on synchronization of coupled oscillators over multi-rate wireless LAN,” *IEICE technical report*, IN2014-153, 114, 478, pp.191–196, Mar. 2015. (in Japanese)

12. R. Ando, R. Hamamoto, H. Obata, C. Takano, and K. Ishida, “An access point control based on media access control method SP-MAC over WLAN ,” *IEICE technical report*, NS2014-249, 114, 477, pp.421–426, Mar. 2015. (in Japanese)

13. Y. Yamamoto, R. Hamamoto, H. Obata, C. Takano, and K. Ishida, “Throughput guarantee method based on media access control method SP-MAC over WLAN,” *IEICE technical report*, NS2014-248, 114, 477, pp.415–420, Mar. 2015. (in Japanese)

14. R. Ando, R. Hamamoto, H. Obata, C. Takano, and K. Ishida, "Performance evaluation of MAC mechanism based on synchronization phenomena of coupled oscillators over wireless LAN coexisting of bidirectional flows," *Proc. the 16th IEEE Hiroshima Section Student Symposium*, B-29, Nov. 2014. (in Japanese, Refereed)

15. H. Obata, R. Hamamoto, C. Takano, and K. Ishida, "Applicability evaluation of MAC mechanism based on synchronization of coupled oscillators on WLAN," *IEICE technical report*, NS2014-105, 114, 252, pp.19–24, Oct. 2014. (in Japanese)

16. H. Obata, R. Hamamoto, C. Takano, and K. Ishida, "Performance evaluation of MAC mechanism based on synchronization of coupled oscillators on WLAN coexisting of DCF terminals," *The 2014 IEICE communications society conference*, B-7-40, Sep. 2014. (in Japanese)

17. R. Hamamoto, C. Takano, M. Aida, and K. Ishida, "Designing method of radio transmission range to improve both communication reachability and power saving based on target problem," *IEICE technical report*, NS2014-82, 114, 206, pp.13–18, Sep. 2014. (in Japanese)

18. H. Obata, R. Hamamoto, C. Takano, and K. Ishida, "Characteristics evaluation of MAC mechanism based on synchronization of coupled oscillators on WLAN," *The 3rd IEICE technical committee on NetSci/CCS workshop*, Aug. 2014. (in Japanese)

19. R. Hamamoto, C. Takano, H. Obata, and K. Ishida, "An adaptive selection mechanism of prediction formulas for high speed throughput prediction method of access point in multi-rate WLAN environment," *IEICE technical report*, IN2014-18, 114, 110, pp.13–18, Jun. 2014. (in Japanese)

20. R. Hamamoto, C. Takano, H. Obata, and K. Ishida, "High speed throughput estimation method for access point in multi-rate wireless LAN environment considering station distribution," *The 2014 IEICE general conference*, B-7-35, Mar. 2014. (in Japanese)

21. H. Obata, R. Hamamoto, C. Takano, K. Ishida, and K. Yamada, "Media access control based on synchronization of coupled oscillators over WLAN," *The 2014 IEICE general conference*, BS-6-2, Mar. 2014. (in Japanese)

22. M. Tomomune, R. Hamamoto, C. Takano, and K. Ishida, "Design method of terminal communication range to improve both power saving and communication reachability using target problem," *The 2014 IEICE general conference*, B-7-27, Mar. 2014. (in Japanese)

23. R. Hamamoto, H. Obata, C. Takano, K. Ishida, and K. Yamada, "Media access control mechanism based on synchronization of coupled oscillators over wireless LAN," *IEICE technical report*, IN2013-157, 113, 473, pp.83–88, Mar. 2014. (in Japanese, 21st Information Network Research Award of IEICE)

24. R. Hamamoto, T. Murase, C. Takano, and H. Obata, K. Ishida, "Characteristics evaluation of an access point selection method considering cooperative moving both access points and users," *IEICE technical report*, IN2013-72, 113, 206, pp.73–78, Sep. 2013. (in Japanese)

25. R. Hamamoto, C. Takano, M. Aida, and K. Ishida, "A study of throughput prediction method for access point in multi-rate wireless LAN environment based on target problem," *IEICE technical report*, IN2013-51, 113, 140, pp.89–94, Jul. 2013. (in Japanese)

26. R. Hamamoto, C. Takano, M. Aida, and K. Ishida, "Evaluation of autonomously configured cluster structure based on local interaction from the point of view of both power consumption and data transfer efficiency," *The 5th IEICE technical committee on Information Network Science* (*NetSci*), May 2013. (in Japanese)

27. R. Hamamoto, C. Takano, M. Aida, and K. Ishida, "A study of power saving method for geocast communication in ad-hoc network based on target problem," *IEICE technical report*, IN2013-12, 113, 36, pp.1–6, May 2013. (in Japanese)

28. R. Hamamoto, C. Takano, M. Aida, and K. Ishida, "Evaluation of autonomously created cluster structure based on power consumption and data transfer efficiency," *IEICE technical report*, IN2012-179, 112, 464, pp.149–154, Mar. 2013. (in Japanese)

29. R. Hamamoto, T. Murase, C. Takano, H. Obata, and K. Ishida, "An access point selection method considering cooperative moving of user and mobile access point," *IEICE technical report*, IN2012-130, 112, 352, pp.51–56, Dec. 2012. (in Japanese)

30. R. Hamamoto, T. Murase, C. Takano, H. Obata, and K. Ishida, "Characteristics evaluation of an access point selection method considering cooperative moving both access points and users," *The 3rd WLAN-QoS workshop*, Oct. 2012. (in Japanese)

31. R. Hamamoto, C. Takano, M. Aida, and K. Ishida, "Application of guaranteeing asymptotic stability of cluster structure by autonomous decentralized structure formation technology for MANET," *IEICE technical report*, IN2012-45, 112, 134, pp.73–78, Jul. 2012. (in Japanese)

32. R. Hamamoto, C. Takano, M. Aida, and K. Ishida, "Power consumption characteristics by autonomous decentralized structure formation technology," *The 2012 IEICE general conference*, B-20-32, Mar. 2012. (in Japanese)

33. R. Hamamoto, C. Takano, M. Aida, K. Ishida, "On guaranteeing asymptotic stability of cluster structure by autonomous decentralized structure formation," *IEICE technical report*, IN2011-117, 111, 346, pp.61–66, Dec. 2011. (in Japanese, 18th Information Network Research Award of IEICE)

Abstract

In recent times, with the wide spread proliferation of wireless Local Area Networks (wireless LANs) based on the IEEE 802.11 standard, Internet connections through wireless LANs have become more common. Moreover, with rapid advancements in mobile terminals such as smartphones, tablets, and mobile access points (APs), the domain available for accessing the Internet has grown. However, several issues of wireless LAN technology have emerged. For instance, in ad hoc networks, both power saving and load balancing are important requirements for prolonging the life of networks. In addition, securing communication reachability for each terminal is an important issue. Further, in infrastructure networks, the AP placement problem and AP selection problem are important considerations in network design. Moreover, media access control methods are actively studied in order to improve the QoS of networks. This thesis describes solutions to the aforementioned problems inspired by natural world.

Specifically, this thesis focuses on two technologies as solutions to the issues in ad hoc networks. First, this thesis focuses on autonomous decentralized clustering based on local interaction. For the clustering mechanism of a MANET, an autonomous decentralized structure formation method based on the local interaction of terminals (referred to as the back-diffusion method) has already been proposed in a previous study; the method can be used to create an autonomous decentralized clustering of MANETs. However, one issue of the clustering method is that the number of clusters decreases with temporal evolution. Power saving and load balancing through hierarchical management of the network cannot be achieved owing to this problem. This thesis proposes a method that maintains the number of clusters (guarantees stability). Furthermore, the back-diffusion method can be used to configure clusters that reflect a network condition such as the residual battery power and the degree of each node. However, the effect of clusters that reflect a network condition has not been evaluated. This thesis configures clusters using the back-diffusion method and a bio-inspired method, which is a type of autonomous decentralized clustering method that is unable to reflect a network condition. Then, this thesis also clarifies the importance of a clustering method that reflects a network condition, with regard to power consumption and data transfer efficiency.

Second, this thesis focuses on a method for designing the radio transmission range considering a target problem. In general, terminals in an ad hoc network are operated by battery powered systems. Thus, extending a network's lifespan through power saving at each terminal is an important issue in an ad hoc network. To address this issue, one solution is to reduce the power consumption of each terminal by suppressing the radio transmission range of each terminal; however, this solution causes degradation of reachability of user data at each terminal. That is, the reachability of each terminal decreases

drastically. This thesis proposes a method for designing the radio transmission range considering a target problem in order to improve both power saving and a terminal's reachability in an ad hoc network.

For infrastructure networks, this thesis proposes and evaluates an acceleration of throughput prediction method for the AP considering the distribution of the terminals. In previous studies, the throughput of the AP in a multi-rate environment was estimated by the harmonic average of terminal's transmission rate. Thus, the complexity is linear order computation. By using the proposal, the calculation cost of the existing method can be reduced to a constant. Moreover, this thesis proposes an AP selection method, where mobile APs move cooperatively in addition to user mobility to avoid performance anomalies in an IEEE 802.11 multi-rate wireless LAN environment. Note that performance anomaly is an issue that it decreases the throughput of an AP when the APs are connected to terminals whose transmission rates are extremely low.

Furthermore, wireless LANs based on the IEEE802.11 standard usually use carrier sense multiple access with collision avoidance (CSMA/CA) for media access control. However, in CSMA/CA, if the number of wireless terminals increases, the back-off time derived by the initial contention window (CW) tends to conflict among wireless terminals. Consequently, data frame collisions often occur, which sometimes results in degradation of the total throughput in the transport layer protocols. In order to improve the total throughput of all terminals, this thesis proposes a new media access control method, SP-MAC, which is based on the synchronization phenomena of coupled oscillators. Moreover, it is demonstrated in this thesis that SP-MAC drastically decreases the data frame collision probability and improves the total throughput compared with the original CSMA/CA method.

Acknowledgments

Special thanks are due to my thesis supervisor Professor Kenji Ishida for his invaluable support and guidance through the hard moments of graduate school. I am also grateful to my dissertation committee: Professor Masaki Aida, Graduate School of System Design, Tokyo Metropolitan University, Professor Yoshiaki Kakuda, Associate Professor Chisa Takano, and Associate Professor Junichi Funasaka, Graduate School of Information Sciences, Hiroshima City University for their support, valuable feedback, and insightful ideas to this research. Moreover, I also received generous support from Lecturer Hiroyasu Obata, Graduate School of Information Sciences, Hiroshima City University. Additionally, I am thankful for discussions on some studies of the QoS guarantee method for wireless LAN using TCP-AV and Receive Opportunity Control in MAC Frame by Mr. Hikaru Tsushima, Graduate School of Information Sciences, Hiroshima City University. Further, I am also grateful for discussions on some studies of the redundancy setting method for TCP congestion control based on FEC over wireless LAN by Mr. Fumiya Teshima, Graduate School of Information Sciences, Hiroshima City University. Moreover, I also thank Mr. Kohei Izui, Graduate School of Information Sciences, Hiroshima City University for discussions on some studies of the transmission rate modeling based on advection-diffusion equation for multi-rate wireless LAN.

Professor Masaki Aida has also offered insightful comments and suggestions for Chapter 3. I am grateful for the constructive discussions I shared with Mr. Takuya Sakamoto and Ms. Miki Tomomune, Faculty of Information Sciences, Hiroshima City University, for Chapter 4. Advice and comments given by Professor Tutomu Murase, Information Technology Center, Nagoya University, and Ms. Natsumi Kumatani, Graduate School of Advanced Integration Science, Ochanomizu University, have been a great help in Chapter 6. Furthermore, I thank Mr. Koutaro Yamada, Faculty of Information Sciences, Hiroshima City University, Mr. Ryoma Ando and Mr. Yuuki Yamamoto, Graduate School of Information Sciences, Hiroshima City University for their help with some experiments in Chapter 7.

In addition, I would also like to thank the faculty members of the department of computer and network engineering, Hiroshima City University for their support. Moreover, I would like to express my appreciation to all my past and present colleagues and friends of the Information Network Laboratory, Graduate School of Information Sciences, Hiroshima City University.

Finally, I would like to express my gratitude to my family for their moral support and warm encouragements.

Table of Contents

List of Publications i

Abstract vii

Acknowledgments ix

Table of Contents x

List of Figures xiii

List of Tables xviii

1 Introduction 1

2 IEEE802.11 Wireless LAN 9
2.1 Overview of IEEE802.11 wireless LAN 9
2.2 Multi-rate transmission mechanism and performance anomaly problem . 11

3 An Autonomous Decentralized Clustering Based on Local Interaction 13
3.1 Introduction 13
3.2 Clustering method based on autonomous decentralized structure formation 15
3.2.1 Overview of back-diffusion based autonomous decentralized structure formation technology 15
3.2.2 Bio-inspired method based on reaction-diffusion equations . . . 19
3.3 Guarantee method of the stability for clusters 19
3.3.1 Problems with applying the back-diffusion method to clustering 19
3.3.2 Method guaranteeing stability of the cluster structure for a vector process 21
3.3.3 Evaluation of guarantee method 23
3.4 Evaluation of the effect which reflects the network condition for clusters 33
3.4.1 Hierarchical routing Hi-TORA 33
3.4.2 Characteristics of power consumption and data transfer efficiency 34
3.4.3 Performance characteristics with varying number of nodes and node mobility 37
3.5 Conclusion 44

4 A Proposal of Design Method for Terminal Communication Range to Improve both Power Saving and Communication Reachability Based on Target Problem 45
4.1 Introduction . . . 45
4.2 Related works . . . 46
4.2.1 Applications of ad hoc network . . . 46
4.2.2 Power consumption and reachability issues of ad hoc networks . 47
4.2.3 Existing methods for designing radio transmission range . . . 48
4.3 Setting the radio transmission range based on a target problem . . . 48
4.3.1 Overview of the two-dimensional target problem and its application to single-hop communication . . . 49
4.3.2 Miss probability estimation method in multi-hop communication 50
4.4 Evaluation . . . 53
4.4.1 Simulation environment . . . 53
4.4.2 Results . . . 54
4.5 Conclusion . . . 58

5 An Acceleration of Throughput Prediction Method for Access Point in Multirate Wireless LAN Considering Terminal Distribution 59
5.1 Introduction . . . 59
5.2 Transmission rate of IEEE802.11 and an existing throughput prediction method . . . 61
5.3 High speed throughput prediction method considering terminal distribution . . . 62
5.3.1 Overview of throughput prediction method based on terminal distribution . . . 62
5.3.2 Throughput prediction based on target problem . . . 63
5.3.3 Throughput prediction based on area ratio . . . 64
5.3.4 Algorithm of the proposed method . . . 64
5.3.5 Adaptive selection mechanism of prediction formulas . . . 65
5.4 Evaluation . . . 67
5.4.1 Results of normal distribution . . . 67
5.4.2 Results of uniform distribution . . . 68
5.4.3 Evaluation for adaptive selection mechanism of prediction formulas . . . 69
5.4.4 Evaluation of calculation cost . . . 72
5.5 Conclusion . . . 74

6 A Proposal of Access Point Selection Method Based on Cooperative Movement of Both Access Points and Users 75
6.1 Introduction . . . 75
6.2 UOMM: AP selection method based on user cooperative movement . . 76
6.3 UACMM: AP selection method based on user-AP-cooperative-mobility 77
6.3.1 Overview of UACMM . . . 77
6.3.2 Determination of communication position of APs and users to maximize system throughput . . . 78

6.4 Throughput evaluations 81
6.4.1 Movable distance of APs and throughput performance 81
6.4.2 Throughput performance vs. number of APs 84
6.4.3 Evaluation of throughput when joining and leaving users exist . 85
6.4.4 Evaluation of throughput considering disconnection methods of a user 87
6.4.5 Realistic solution 90
6.5 Conclusion 92

7 A Media Access Control Method Based on the Synchronization Phenomena of Coupled Oscillators over Wireless LAN 93
7.1 Introduction 93
7.2 Related works 94
7.2.1 Synchronization model of coupled oscillators 94
7.2.2 Existing media access controls for collision avoidance 95
7.3 SP-MAC: A media access control method based on the synchronization phenomena of coupled oscillators 97
7.3.1 Overview of SP-MAC 97
7.3.2 Detailed procedures of SP-MAC 98
7.4 Simulation experiments 100
7.4.1 Simulation settings 100
7.4.2 Basic performance evaluations 101
7.4.3 Comparative evaluation with existing method for collision avoidance 104
7.4.4 Performance evaluation when both SP-MAC and CSMA/CA exist 107
7.4.5 Performance evaluation when join and leave wireless terminals exist 110
7.4.6 Performance evaluation of SP-MAC over multi-rate wireless LAN environment 111
7.5 Conclusion 113

8 Conclusion 115

References 117

List of Figures

1.1 Layer structure of nature: Snake of uroboros. 2
1.2 The relationship among behavior, models, and advanced technologies in the thesis. 5
1.3 The location of installation for advanced technologies of the thesis. . . . 6
1.4 The technical area of each advanced technology. 7
1.5 The correspondence between TCP/IP protocol and advanced technologies of the thesis. 7

2.1 Example of CSMA/CA. 10
2.2 Performance anomaly problem. 11

3.1 Determining $\Phi(\boldsymbol{x}, t)$ according to back-diffusion. 16
3.2 Diffusion and back-diffusion. 16
3.3 Cluster structure formation by the back-diffusion method (initial state, after 5, 20). 17
3.4 The effect of the back diffusion in one-dimension model. 17
3.5 Examples of Turing pattern. 19
3.6 Issues in parameter setting. 20
3.7 Decay of the range of the distribution. 20
3.8 Problems with dynamic network topologies. 21
3.9 Temporal evolution of $\boldsymbol{Q}(t_k)$ for each node. 21
3.10 Torus topology. 24
3.11 Initial conditions (1). 24
3.12 Temporal variation of the distribution range due to diffusion. 25
3.13 Damping characteristics in the distribution range due to diffusion. . . . 25
3.14 Temporal variation of the distribution range due to diffusion and drift. . 26
3.15 Relation of the decay rate and c in the distribution range due to diffusion and drift. 26
3.16 Initial conditions (2). 27
3.17 Cluster structures for the 5th and 20th components of $\boldsymbol{Q}(t_k)$. 27
3.18 Temporal variation in the distribution range for the 5th and 20th components of $\boldsymbol{Q}(t_k)$. 28
3.19 Unit disk graph network. 29
3.20 Initial conditions (3). 29
3.21 Temporal variation in the range of the distribution for the 5th and 20th components of $\boldsymbol{Q}(t_k)$ (Nodes move every 100 sec. Node mobility frequency is low.). 30

3.22 Temporal variation in the range of the distribution for the 5th and 20th components of $\boldsymbol{Q}(t_k)$ (Nodes move every 10 sec. Node mobility frequency is moderate.). 30
3.23 Temporal variation in the range of the distribution for the 5th and 20th components of $\boldsymbol{Q}(t_k)$ (Nodes move every 1 sec. Node mobility frequency is high.). 31
3.24 Time average of the number of clusters for the 5th and 20th components of $\boldsymbol{Q}(t_k)$ (Nodes move every 100 sec. Node mobility frequency is low.). . 31
3.25 Time average of the number of clusters for the 5th and 20th components of $\boldsymbol{Q}(t_k)$ (Nodes move every 10 sec. Node mobility frequency is moderate.). 32
3.26 Time average of the number of clusters for the 5th and 20th components of $\boldsymbol{Q}(t_k)$ (Nodes move every 1 sec. Node mobility frequency is high.). . 32
3.27 The distribution of initial battery power. 35
3.28 Temporal evolution of percentage of live nodes. 36
3.29 Relationship between the percentage of live nodes and the number of nodes (back-diffusion). 38
3.30 Relationship between the percentage of live nodes and the number of nodes (bio-inspired). 38
3.31 Relationship between the FND time and the number of nodes. 39
3.32 Relationship between the standard deviation of FND time and the number of nodes. 39
3.33 Relationship between the amount of received data and the number of nodes. 40
3.34 Relationship between the standard deviation of the amount of received data and the number of nodes. 40
3.35 Relationship between the percentage of live nodes and the average node velocity (back-diffusion). 41
3.36 Relationship between the percentage of live nodes and the average node velocity (bio-inspired). 41
3.37 Relationship between the FND time and the average node velocity. . . . 42
3.38 Relationship between the standard deviation of the FND time and the average node velocity. 42
3.39 Relationship between the amount of received data and the average node velocity. 43
3.40 Relationship between the standard deviation of the amount of received data and the average node velocity. 43

4.1 Overview of geocast communication. 47
4.2 Relationship between the distance from the origin and the χ distribution in the two-dimensional target problem. 50
4.3 Relationship between the transmission range r and miss probability for each N ($\sigma = 1.0$). 51
4.4 Relationship between the transmission range r and effective radius R_{ef} for each σ ($N = 1,000$). 51
4.5 Relationship between α and σ. 51

4.6 Relationship between β and σ. 51
4.7 Comparison of the simulation value and the theoretical value Eq.(4.9) (σ = 1.0). 52
4.8 Relationship between σ and the distance of the node farthest from the GWN. 53
4.9 Total goodput for each σ (N = 100, DSDV, CSMA/CA). 54
4.10 Total goodput for each σ (N = 100, DSDV, TDMA). 54
4.11 Total goodput for each σ (N = 100, AODV, CSMA/CA). 55
4.12 Total goodput for each σ (N = 100, AODV, TDMA). 55
4.13 Relationship between the transmission range r and the total power consumption and total goodput (σ = 30.0, DSDV, CSMA/CA). 56
4.14 Relationship between the transmission range r and the total power consumption and total goodput (σ = 30.0, DSDV, TDMA). 57
4.15 Relationship between the transmission range r and the total power consumption and total goodput (σ = 30.0, AODV, CSMA/CA). 57
4.16 Relationship between the transmission range r and the total power consumption and total goodput (σ = 30.0, AODV, TDMA). 58

5.1 Stepped transmission rate. 61
5.2 Throughput prediction using target problem. 64
5.3 Throughput prediction using area ratio. 64
5.4 Ratio of terminals that use the maximum transmission rate. 66
5.5 Throughput of an AP that is predicted by each method (normal distribution, 10 terminals). 67
5.6 Throughput of an AP that is predicted by each method (normal distribution, 20 terminals). 67
5.7 Relative error between the proposed method and the existing method in each σ. 67
5.8 Throughput of an AP that is predicted by each method (uniform distribution, 10 terminals). 69
5.9 Throughput of an AP that is predicted by each method (uniform distribution, 20 terminals). 69
5.10 Relative error between the proposed method and the existing method in each L_r. 69
5.11 Throughput of an AP that is predicted by each method in each σ using the adaptive selection mechanism of the prediction formulas (normal distribution, v = 1.0 m/s). 70
5.12 Throughput of an AP that is predicted by each method in each L_r using the adaptive selection mechanism of the prediction formulas (uniform distribution, v = 1.0 m/s). 71
5.13 Number of terminals v.s. complexity. 73
5.14 Accumulated complexity. 73

6.1 AP selection method based on AP cooperative movement of both the AP and the user. 78
6.2 Initial position of APs and users. 78

6.3 Determination of communication position of APs and new users. 78
6.4 Initial configuration of system (1). 81
6.5 Relationship between system throughput and movable distance of both the AP and new user (vs. minimum distance selection method). 82
6.6 Relationship between system throughput and movable distance for both the AP and new user (vs. UOMM). 82
6.7 Relationship between system throughput and movable distance (total movable distance is 60 m). 84
6.8 Initial configuration of system (2). 84
6.9 Throughput performance vs. the number of APs in the system (movable distance; AP 10 m, new user 10 m). 85
6.10 Throughput performance vs. number of APs in the system (movable distance; AP 30 m, new user 30 m). 85
6.11 Utilization rate (ρ) vs. improvement ratio of system throughput (new user movable distance: 10 m). 86
6.12 Utilization rate (ρ) vs. improvement ratio of system throughput (new user movable distance: 30 m). 86
6.13 Relationship between system throughput and each option (AP capacity: 2, new user movable distance: 10 m). 88
6.14 Relationship between system throughput and each options (AP capacity: 2, new user movable distance: 30 m). 88
6.15 Relationship between system throughput and each option (AP capacity: 10, new user movable distance: 10 m). 89
6.16 Relationship between system throughput and each option (AP capacity: 10, new user movable distance: 30 m). 89
6.17 Initial configuration of system (3). 90
6.18 System throughput with discrete and continuous destination points. . . . 90
6.19 Comparing system throughput achieved with gravity point and p-median. 91

7.1 Example: cosine curves of synchronized oscillators with phase shifting. 97
7.2 Relationship between the phase and back-off time of SP-MAC. 99
7.3 Simulation model. 101
7.4 The total throughput for each flow (UDP). 103
7.5 The total throughput for each flow (TCP-Reno with Sack). 103
7.6 The total throughput for each flow (CUBIC-TCP). 104
7.7 The standard deviation of each flow (CUBIC-TCP). 104
7.8 The total throughput of UDP for each flow when comparing SP-MAC to PCF, TDMA, and SRB. 105
7.9 The rate of the sum of receipt control frame size and management frame size compared to total receipt frame size. 105
7.10 The total throughput of UDP for each flow in the unsaturated flow case. 106
7.11 The total throughput of UDP when both SP-MAC and CSMA/CA exist. 108
7.12 The average throughput of UDP when both SP-MAC and CSMA/CA exist. 108
7.13 The total throughput of CUBIC-TCP when both SP-MAC and CSMA/CA exist. 109

7.14 The average throughput of CUBIC-TCP when both SP-MAC and CSMA/CA exist. 109
7.15 The total throughput of UDP when join and leave wireless terminals exist. 110
7.16 The time change of total throughput (UDP) when join and leave wireless terminals exist (SP-MAC, CSMA/CA, and SRB). 110
7.17 The total throughput for each flow (Case1). 112
7.18 The total throughput for each flow (Case2). 112
7.19 Improvement ratio of the SP-MAC's average throughput compared to CSMA/CA (Case1). 114
7.20 Improvement ratio of the SP-MAC's average throughput compared to CSMA/CA (Case2). 114

List of Tables

1.1 The local rule and aim of the technology. 5
1.2 The relationship between the control form and advanced technologies of the thesis. 6

2.1 IEEE 802.11 standards. 10

3.1 Experimental parameters (diffusion only). 24
3.2 Experimental parameters (the two-dimensional network $\boldsymbol{Q}$ does not change over time). 27
3.3 The converged value of the range α. 28
3.4 Experimental parameters (MANET $\boldsymbol{Q}$ changes over time). 29
3.5 The range of fluctuation b. 31
3.6 Experimental environments (power consumption). 34
3.7 Parameters of the back-diffusion method. 35
3.8 Parameters of the bio-inspired method. 35
3.9 FND time. 37
3.10 Standard deviation of FND time. 37
3.11 Amount of total received data. 37
3.12 Standard deviation of total received data by the sink node. 37

4.1 Value of $\phi(N)$. 52
4.2 Applicability of the proposed method. 58

5.1 Relationship between distance and transmission rate (IEEE 802.11a/g). 61
5.2 Relative error between the proposed method and the existing method in each σ using the adaptive selection mechanism of the prediction formulas (v = 1.0 m/s). 70
5.3 Relative error between the proposed method and the existing method in each L_r using the adaptive selection mechanism of the prediction formulas (v = 1.0 m/s). 71

7.1 Simulation parameters. 101
7.2 The number of collisions for each flow (UDP). 102
7.3 The number of collisions for each flow (TCP-Reno with Sack). 102
7.4 The number of collisions for each flow (CUBIC-TCP). 102
7.5 Estimated total throughput of all terminals when CSMA/CA is used for MAC protocol. 111
7.6 The number of data frame collisions for each flow (Case1). 113

7.7 The number of data frame collisions for each flow (Case2). 113

Chapter 1

Introduction

In recent years, wireless Local Area Networks (wireless LANs) based on IEEE 802.11 standard [1, 2] have become increasingly popular. Wireless LANs can be introduced at lower costs compared to wired LANs as they can be configured without hard-wiring between terminals and Access Points (APs). If APs have access to the Internet, terminals in the transmission area of the AP can access the Internet regardless of their location. Owing to these advantages, currently, wireless LANs are used in various environments such as homes, offices, and schools . Further, owing to rapid advancements in mobile terminals such as smartphones, tablets, and mobile APs, public Wi-Fis [3] have widely proliferated [4]. Moreover, remote campus systems [5] and telemedicine systems [6–8] can be constructed through wireless LAN systems, thereby connecting remote locations, such as isolated islands with universities and hospitals.

There are two modes of wireless LANs based on IEEE 802.11 [1, 2]: infrastructure mode and ad hoc mode. In the infrastructure mode, wireless LAN systems consist of APs connected to external networks via wired LAN (e.g. Ethernet) as well as a number of terminals located within the radio transmission range of the APs. The infrastructure mode is typically used for public wireless LAN service areas. Conversely, the networks using the ad hoc mode can be configured autonomously using wireless terminals such as laptops and tablets, without requiring network infrastructure such as APs. Moreover, the ad hoc mode networks can be configured rapidly and inexpensively. In addition, when a large-scale disaster such as an earthquake or tsunami occurs, the wireless ad hoc networks are beneficial because they can be configured without network infrastructures [9–13]. As a specific example, [9] have proposed *SKYMESH*, which is an instance of the ad hoc network configured using aircrafts equipped with the AP of wireless LAN. Because of the above reasons, the wireless LAN is one of the most important communication infrastructure not only in times of peace but also in the event of a disaster. However, the wireless LAN technology has various issues. For example, in the ad hoc mode wireless LANs, both power saving and load balancing are important issues for life prolongation of networks. In addition, securing communication reachability for each terminal is a significant issue. On the other hand, in the infrastructure mode wireless LANs, an AP placement problem and an AP selection problem are important considerations in the network design. Furthermore, a Quality of Service (QoS) control method and a media access control (MAC) method are actively studied.

This thesis focuses on power saving and communication reachability for the ad hoc

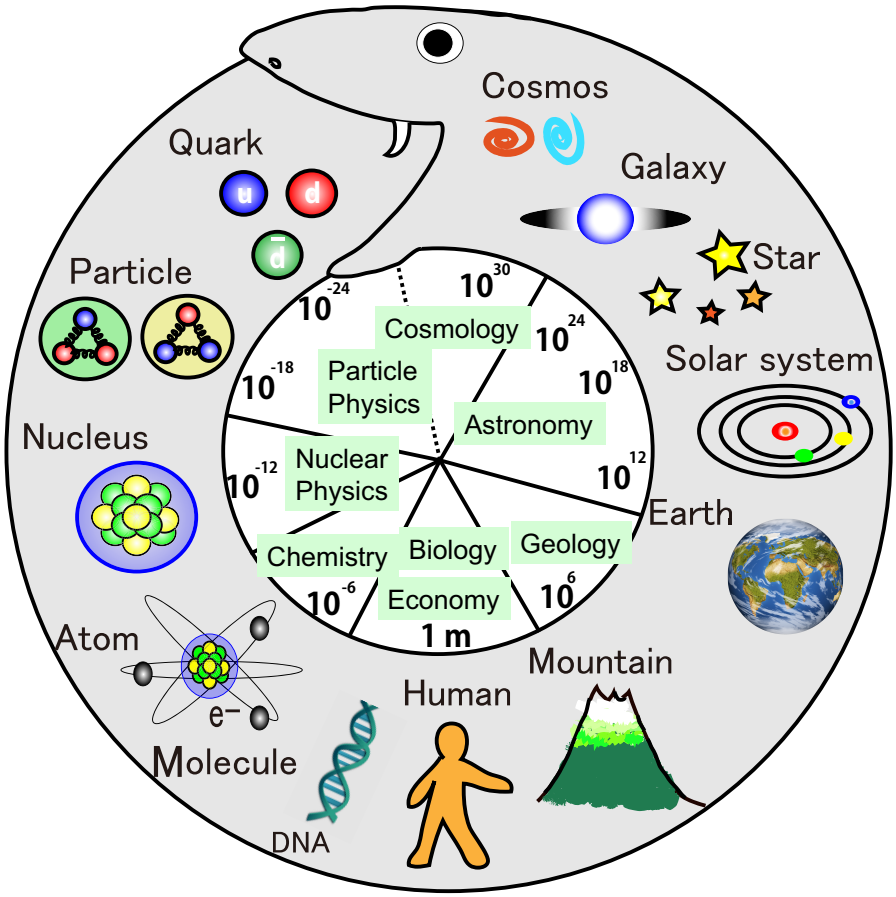

Figure 1.1: Layer structure of nature: Snake of uroboros.

networks. Furthermore, the AP selection method, the throughput prediction method, and the MAC method are proposed to address the issues of the infrastructure mode. Previous studies have proposed clustering methods for networks and transmission range management technologies for terminals in the ad hoc networks. Moreover, to address the issues of the infrastructure mode, various AP selection or AP placement algorithms and throughput prediction methods have been proposed. Additionally, some MAC methods have been proposed to improve the QoS of users. One of the example of these solutions is to control the entire system by behavior of individual elements constituting a system which is according to the local rule.

An example of the system which realize the above solution is *natural world*. The natural world is controlled with the order. The structure of hierarchy is found in the order of nature, and it is a complexly intertwined hierarchical structure from small scale to large scale [14]. As an example, substances are constructed by some atoms or molecules. Moreover, the atom is constructed by the set of smaller materials such as nucleus, protons, electrons, and quarks. On the other hand, both organic materials such as organisms and inorganic materials such as minerals are composed by many atoms. Further, the earth was formed by a living entity and minerals, and the earth is a part of the solar system. The solar system is a part of the galaxy, and the cosmos is constructed

by many galaxies. Thus, the entire natural world is formed by configuring the structure of the macro-scale (10^{30} order) which is stacking components of a micro-scale (10^{-24} order) hierarchically (see Fig.1.1). As described above, the components of nature is controlled by the local behavior of the components in the lower hierarchy from it. Here, by considering the control which imitates the behavior of the natural world, the solution of the issues which is described above can be proposed. However, in order to achieve the purpose, it is necessary to clarify what gimmicks operates in the natural world. To elucidate the natural world, many researchers have already tried a variety of approaches.

Here, the challenge of elucidate the natural world include to clarify the various phenomena and behavior which are caused by the components of the natural world. In fact, various phenomena are caused by the behavior of the components for the natural world. As a specific example, several biological phenomena such as pattern formation of animals and plants [15] and beating of the heart [16] exist. Further, social phenomena such as traffic congestion [17] and economic recession/inflation [18] also are known. These phenomena are an interesting subject for study in order to clarify the natural world. There are *social sciences* and *natural sciences* as academic to elucidate the natural world. To study the behavior which caused by the human interaction, social sciences have been established. Examples of the social sciences are the economy, the geography, and the historiography. Moreover, natural sciences have been proposed in order to clarify the natural phenomena. The physics, the chemistry, and the biology are representative examples of the natural sciences.

Here, an important requirement in order to analyze the phenomena is that quantitative reproduction of the phenomena is necessary. To achieve this requirement, *modeling*, which is a method for representing a phenomenon by a formula, is a useful tool in both the social sciences and natural sciences. That is, both natural sciences and social sciences have a common goal of revealing the natural world through the model. Previous studies have already proposed the model of phenomena, and characteristics of the natural world is shown in the model. Thus, by utilizing the proposed models, it is possible to realize a control which uses the behavior of nature. So far, some studies have proposed and evaluated nature-inspired (social/natural sciences inspired) technologies [19–22]. These are the systems that take advantage of the harmony of the natural world. This thesis proposes advanced technologies for wireless LANs using models of natural phenomena proposed by pioneers. Especially, this thesis proposes advanced technologies for wireless LANs which controls the entire system by behavior of according to the local rule with individual elements constituting a system as the natural world.

This thesis focuses on two technologies as solutions to the issues of the ad hoc networks. First, this thesis focuses on an autonomous decentralized clustering based on local interaction. For the clustering mechanism of the ad hoc networks, an autonomous decentralized structure formation method (the back-diffusion method [23]) which is based on the local interaction of terminals has already been proposed and evaluated in a previous study. However, the problem of the back-diffusion method is that the number of clusters decreases with temporal evolution. Power saving and load balancing through hierarchical management of the network cannot be achieved owing to this problem. This thesis proposes a method that maintains the number of clusters (guarantees stability) [24–26]. Furthermore, the back-diffusion method is known to configure clusters that reflect the network condition, such as residual battery power and the de-

gree of each node. However, the effect of clusters that reflect the network condition has not been evaluated. This thesis configures clusters using the back-diffusion method and a bio-inspired method, which is an instance autonomous decentralized clustering that cannot reflect a network condition. Next, this thesis clarifies the importance of clustering for reflecting a network condition, with regard to the power consumption and the data transfer efficiency [27–29]. Second, this thesis focuses on the design method for the radio transmission range considering the target problem [30]. In general, terminals in the an ad hoc network are operated with battery powered systems. Thus, extending the network lifetime through power saving for each terminal is an important issue in the ad hoc networks. One method to address this issue is to reduce the power consumption of each terminal by reducing the radio transmission range of each terminal; however, it could lead to degradation in reachability of user data for each terminal. That is, reachability of each terminal could decrease drastically. This thesis proposes a method for designing the radio transmission range considering the target problem in order to improve both power saving and a terminal's reachability in the ad hoc network. For the infrastructure mode wireless LANs, this thesis proposes and evaluates an acceleration of throughput prediction method for the AP considering the distribution of the terminals [31]. In previous studies, the throughput of the AP in the IEEE 802.11 multi-rate environment was estimated by the harmonic average of terminal's transmission rate. Thus, the complexity is linear order computation. By using [31], however, the calculation cost of the existing method can be reduced to a constant. Note that the terminal distribution is approximated by a probability distribution. Moreover, this thesis proposes an AP selection method [32–34], where mobile APs move cooperatively in addition to user mobility to avoid performance anomalies in the multi-rate wireless LAN environment. The proposed AP selection method is based on Pareto optimization. Note that a performance anomaly is an issue that it decreases the throughput of an AP because APs are connected to terminals whose transmission rates are extremely low. Furthermore, wireless LANs based on the IEEE802.11 standard usually use carrier sense multiple access with collision avoidance (CSMA/CA) for MAC method. However, in CSMA/CA, if the number of wireless terminals increases, the back-off time derived by the initial contention window (CW) tends to conflict among wireless terminals. Consequently, a data frame collision often occurs, which results in degradation of the total throughput in the transport layer protocols. In order to improve the total throughput, this thesis proposes a new media access control method, SP-MAC [35–38], which is based on the synchronization phenomena of coupled oscillators. Moreover, this thesis shows that SP-MAC drastically decreases the data frame collision probability and improves the total throughput compared with the original CSMA/CA.

The remainder of this thesis is organized as follows: Chapter 2 introduces related works of this study. Chapter 3 explains the studies about the autonomous decentralized clustering based on the local interaction. Chapter 4 describes the method for designing the radio transmission range using target problem in order to improve both power saving and a terminal's reachability. Chapter 5 proposes the throughput prediction method for the AP considering the terminal's distribution. Chapter 6 summarizes the AP selection method based on cooperative moving of both users and APs. Chapter 7 elucidates the media access control method based on the synchronization phenomena of coupled oscillators. Finally, Chapter 8 shows the conclusion and future works.

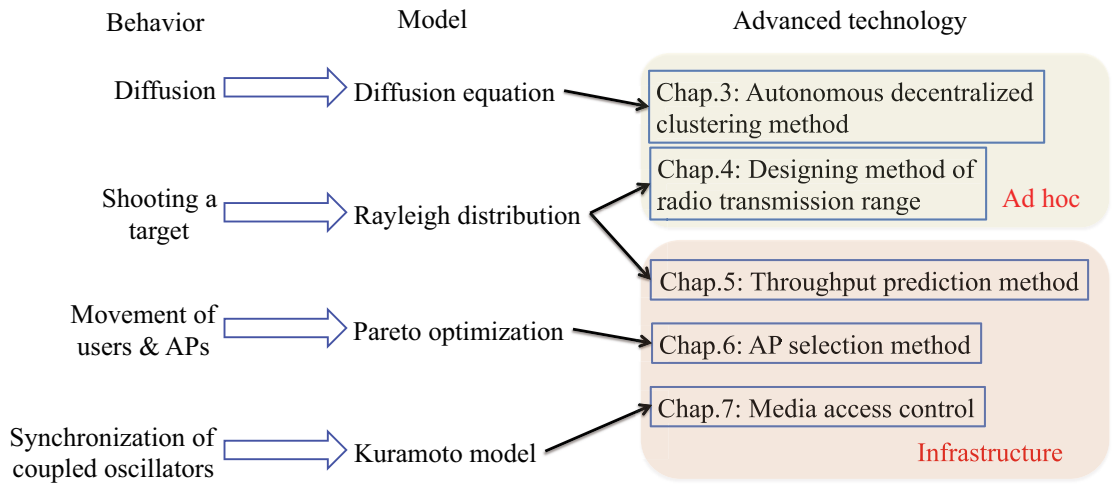

Figure 1.2: The relationship among behavior, models, and advanced technologies in the thesis.

Table 1.1: The local rule and aim of the technology.

Chapter	Local rule	Aim of the technology
3	Calculation of the clustering metric	To configure clusters
4	Calculation of the transmission range	To improve the reachability
5	Calculation of the ratio of the terminal connecting near the AP	To predict the AP throughput quickly
6	Minimization of the distance between the AP and the terminal	To Maximize the AP throughput
7	Calculation of the Kuramoto model	To avoid the data frame collision

Here, the chapters of this thesis are categorized from the point of view of the model and local rule for the technologies, the location of installation for the technologies, the control form of the technologies, the technical area for the technologies, and the correspondence between TCP/IP protocol and the technologies.

The model and local rule for each technology

Figure 1.2 shows the relationship among the behavior of the natural world, the models of each behavior, and the advanced technologies for the wireless LAN. In Fig.1.2, Diffusion equation, Rayleigh distribution, and Kuramoto model are proposed by natural sciences. On the other hand, Pareto optimization is a kind of model which is devised for the microeconomics. That is, Pareto optimization is proposed by social sciences. Moreover, Table 1.1 summarizes the relationship between the aim of the technology and the local rule that the components of the wireless LAN system (terminal and AP) performs in each technology. In any technology of this thesis, the control aimed by the wireless LAN system can be realized by performing the local rules of the terminal or the AP. That is, these technologies realize the control for the entire system by behavior of components as the natural world.

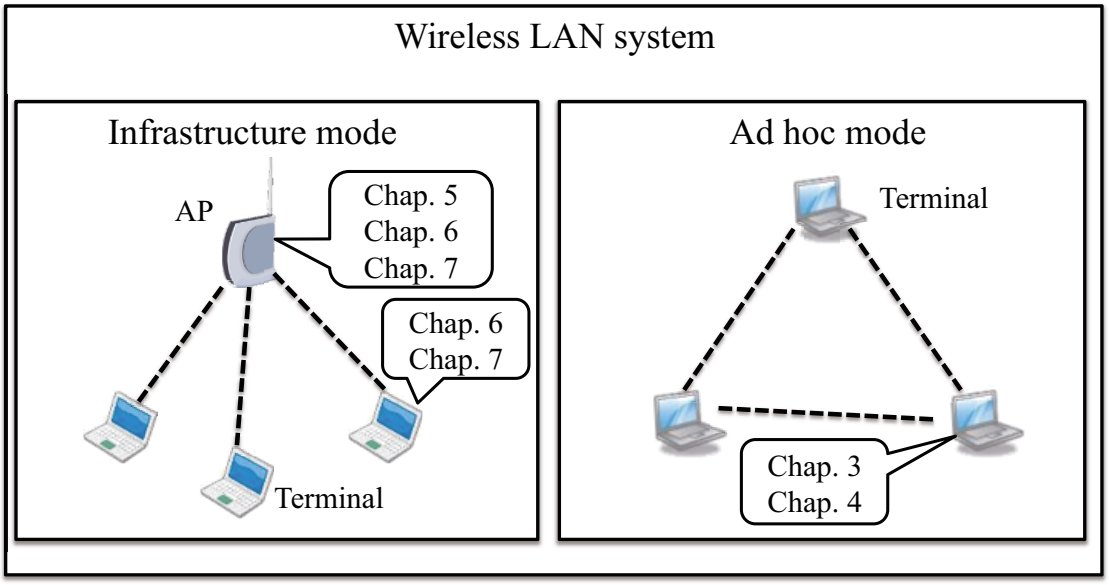

Figure 1.3: The location of installation for advanced technologies of the thesis.

Table 1.2: The relationship between the control form and advanced technologies of the thesis.

Chapter	Control form
3	Decentralized
4	Centralized
5	Centralized
6	Centralized
7	Centralized

The location of installation for each technology

Figure 1.3 summarizes the location of installation for the advanced technologies of the thesis. That is, Fig.1.3 shows who performs the local rule in order to control the wireless LAN system in each technology. From Fig.1.3, in order to solve the issue of the ad hoc mode wireless LAN, both the autonomous decentralized clustering which is proposed in Chapter 3 and the designing method of the transmission range for wireless terminals which is proposed in Chapter 4 are installed in the terminal only. On the other hand, the AP throughput prediction method which is proposed in Chapter 5 is installed in the AP only. Moreover, both the AP selection method which is proposed in Chapter 6 and the media access control method which is proposed in Chapter 7 are needed to install in both the terminal and the AP.

The control form of each technology

The relationship between the control form and the advanced technologies of the thesis is shown in Table 1.2. From Table 1.2, the technology proposed in Chapter 3 is only the distributed control system. Moreover, the technologies which are proposed in Chapter 4, Chapter 5, Chapter 6, and Chapter 7 are the centralized control system.

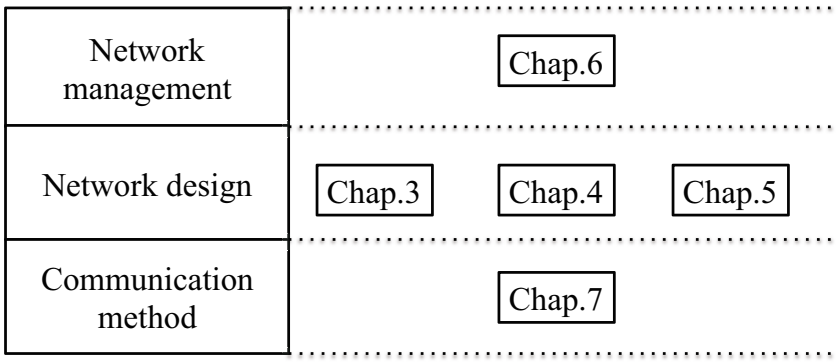

Figure 1.4: The technical area of each advanced technology.

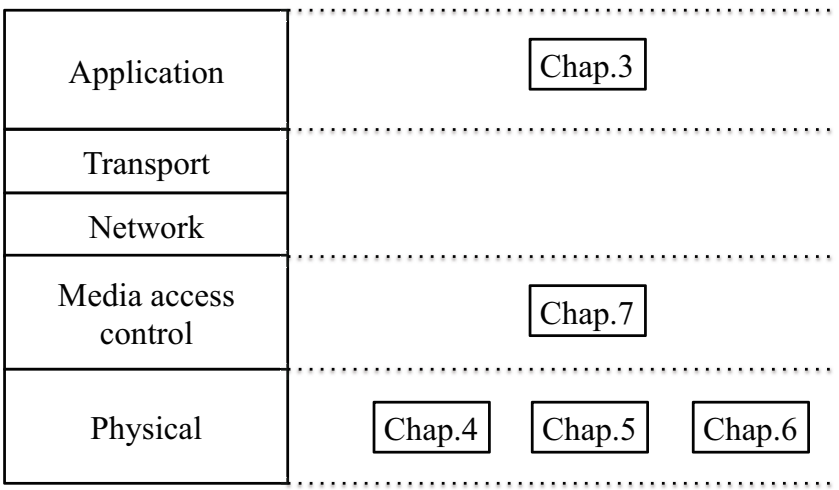

Figure 1.5: The correspondence between TCP/IP protocol and advanced technologies of the thesis.

The technical area for each technology

Figure 1.4 summarizes the technical area of the advanced technologies which are proposed in the theses. From Fig.1.4, the technology proposed in Chapter 7 is associated with the communication method. Moreover, Chapter 3, Chapter 4, and Chapter 5 propose the advanced technologies for the network design. In addition, proposals of Chapter 6 is the advanced technology for the network management. That is, frames are sent by the technology proposed in Chapter 7. Furthermore, using the information which is included in the frames, the network design technologies which are proposed in Chapter 3, Chapter 4, and Chapter 5 are operated. Finally, to improve the performance of the network, network administrators manage the network using the technology proposed in Chapter 6.

The correspondence between TCP/IP protocol and each technology

Finally, Fig.1.5 shows the correspondence between TCP/IP protocol and the advanced technologies of the thesis. From Fig.1.5, the proposals in Chapter 4, Chapter 5,

and Chapter 6 are the technologies corresponding to the physical layer of TCP/IP protocol. They are technologies for the physical connection of the wireless terminals and the AP. Moreover, the proposal in Chapter 7 is the MAC layer protocol. It is the technology of the access timing control for the wireless terminal and the AP. Further, the proposal in Chapter 3 is associated with the application layer. It is the technology of both the power saving and the load balancing of the wireless terminals.

Chapter 2

IEEE802.11 Wireless LAN

THIS chapter presents an overview of IEEE802.11 wireless LAN [1].

2.1 Overview of IEEE802.11 wireless LAN

The IEEE802.11 wireless LAN is one of the most popular standards for wireless Internet access. It has several versions (Table 2.1) such as IEEE802.11b [39], IEEE802.11g [40], IEEE802.11n [41], and IEEE802.11ac [42]. These versions use 2.4 GHz and 5 GHz bands. Note that in Table 2.1, the Data rate shows the maximum data rate in each standard.

There are two forms of wireless LANs based on the IEEE 802.11, infrastructure mode and ad hoc mode. In the infrastructure mode, wireless LAN systems consist of APs connected to external networks via a wired network (e.g. Ethernet) as well as a number of terminals located within the radio transmission range of the APs. Conversely, networks using ad hoc mode can be configured autonomously using wireless terminals such as laptops and tablets, without network infrastructure such as APs. Moreover, ad hoc mode networks can be configured rapidly and inexpensively. For example, ad hoc networks can construct sensor networks [43] for the purpose of environmental monitoring. Additionally, they can be used in vehicle to vehicle (V2V) communication systems [44] for delivering traffic information such as traffic jam and traffic accident.

In ad hoc networks, there are two communication methods, single-hop and multi-hop. In single-hop communication, each terminal communicates directly (1 hop). Thus, a sender must increase the transmission power if the distance between the sender and receiver is relatively large. Therefore, single-hop communication is not suitable for extending an ad hoc network's lifetime. Note that the infrastructure mode uses single-hop communication. Conversely, in multi-hop communication, the sender and the receiver are not required to communicate with other terminal directly; packets can be relayed by terminals in between a sender and a receiver. In other words, terminals in multi-hop communication networks can receive packets from neighboring terminals. Thus, multi-hop communication is suitable for extending the lifetime of ad hoc networks.

In IEEE802.11 wireless LANs, a wireless terminal uses carrier sense multiple access with collision avoidance (CSMA/CA) as the MAC method and autonomously sends data frames (see Fig.2.1). Thus, each wireless terminal individually decides the timing

Table 2.1: IEEE 802.11 standards.

Standard	Release year	Frequency range	Bandwidth	Modulation	Data rate
802.11	1997	2.4 GHz	20 MHz	DSSS, FHSS	2 Mbps
802.11b	1999	2.4 GHz	20 MHz	DSSS	11 Mbps
802.11a	1999	5 GHz	20 MHz	OFDM	54 Mbps
802.11g	2003	2.4 GHz	20 MHz	DSSS, OFDM	54 Mbps
802.11n	2009	2.4/5 GHz	20/40 MHz	OFDM	600 Mbps
802.11ac	2013	5 GHz	40/80/160 MHz	OFDM	6.93 Gbps

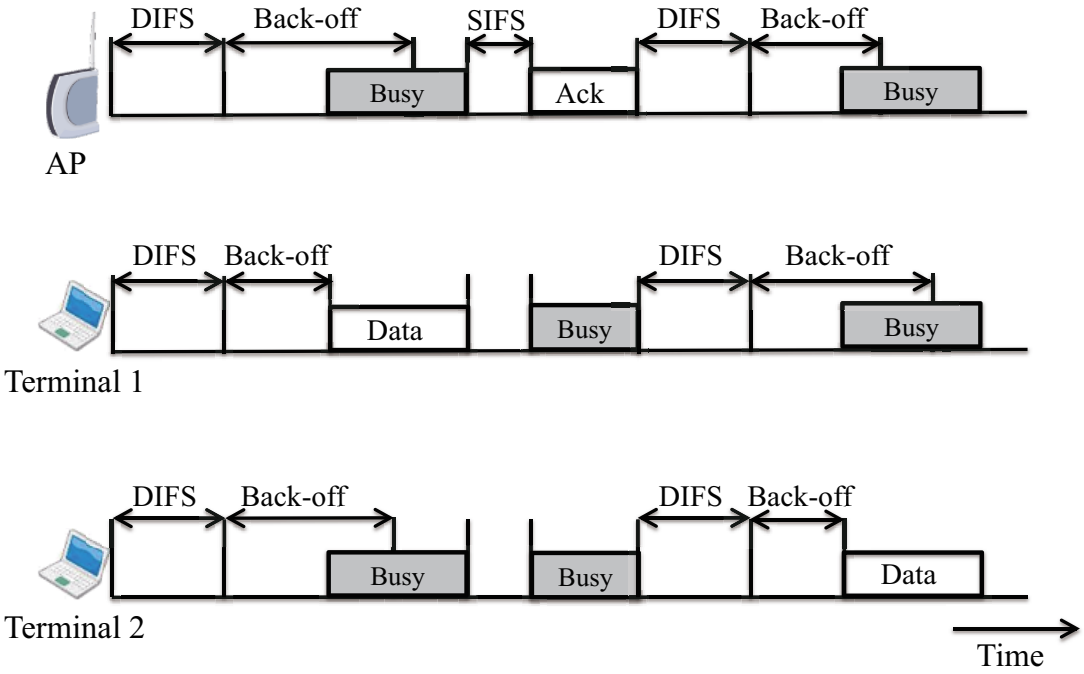

Figure 2.1: Example of CSMA/CA.

of data transmission. In CSMA/CA, if the channel becomes idle when a data frame arrives in the transmission queue, it defers to DCF inter frame space (DIFS) time. Then, if the channel remains idle after DIFS, CSMA/CA waits for the back-off time, which is randomly calculated using a CW. Subsequently, if the channel remains idle after the back-off time, the terminal sends the data frame. The back-off time is determined using Eq.(2.1), which is calculated independently for each terminal.

$$\text{Backoff} = \textit{Random}() \times \text{SlotTime} \tag{2.1}$$

In Eq.(2.1), *Random*() and SlotTime indicate a random integer derived from a discrete uniform distribution [0,CW] and the slot time interval specified in IEEE802.11, respectively. Note that CW satisfies $CW_{\text{min}} \leq CW \leq CW_{\text{max}}$ At this point, the initial CW is set to CW_{min}. If a collision causes the data frame transmission to fail, then the terminal sets the back-off time using Eq.(2.1) again. In this case, the CW becomes twice as large

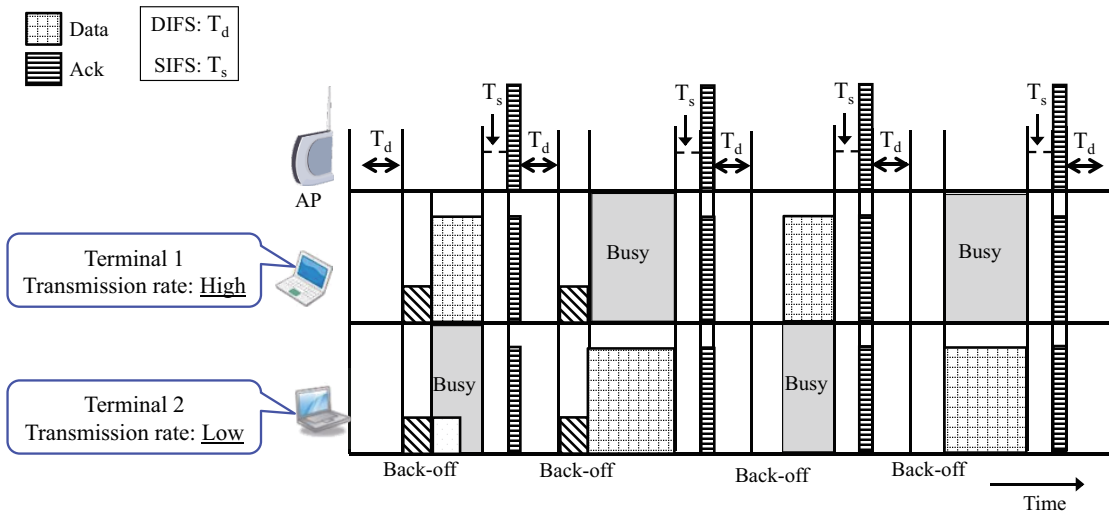

Figure 2.2: Performance anomaly problem.

as the previous value, and the upper bound is CW_{max} (= 1023). If the retransmission exceeds the maximum retry limits (usually 7), the terminal discards the data frame.

2.2 Multi-rate transmission mechanism and performance anomaly problem

Most IEEE802.11b/a/g wireless LANs [1] employ multi-rate transmission for effective communication. In IEEE802.11b, the transmission rates are 11, 5.5, 2, and 1 Mbps, whereas IEEE802.11 a/g offers 54, 48, 36, 24, 18, 12, 9, and 6 Mbps. These protocols specify multiple transmission rates, and an appropriate transmission rate can be selected so as not to exceed a certain bit error rate or frame error rate [45]. The appropriate transmission rate is usually selected by each vendor's original algorithm. However, some products allow the transmission rate to be manually selected. For example, in transmission rate control [46], if the electric wave environment worsens and high-speed transmission cannot be maintained, the AP drops the transmission rate.

In a multi-rate environment, however, a performance anomaly [47] degrades the throughput of all terminals connected to one AP (Fig.2.2). The throughput of the terminal connected to the same AP becomes nearly equal to that of the terminal with the lowest transmission rate. This problem is caused by CSMA/CA. In a wireless LAN environment, each terminal can obtain a fair transmission opportunity. Specifically, CSMA/CA provides each terminal with the same number of accesses to the communication channel. However, in a multi-rate environment, the time for which a terminal occupies the channel depends on its transmission rate. Since a terminal with a high transmission rate has a short channel occupancy time, the wait time of other terminals decreases. Conversely, since the channel occupancy time of a low transmission rate terminal is long, the wait time of other terminals increases. In this situation, the transmission cycle of terminals with high transmission rates becomes the almost the same as

that of the terminal with the lowest transmission rate. Accordingly, the throughput of the high transmission rate terminals decreases.

In a multi-rate environment, it is known that the throughput of the AP (the total throughput of all terminals connected to the AP) Th can be estimated by Eq.(2.2) [48]. Equation (2.2) shows that AP throughput Th is equal to the harmonic average value of the transmission rate of terminals connected to the same AP in a multi-rate environment.

$$Th = \frac{n_{cnt}}{\sum_{\{j|1 \leq j \leq N,\ b_j > 0\}} (b_j)^{-1}} \tag{2.2}$$

In Eq.(2.2), N means the number of all terminals in the system, and n_{cnt} ($\leq N$) denotes the number of terminals connected to the AP with transmission rates larger than 0 bps. Moreover, b_j is the transmission rate of the jth terminal connected to the AP, and b_j changes according to the distance between the AP and the terminal. Note that the transmission rate that equals 0 bps is dropped from the denominator of Eq.(2.2). This study assumes that Eq.(2.2) indicates AP throughput. The throughput of the terminal connected to the AP Th_u is obtained by dividing by n_{cnt} (Eq.(2.3)) because all terminals connected to the same AP have the same Th_u values.

$$Th_u = \frac{Th}{n_{cnt}} \tag{2.3}$$

Chapter 3

An Autonomous Decentralized Clustering Based on Local Interaction

This chapter describes studies about the autonomous decentralized clustering based on local interaction [23].

3.1 Introduction

Large-scale disasters such as tsunamis and earthquakes can seriously damage or destroy network infrastructure. In the aftermath of such disasters, it is crucial to quickly gather information about the disaster and to promptly issue according evacuation orders. In order to realize these goals, failures in network functionality must be corrected as quickly as possible. Because confusion tends to abound immediately after a catastrophe, network protocols designed with the assumption of a normal environment may not satisfy operating requirements, and hence prompt network recovery may not be possible. This problem can be solved by creating an environment in which the remaining devices can operate effectively.

One solution is mobile ad hoc networks (MANETs) [49], where mobile terminals directly connect to one another to create a communication network without recourse to network infrastructure, such as base stations and/or APs of wireless LANs connected to wired backbone networks. One of the most important issues in MANETs is to reduce the power consumption of the network in order to extend its life span. The research has been conducted on methods to reduce the power consumption of networks [50–52]. Clustering mechanisms for MANETs have been proposed for power saving and load balancing [53,54]. They are important because they help reduce the power consumption of each node and extend the life of the entire network. These mechanisms use metrics such as the battery reserves [55] and the performance (e.g., processing speed, memory, and other parameters) [56] of each node in the network.

Various clustering methods have been studied [57–62]. However, all these method require non-local information. In other words, they are not strictly autonomous decentralized algorithms, and global information regarding the state of the network is needed to obtain a globally optimal solution for the cluster structure. It is practically difficult to acquire global network information because information exchange is structurally lim-

ited in MANETs. This emphasizes the importance of autonomous decentralized cluster configuration methods, whereby globally optimum structures can be developed from local information, and can be used to execute traffic control, path control, and network resource management.

Methods proposed in [63, 64] are based on local information, and include the well-known *bio-inspired method*, which uses a Turing pattern of reaction-diffusion equations. However, these clustering methods use seven parameters, and thus parameter setting is difficult for them. Moreover, clusters configured using the bio-inspired method cannot reflect the characteristics of the given network conditions (e.g., the distribution of the residual battery power of terminals, the position of power supplies, or the degree of mobile terminals).

In the past, [65] has proposed a framework for a novel autonomous decentralized mechanism based on local interaction. This framework is founded on the interplay between local interaction and the solution provided by a partial differential equation. As a specific example, [23] proposed the autonomous decentralized formation of structures with finite spatial size and showed the applicability of the method to autonomous clustering in MANETs. This clustering method, the *back-diffusion method*, can configure clusters using only local information about neighboring nodes. Moreover, it allows each node to act flexibly based only on the information available to it, i.e., its own situation. Consequently, the back-diffusion method can yield clustering structures that reflect the characteristics of the network condition. [66] shows that the back-diffusion method can configure clusters faster than an existing method [63] by a factor of 10 or more. This means that communication can be recovered more quickly through the back-diffusion method. Furthermore, the clusters yielded by the back-diffusion method have approximately double the lifetime of those generated by the bio-inspired method in the control packet transfer phase [27]. Note that [27] makes no mention of the effect of the routing algorithm on the data packet transfer phase.

However, the problem of [23] is that the number of clusters decreases with temporal evolution. The power saving and the load balancing by the hierarchical management of the network cannot be performed by this problem. This chapter proposes a method which maintains the number of clusters (guarantees stability) [24–26]. So, the aim is to maintain the hierarchical network configuration created by clusters. This study focuses on the hierarchical network configuration as a preliminary study which is necessary to realize the real communication considering data transfer by network protocols.

Moreover, the effect of clusters that reflect the network condition has not been evaluated. To show the effectiveness, this chapter configures clusters using the back-diffusion method [23] and the bio-inspired method [63]. Then, this chapter evaluates the effect which reflects the network condition for clusters from the point of view of both power consumption and data transfer efficiency [28]. In particular, this chapter shows the characteristics of power consumption using the metrics of both the first node die (FND) time [67] (FND time is the time period until the first failure of a node due to battery exhaustion) and the percentage of live nodes. Live nodes are those that have battery power remaining. Moreover, this chapter evaluate the amount of the received packets by the destination node of the network, which is configured by the back-diffusion method and the bio-inspired method, to determine data transfer efficiency. Further, this chapter shows the performance characteristics of each method in terms of the number of

nodes and node mobility [29]. A hierarchical temporally ordered routing algorithm (Hi-TORA) [68] is used in order to evaluate the data transfer efficiency of the cluster. Note, however, that the aim of this chapter is not to find the most suitable routing algorithm for the back-diffusion method.

This chapter consists of the following sections: Section 3.2 presents the framework of the autonomous decentralized structure formation technology and explain the bio-inspired method, which is an autonomous decentralized structure formation approach that uses Turing patterns. Furthermore, Sect. 3.3 proposes and evaluates a guarantee method of the stability for clusters configured by the back-diffusion method. Section 3.4 shows evaluations of the characteristics for the back-diffusion method about the power consumption and the data transfer efficiency. Finally, Sect. 3.5 provides the concluding remarks.

3.2 Clustering method based on autonomous decentralized structure formation

This section provides an overview of the autonomous decentralized structure formation that uses back-diffusion drift. Moreover, the bio-inspired method based on reaction-diffusion equations is also described in this section.

3.2.1 Overview of back-diffusion based autonomous decentralized structure formation technology

This section first introduces the autonomous decentralized structure formation technology (back-diffusion method) for an one-dimensional network model to provide an intuitive understanding of the behavior of the method. Let the density function (density distribution) of a certain *quantity* at time t and position x be $q(x,t)$. The initial value of $q(x,0)$ can be considered as the metric, e.g., the residual battery power of each node in a MANET. Local behavior corresponds to changing the value of $q(x,t)$ at each point, x, by controlling the information exchange between adjacent nodes. Note that $q(x,t)$ $(t > 0)$ is used for cluster configuration and is independent of residual battery power, whereas $q(x,0)$ reflects initial battery power. Therefore, changing the value of $q(x,t)$ at each point does not mean that each node changes its own battery power. In an autonomous decentralized structure formation, flow $J(x,t)$ (the operation rule that changes the value of $q(x,t)$) is expressed as

$$J(x,t) = -c\, f(x,t)\, q(x,t) - c\, \sigma^2 \frac{\partial}{\partial x} q(x,t), \tag{3.1}$$

where the first and second terms denote the drift and diffusion terms, respectively. The temporal evolution of distribution $q(x,t)$ that corresponds to this change is given by

$$\frac{\partial}{\partial t} q(x,t) = c \left(\frac{\partial}{\partial x} f(x,t) + \sigma^2 \frac{\partial^2}{\partial x^2} \right) q(x,t). \tag{3.2}$$

In the above equation, c (> 0) denotes the rate of temporal evolution of $q(x,t)$ and σ^2 denotes the variance of the normal distribution on which the function converges. In

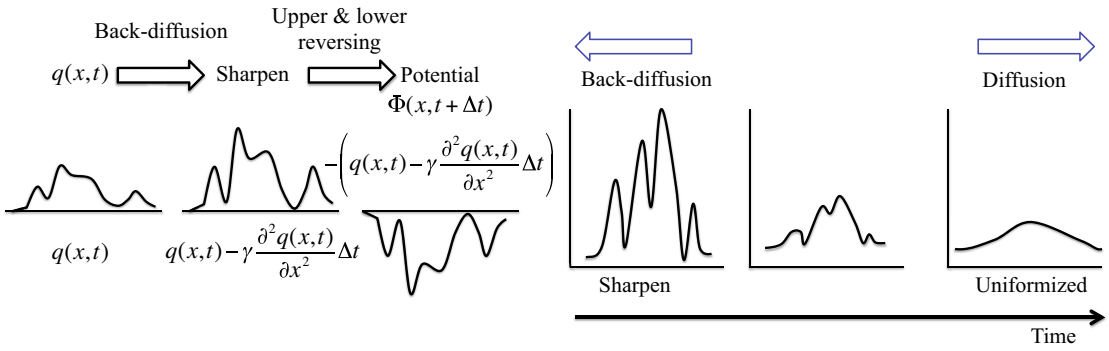

Figure 3.1: Determining $\Phi(\boldsymbol{x}, t)$ according to back-diffusion.

Figure 3.2: Diffusion and back-diffusion.

Eq.(3.1), moreover, $J(x,t)$ represents the extent of spatial movement of $q(x,t)$; note that the total amount of $q(x,t)$ does not change over time. Equation (3.2) is a second-order differential equation. Therefore, this operation rule can be determined through interaction with adjacent nodes.

The introduction of $f(x,t)$ eliminates the need to set a coordinate system in the network. As a more intuitive explanation, this section considers the potential function $\Phi(x,t)$ instead of $f(x,t)$ as Eq.(3.3):

$$f(x,t) = -\frac{\partial \Phi(x,t)}{\partial x}. \tag{3.3}$$

Choosing an appropriate $\Phi(x,t)$ yields autonomous decentralized control that does not depend on a coordinate system. Now, the calculation of the drift term from $q(x,t)$ at each point x is investigated. Since $\Phi(x,t)$ should result in the maintenance of the distribution within a finite spatial size, contrary to the effect of diffusion, $\Phi(x,t)$ is, after discrete time Δt, given by

$$\Phi(x, t+\Delta t) = -\left(q(x,t) - \gamma\frac{\partial^2 q(x,t)}{\partial x^2}\,\Delta t\right), \tag{3.4}$$

where $\gamma > 0$, and $\Phi(x,t)$ is periodically renewed at intervals of Δt. The above equation is obtained by the sign inversion of the space derivative term in the diffusion equation. Note that Eq.(3.4) uses periodic time with interval Δt instead of $\mathrm{d}t$. This is because the effect of the second term vanishes at the limit where $\mathrm{d}t$ approaches 0 [23].

The method of generating potential $\Phi(x, t+\Delta t)$ by using $q(x,t)$ is shown in Fig.3.1. The meaning of this figure is expressed as follows:

- This method lets the time progression of the diffusion phenomenon with diffusion coefficient γ be reversed (back-diffusion).
- This method then reverses the distribution (up and down) and regards the completed distribution as the potential.

Because of the effect of the drift term, including the potential, the peak of $q(x,t)$ is emphasized and the shape of the distribution is sharpened (Fig.3.2). The effect of

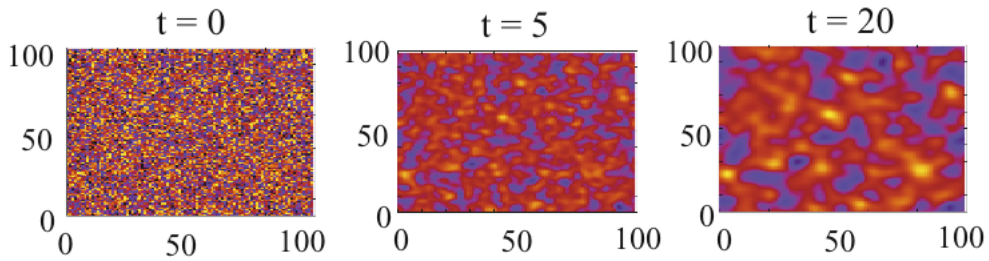

Figure 3.3: Cluster structure formation by the back-diffusion method (initial state, after 5, 20).

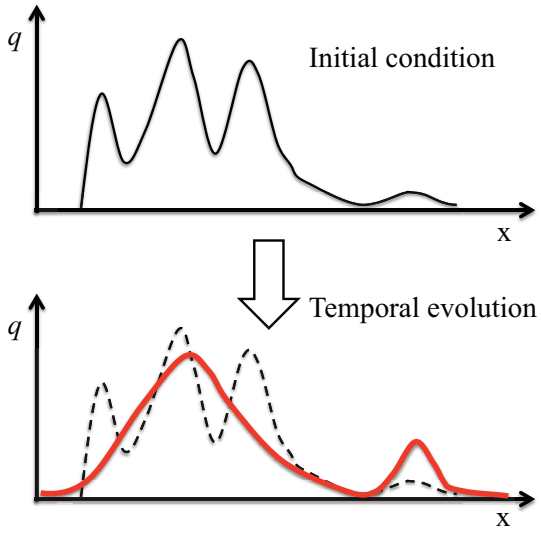

Figure 3.4: The effect of the back diffusion in one-dimension model.

the diffusion term, on the other hand, is to flatten the distribution. Figure 3.3 shows an example of the structure with a finite spatial size that can be formed by balancing one effect against the other. In Fig.3.3, the peak of $q(x,t)$ is the representative node of the cluster and the minimum value of the distribution is the boundary of the cluster.

Here, this section explains the characteristics of the proposed method using Fig.3.4. For example, the initial condition on a one-dimension model in which there are two or more peaks on the left, and there is one small-scale peak in the right. In areas that have multiple peaks, the peaks are integrated autonomously to form one cluster. On the other hand, when there is no peak in the surrounding, the peak is emphasized even if it is not a powerful peak. This effect derives from the back diffusion, and the proposal adopts back diffusion to form the cluster even for a remote weak peak.

Moreover, [23] has shown that the approach can be applied to an arbitrary network as well as a one-dimensional network because diffusion and back-diffusion can be defined based only on the states of the node and nodes adjacent to it. The author now concretely describes the local action rule in the network. First, the set of nodes that are adjacent to node i (the set of nodes that are linked to node i) is defined as N_i. The author also discretizes time and set the time interval of autonomous control as Δt. In the following, the action rule for spatial discretization that corresponds to nodes in the network, and time discretization that corresponds to control timing were described. The distribution

$q_i(t_k)$ at time t_k ($:= k \times \Delta t$) at node i changes (after Δt) as Eq.(3.5):

$$q_i(t_{k+1}) = q_i(t_k) - \Delta t \sum_{j \in N_i} \left(J^{\text{drift}}_{i,j}(t_k) + J^{\text{diff}}_{i,j}(t_k) \right), \tag{3.5}$$

where $J^{\text{drift}}_{i,j}(t)$ and $J^{\text{diff}}_{i,j}(t)$ are variations created by the drift effect and the diffusion effect within each unit time, respectively. $J^{\text{drift}}_{i,j}(t)$ and $J^{\text{diff}}_{i,j}(t)$ satisfy Eq.(3.6), Eq.(3.7), and Eq.(3.8):

$$J^{\text{drift}}_{i,j}(t_k) := \begin{cases} c\, f_{i,j}(t_k)\, q_i(t_k), & (f_{i,j}(t_k) > 0), \\ -c\, f_{j,i}(t_k)\, q_j(t_k), & (f_{j,i}(t_k) > 0), \end{cases} \tag{3.6}$$

$$f_{i,j}(t_k) := -(\Phi_j(t_k) - \Phi_i(t_k)), \tag{3.7}$$

$$J^{\text{diff}}_{i,j}(t_k) := -\sigma^2 \left(q_j(t_k) - q_i(t_k) \right). \tag{3.8}$$

Due to the drift effect, the distribution moves in direction $i \to j$ ($j \to i$) in the case of $f_{i,j}(t_k) > 0$ ($f_{i,j}(t_k) < 0$). Here, equation $f_{i,j}(t_k) = -f_{j,i}(t_k)$ holds. The variation is proportional to the product of the velocity of the drift $f_{i,j}(t_k)$ ($f_{j,i}(t_k)$) and $q_i(t_k)$ ($q_j(t_k)$) in node i (j). The above description is formalized by Eq.(3.6). The variation due to the diffusion effect is proportional to the gradient of the distribution in Eq.(3.8).

The author now explains how to determine the potential $\Phi_i(t_k)$ that is related to drift. The potential value $\Phi_i(t_{k+1})$ of node i at time t_{k+1} is decided by the value of the distribution $q_i(t_k)$ and the back-diffusion of $q_i(t_k)$ as Eq.(3.9):

$$\Phi_i(t_{k+1}) = -\left(q_i(t_k) - \gamma \Delta t \sum_{j \in N_i} \left(J^{\text{back}}_{i,j}(t_k) - J^{\text{back}}_{j,i}(t_k) \right) \right), \tag{3.9}$$

where $J^{\text{back}}_{i,j}(t_k)$ is generated by the back-diffusion of $q_i(t_k)$, and is the variation in a unit time period in the direction of node $i \to j$. The variation $J^{\text{back}}_{i,j}(t_k)$ is given by

$$J^{\text{back}}_{i,j}(t_k) = \begin{cases} q_j(t_k) - q_i(t_k), & (\Delta q^{\max}_i(t_k) = q_j(t_k) - q_i(t_k)), \\ 0, & (\text{otherwise}). \end{cases} \tag{3.10}$$

$$\Delta q^{\max}_i(t_k) := \max \left(\max_{j \in N_i} \left(q_j(t_k) - q_i(t_k) \right), 0 \right). \tag{3.11}$$

$\Delta q^{\max}_i(t_k)$ is the difference between the distribution value of node i and the distribution value of the adjacent node j in the direction of the steepest ascent from node i (Eq.(3.11)). In the above-mentioned action rule for discretization in the network (Eq.(3.10)), local interaction is guaranteed because the summations of nodes $j \in N_i$ in the above equations involve only the nodes adjacent to node i.

To achieve the above-mentioned control, it is necessary to exchange information about the values of the distribution $q_j(t_k)$ for the adjacent nodes at the interval of Δt. The complexity of this information exchange does not depend on network size because the communication range is only one hop. Therefore, it is scalable against the number of nodes.

Note that $c\sigma^2$ need to satisfy Eq. (3.12)

$$c\sigma^2 < \frac{1}{d_{max}} \tag{3.12}$$

where d_{max} means the maximum degree of nodes in the network. If $c\sigma^2$ do not meet Eq. (3.12), $q(.)$ of some nodes becomes negative value by the diffusion effect [69].

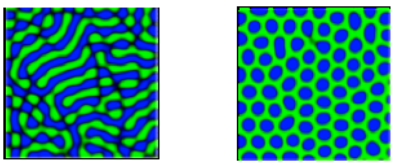

Figure 3.5: Examples of Turing pattern.

3.2.2 Bio-inspired method based on reaction-diffusion equations

The bio-inspired method [63] is an autonomous decentralized structure formation approach that uses Turing patterns. Invented by Alan Mathison Turing, a Turing pattern is a mathematical method used to describe pattern formation on the bodies of animals. A Turing pattern is formed through reaction-diffusion equations (Eq.(3.13) and Eq.(3.14)). Each node in the network contains two factors, activator A and inhibitor H, and these values change over time according to the following differential equations:

$$\frac{\partial A}{\partial t} = \frac{CA^2}{h} - \iota A + \rho_0 + D_A \nabla^2 A, \tag{3.13}$$

$$\frac{\partial H}{\partial t} = CA^2 - \upsilon H + \rho_1 + D_H \nabla^2 H, \tag{3.14}$$

where C, ρ_0, and ρ_1 are parameters that enhance the effects of the activator and the inhibitor, and ι and υ are parameters that reduce the effects of the activator and the inhibitor, respectively. Moreover, D_A and D_H are parameters that describe the rate of diffusion of the activator and the inhibitor, respectively. From Eq.(3.13) and Eq.(3.14), the spatial pattern appears gradually over time (Fig.3.5), and the peak of the created pattern denotes the representative node of the cluster whereas the extent of the pattern denotes the extent of the cluster. [70] presents research on parameter design for systems based on reaction-diffusion equations. It is, in general, significantly more difficult to design parameters for the bio-inspired method than the back-diffusion method because the former has many more parameters.

3.3 Guarantee method of the stability for clusters

This section discusses the issues raised by applying the back-diffusion method to MANETs. Also this section proposes a guarantee method of the stability for clusters.

3.3.1 Problems with applying the back-diffusion method to clustering

The back-diffusion method described in Sect. 3.2.1 forms some clusters by balancing the diffusion term (diffusion effect of the distribution) against the drift term (emphasizing effect of the peak of the distribution). If the diffusion effect is greater than the drift effect, the distribution of the formed structure is smoothed over time and the range of the distribution decays (Fig.3.6). Here, the range $R(t)$ denotes the difference in the

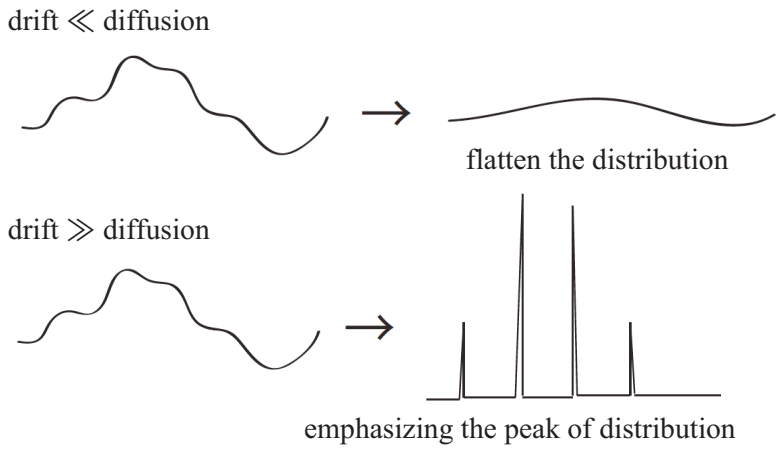

Figure 3.6: Issues in parameter setting.

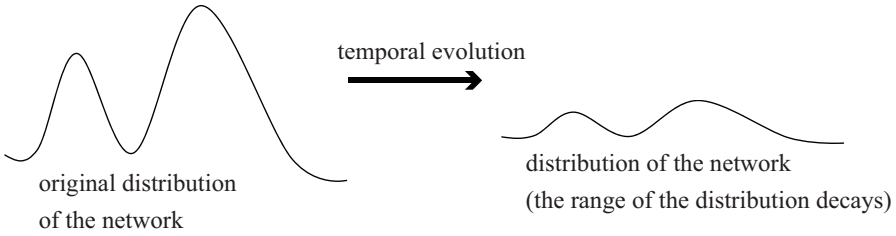

Figure 3.7: Decay of the range of the distribution.

maximum value and the minimum value of the distribution for each time as Eq.(3.15):

$$R(t) = \max_x(q(x,t)) - \min_x(q(x,t)). \tag{3.15}$$

On the other hand, if the drift effect is stronger than the diffusion effect, the peak of the structure is emphasized, and the unevenness of initial distribution becomes excessive. Therefore, it is necessary to balance of the strengths of the diffusion and drift terms, but designing the optimum parameters is very difficult. As mentioned earlier, however, if the diffusion effect is stronger than the drift effect, the range of the distribution decays over time (Fig.3.7). Note that this chapter evaluates the characteristics of the decay of the range in Sect. 3.3.3.

The decay characteristics cause two problems. First, the representative nodes and the boundaries of clusters cannot be determined when the range of the distribution becomes zero (complete harmonization) by the diffusion effect. In the mathematical expression, the complete harmonization practically requires infinite time; however, the range of the distribution becomes zero in finite time owing to the limits of the calculation accuracy, which means that the proposed method cannot configure the clusters. That is, the power saving and the load balancing by the hierarchical management of the network cannot be performed by this problem. Second, it should consider a situation where the distribution of one network is compared to the distribution of another network. This problem may occur in an MANET when new terminals connect or other terminals move into the area under consideration. For example, *network A* has a small range of the distribution by the diffusion effect, whereas *network B* has a large range of the distribution. Note that this situation is that the initial range of the distribution of network A is the same as

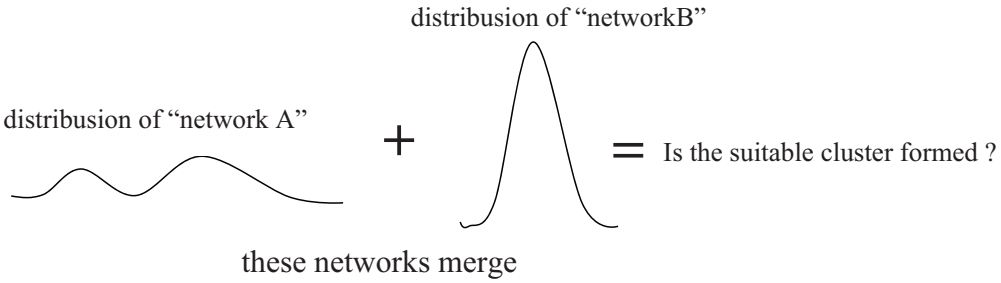

Figure 3.8: Problems with dynamic network topologies.

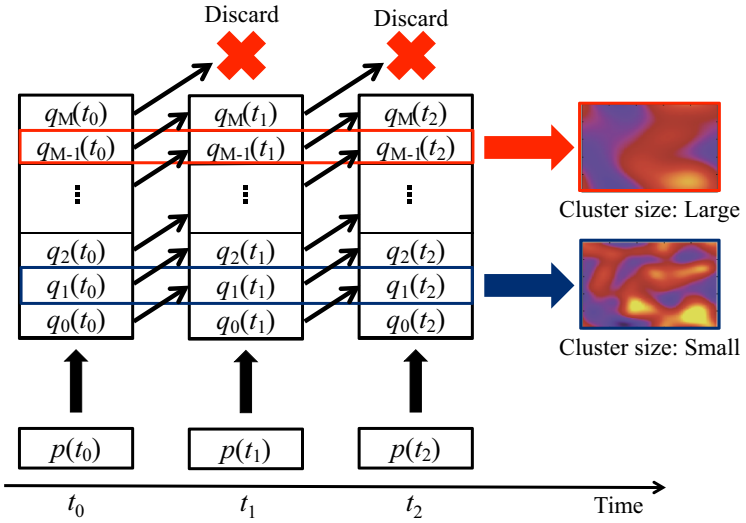

Figure 3.9: Temporal evolution of $\boldsymbol{Q}(t_k)$ for each node.

that of network B, but the range of the distribution of network A decays because of a lapse of time from the cluster formation and is smaller than that of network B. When these networks merge, network A will not be able to preserve its form, because their networks have the different measures for the ranges of the distributions (Fig.3.8). In other words, a cluster which has large range of the distribution has a huge effect on the cluster compared to a cluster which has small range of the distribution.

The details of the problems of merging networks have been discussed in [71]. To solve these problems, it is necessary to restrain the decay of the range caused by the time progression.

3.3.2 Method guaranteeing stability of the cluster structure for a vector process

This section discusses the requirement that the range of the distribution should satisfy in order to restrain the decay of it, and then proposes a method which meets the requirement.

As mentioned in Sect. 3.3.1, it is necessary to restrain the decay of the range caused by the time progression in order to maintain the cluster structure. This is the requirement for the range of the distribution. To show the requirement for the range of the distribution, the asymptotic stability for the range of the distribution is introduced as

follows:

$$\lim_{t\to\infty} R(t) = \alpha, \tag{3.16}$$

where $R(t)$ is defined in Eq.(3.15) and α is a positive constant. This equation means that the range of the distribution converges on a positive constant value over infinite time. Unless it is satisfied, on the other hand, $R(t)$ approaches zero with time.

Next, this section explains the method which restrains the decay of the range and guarantees the asymptotic stability of the range. To guarantee the stable range of the distribution, each node has its own vector with M components to keep the history information of the distribution. Each node has its own value, $p(t_k)$, that denotes the distribution (for example, battery residual power) at time t_k ($k = 0, 1, \cdots$). $\boldsymbol{Q}(t_k)$ shows the distribution used for configuring the cluster structure at t_k; it is given as Eq.(3.17) and Eq.(3.18):

$$\boldsymbol{Q}(t_k) = (q_0(t_k), q_1(t_k), \cdots, q_M(t_k)), \tag{3.17}$$

$$q_0(t_k) = p(t_k). \tag{3.18}$$

The vector's 0th component is set to $p(t_k)$. In each step, the diffusion and drift (back diffusion) operations are performed for every component of $\boldsymbol{Q}(t_k)$. In other words, each component of the vector is calculated by the diffusion and the back diffusion. When the operations are completed for every component of $\boldsymbol{Q}(t_k)$, the nth ($n = 0, 1, \cdots, M$) component of the vector is shifted to the $(n + 1)$th component in the following step (Fig.3.9). Note that $(M + 1)$th component is discarded. If $p(t_k)$ does not change over time, $\boldsymbol{Q}(t_k)$ will not change either. A cluster is constructed by using $q_n(t_k)$ (a specified n within $n = 0, 1, \cdots, M$) which each node has, and larger clusters can be configured by specifying the larger n.

In general clustering, it is demanded that the number of cluster heads (the representative nodes) in the network is small (in other words, the average cluster size is large) because nodes chosen as cluster heads have a heavy load due to the management of the control information for both the inter- and the intra-cluster. If the cluster size is large (the number of clusters is small), on the other hand, significant traffic occurring in bursts within the cluster causes the overload of functions for the cluster head because each cluster head attends to many member nodes in the cluster. Here, the main purpose of this section is not to argue about the optimal cluster size but is to maintain the hierarchical network structure created by clusters. Note that the proposed method can adjust the mean number of clusters to some extent according to the network situation by only using local information exchange. The vector process of the proposed method can be simply expressed as follows: Each node keeps M distribution values for each time by using the vector structure $q_n(t_k)$. The values have a hardly diffused distribution when n is small and an almost completely diffused distribution when n is large.

Here, $R_n(t_k)$ ($n = 0, 1, \cdots, M$) is the range of the distribution for the nth component at time t_k as follows:

$$R_n(t) = \max_x(q_n(x, t_k)) - \min_x(q_n(x, t_k)). \tag{3.19}$$

In the proposed method, if the distribution $p(t_k)$ (e.g. the battery capacity) does not change with time, the vector structure $\boldsymbol{Q}(t_k)$ that each node keeps does not change as

well. That is to say, the asymptotic stability of the range in Eq.(3.16) is expressed as follows:

$$R_n(t) = \alpha \quad (t \geq t_n), \tag{3.20}$$

where $R_n(t_k)$ can be calculated by Eq.(3.19), and t_n is the period of time used to form the n components of the vector structure from nothing. Equation (3.20) shows the requirement to stabilize the range of the distribution not *asymptotically* but *completely*, if nodes are immovable and the initial distribution for each node does not change. When the distribution $p(t_k)$ becomes smaller with time, the decay of the range of the distribution cannot be stopped, but the proposed method can restrain the range decay phenomenon caused by diffusion effects. The issue for this method is that a certain time t_n is required when creating a vector structure from nothing. The range of the distribution decays by the diffusion effect until the vector structure is formed. This issue will be addressed in future work. In addition, this proposed method can be applied to other clustering methods [72].

3.3.3 Evaluation of guarantee method

This section investigates the decay characteristics of the range of the distribution shown in Sect.3.3.1, and the stability of the proposed method is evaluated using a two-dimensional lattice model and an MANET model in this section.

Decay characteristics of the range

First, this section examines the decay characteristics of the range drift effect and diffusion effect. As preliminary research, this evaluation assumes a two-dimensional lattice model with 100×100 nodes to make the space structure easy to display. The network model has a torus topology to exclude the influence of the boundary (Fig.3.10). Each node has a degree of four ($d_{max} = 4$) because each node has four neighbors, and sends a control packet to their neighbors at every step ($\Delta t = 1$ step), which is the normalized time. In this evaluation, the node sends control parameters for adjacent nodes at the same time. Moreover, each node does not move in this evaluation. This evaluation assumes that initial state of the distribution is the state where clusters have been already formed to some extent (Fig.3.11). Because the purpose of the study is to investigate the range characteristics of the distribution due to the diffusion effect and the drift effect, intense unevenness of the initial state of the distribution quantity is not needed. The horizontal and vertical axes in Fig.3.11 represent the coordinates, and the color of each node indicates the distribution height.

Figure 3.12 shows the temporal variation of the range of the distribution due to the diffusion effect (without the drift effect). This figure is a semilog plot, and the unit of time is the number of steps. Each node computes its own distribution at every step. The clustering parameters are listed in Table 3.1. It is seen that exponential decay occurs regardless of the value of σ^2. The relationship of σ^2 and the decay rate is shown in Fig.3.13; σ^2 is proportional to the decay rate of the diffusion effect.

Figure 3.14 is a representation of the temporal variation of the range of the distribution due to the diffusion and drift effects. The parameters used in the simulation are

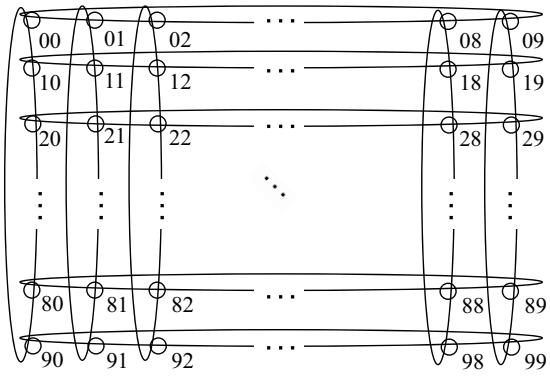

Figure 3.10: Torus topology.

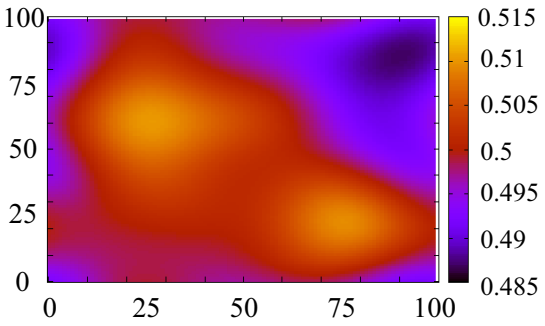

Figure 3.11: Initial conditions (1).

Table 3.1: Experimental parameters (diffusion only).

c	σ^2	γ
0.01	varied	0.1

$c\sigma^2 = 0.01$ and $\gamma = 0.1$; c is varied. This figure is a semilog plot, and the unit of time is the number of steps. From Fig.3.14, exponential decay occurs regardless of the value of c. Figure 3.15 shows the relation of the decay rate and c. From these results, c is proportional to the decay rate for the diffusion and drift effects.

As mentioned above, the range of the distribution exponentially decays with time and will become zero within finite time, that is to say that it does not satisfy the asymptotic stability shown in Eq.(3.16).

Next, this section evaluates the characteristics of the decay for the proposed method using the vector process in Sect. 3.3.2 and the existing method. Two situations were assumed as follows:

- the initial distribution, $p(t_k)$, (ex. residual battery power) does not change over time, and all nodes are immovable
- the initial distribution, $p(t_k)$, decreases gradually by power consumption, and all nodes can move

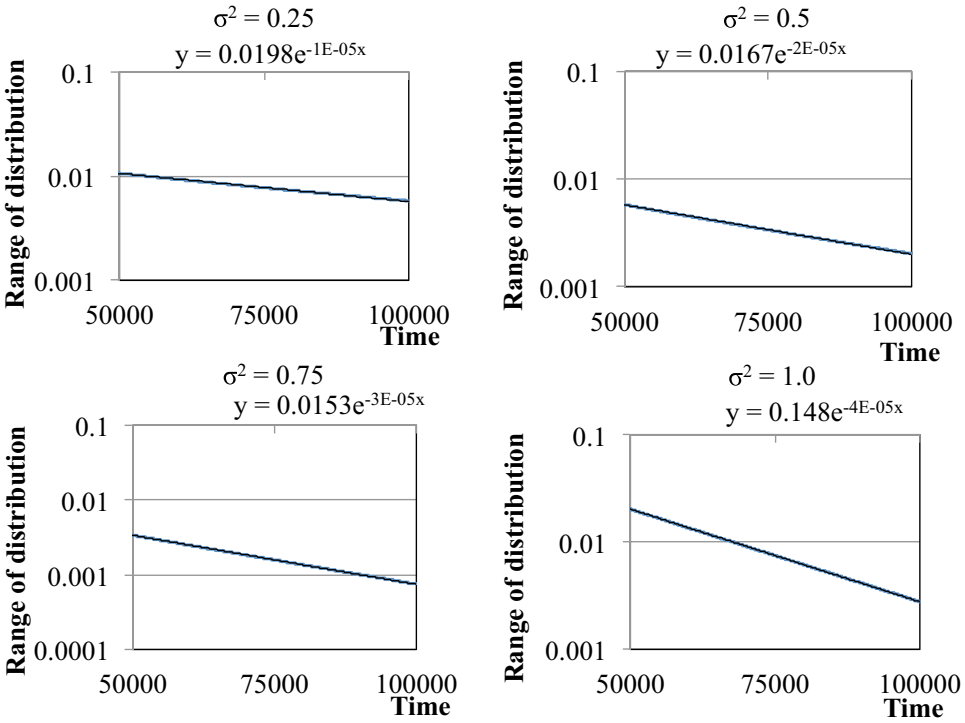

Figure 3.12: Temporal variation of the distribution range due to diffusion.

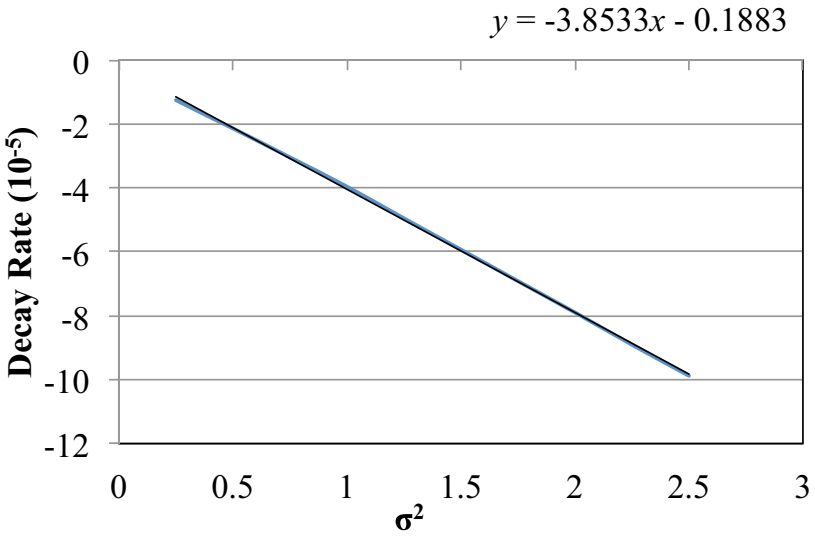

Figure 3.13: Damping characteristics in the distribution range due to diffusion.

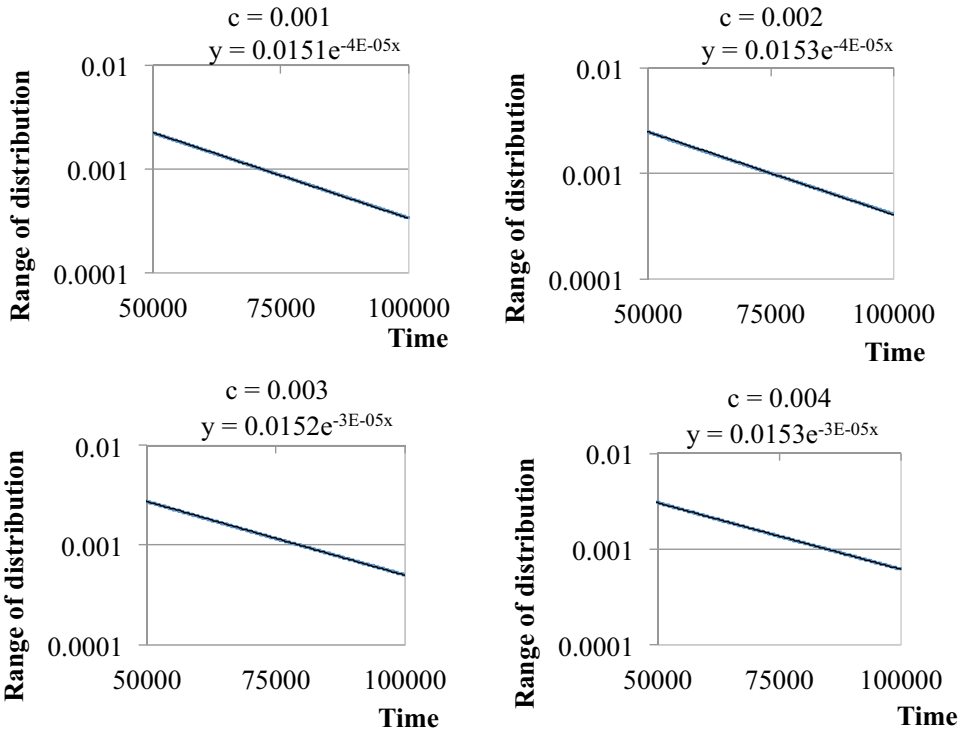

Figure 3.14: Temporal variation of the distribution range due to diffusion and drift.

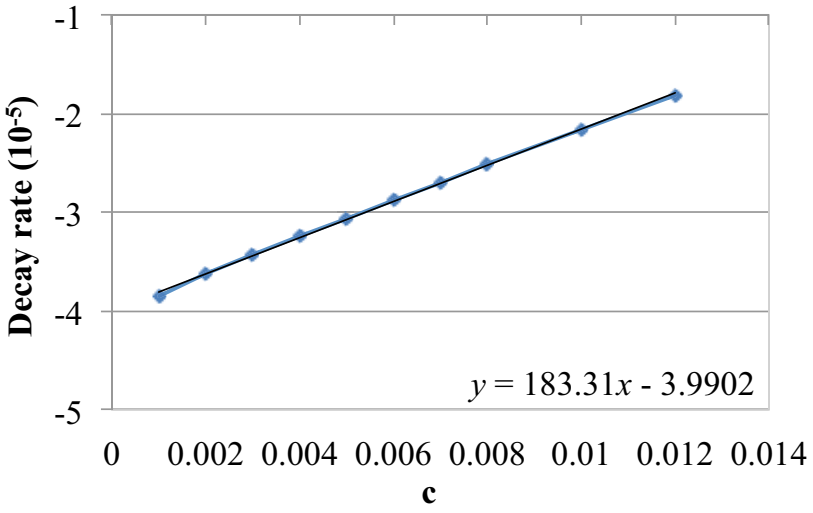

Figure 3.15: Relation of the decay rate and c in the distribution range due to diffusion and drift.

Table 3.2: Experimental parameters (the two-dimensional network $\boldsymbol{Q}$ does not change over time).

c	σ^2	γ
0.001	200.0	0.0001

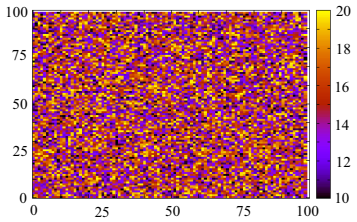

Figure 3.16: Initial conditions (2).

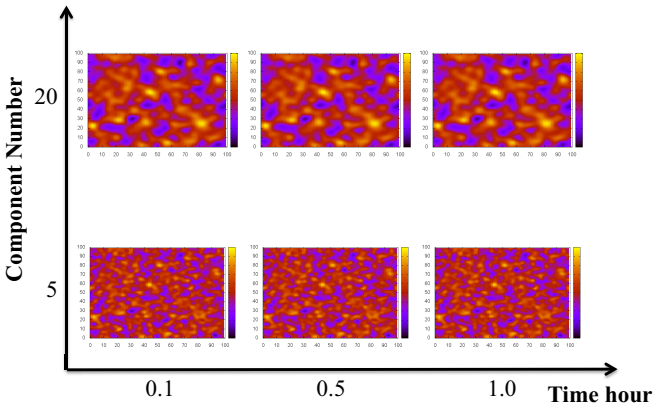

Figure 3.17: Cluster structures for the 5th and 20th components of $\boldsymbol{Q}(t_k)$.

Evaluation of stability (in two-dimensional lattice model)

This section assume a two-dimensional lattice model with 100×100 nodes in a torus topology; nodes do not move (fixed nodes). The ith node's initial distribution (the initial battery capacity), $p_i(0)$, is set to a random number uniformly distributed in $[10, 20]$ (Fig.3.16). In this experiment, $p_i(t_k)$ does not change over time. Furthermore, nodes in the network do not move in this simulation. The parameters used are summarized in Table 3.2, and the number of components of the vector for the proposed clustering model is 21 ($n = 0, 1, \cdots, 20$). These parameters satisfy the conditions of Eq.(3.12). For these parameters, the range of the distribution is due to the diffusion effect being greater than the drift effect [23]. Each node sends control packets every 1 sec ($\Delta t = 1$ sec) [73] and deals with the diffusion and drift processing on the basis of the information in the received packets. In the evaluation, the node sends control parameters for its adjacent nodes at the same time. Moreover, the simulation time is 1.0 hour.

Figure 3.17 shows the cluster structures for the 5th and 20th components of the vector at time t_k ($t_k = 0.1, 0.5, 1.0$ hour). From Fig.3.17, the cluster of the 5th component has a finer structure than that of the 20th component. This is because the latter is strongly influenced by the diffusion effect. In other words, if the vector component's number to a large value is set, larger clusters can be configured.

Figure 3.18 shows the temporal variation in the distribution range for the 5th and 20th components of $\boldsymbol{Q}(t_k)$. This figure includes results for the existing method [23] for comparison with the proposal. From Fig.3.18, the range of the distribution for the existing method always decays, which means that the existing method cannot guarantee the stability for the range of the distribution shown in Eq.(3.16).

For the proposed method, on the other hand, the range of the distribution is completely stable (guarantees the stability in Eq.(3.20)) after time t_n, which is the period of

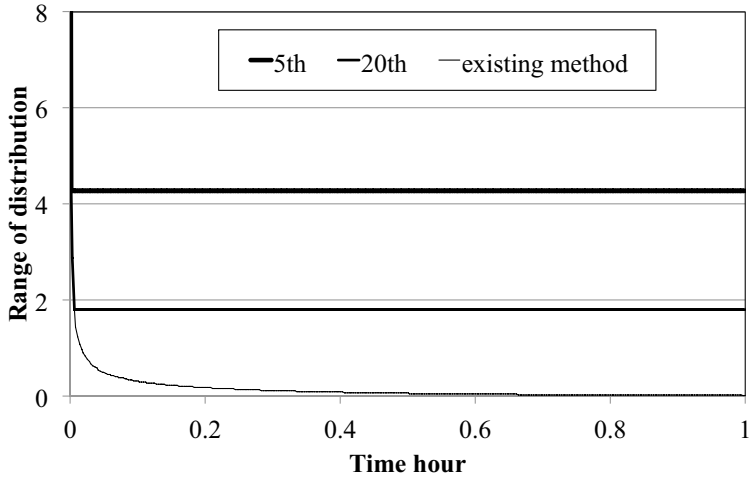

Figure 3.18: Temporal variation in the distribution range for the 5th and 20th components of $\boldsymbol{Q}(t_k)$.

Table 3.3: The converged value of the range α.

5th	20th
4.269	1.804

time needed to form the n components of the vector structure from nothing, because the initial value of the distribution of each node does not change over time. In the case with the 5th and 20th components, $t_n = 5 \times 1$ sec $= 5$ sec and $t_n = 20 \times 1$ sec $= 20$ sec, respectively.

Moreover, Table 3.3 shows the converged value of the range of the distribution in each component of the vector. This result shows that the converged value of the 5th component is greater than that of the 20th component, because the latter is strongly influenced by the diffusion effect.

Evaluation of stability (in MANET)

This section evaluates the decay characteristics of the proposed method in a network model supposing an MANET. The network model is the unit disk graph (UDG) with dimensions of $1,500$ m $\times$ $1,500$ m and a torus topology (Fig.3.19). UDG is a type of intersection graph based on circles of the same size. UDG is suitable as a model of an ad hoc network because it can describe various radio transmission ranges between nodes, but it cannot reflect more realistic wireless network characteristics such as packet collisions. This issue will be addressed in future work.

The simulation conditions are as follows. 100 nodes are randomly placed in the area. The initial distribution $p_i(0)$ for node i is a uniform random number in the range of [10, 20] (Fig.3.20); the radio transmission range for each node is 125 m. Regarding mobility, all nodes move every 100 sec, 10 sec, or 1 sec in consideration of the convergence time of cluster formation. The range to which each node moves at the above intervals yields an average movement distance of 1.3 m (uniform random number [0, 2.6]); the direction is based on the random direction model [74]. The parameters of the proposed model are

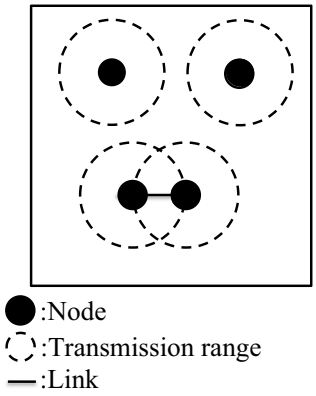

Figure 3.19: Unit disk graph network.

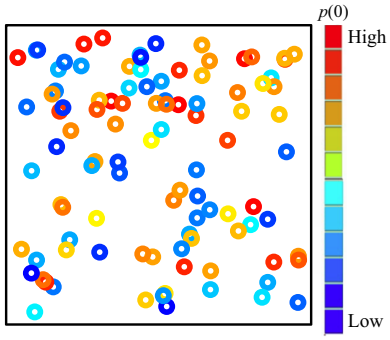

Figure 3.20: Initial conditions (3).

Table 3.4: Experimental parameters (MANET $\boldsymbol{Q}$ changes over time).

c	σ^2	γ
0.001	30.0	0.0001

listed in Table 3.4. Note that these parameters meet the conditions of Eq.(3.12). This section assumes that the initial distribution of each node, is identical to the random initial battery capacity, and the battery capacity of each node decreases by transmitting and processing control packets to and from neighbor nodes. Each node sends control packets every 1 sec (Δt = 1 sec) and deals with the diffusion and drift processing on the basis of the information in the received packets. Note that the node sends control packets for adjacent nodes simultaneously. Each node consumes the battery reserves at 1 μ J/bit for the transmission and reception of packets, and that of each representative node is 0.1 μ J/s for processing, which is self-performed [75]. In addition, the distribution $p_i(t_k)$ of node i is the residual battery capacity at t_k. This evaluation assumes that nodes whose residual battery capacities become zero become unavailable and secede from the network. This evaluation pays attention to the decay characteristics of the range of the cluster configured by the 5th and 20th components. Note that in the case with the 5th and 20th components, $t_n = 5 \times 1$ sec = 5 sec and $t_n = 20 \times 1$ sec = 20 sec, respectively.

Figures 3.21, 3.22, and 3.23 show temporal variation in the distribution range for the 5th and 20th components for each mobility frequency. In these figures, the horizontal axis and vertical axis represent time and the range of the distribution, respectively. These results show that the range of the distribution for the existing method decreases sharply regardless of the node mobility frequency. The range for the existing method approaches zero very fast, and the existing method cannot guarantee the stability in Eq.(3.16). On the other hand, the characteristics of the range for the proposed method maintain nearly a fixed value after time t_n (t_n = 5 or 20 sec) for all patterns of the node mobility frequency. The proposed method does not satisfy Eq.(3.20), but it can maintain the range of the distribution at a positive value for a long time. Table 3.5 summarizes the fluctuation b of the range for the mobility frequency and the component number. The fluctuation b is the maximum deviation between the range at time t_n and the range at time t ($> t_n$). From this result, the value of b becomes large as the node mobility frequency grows, and the difference between the component numbers does not influence

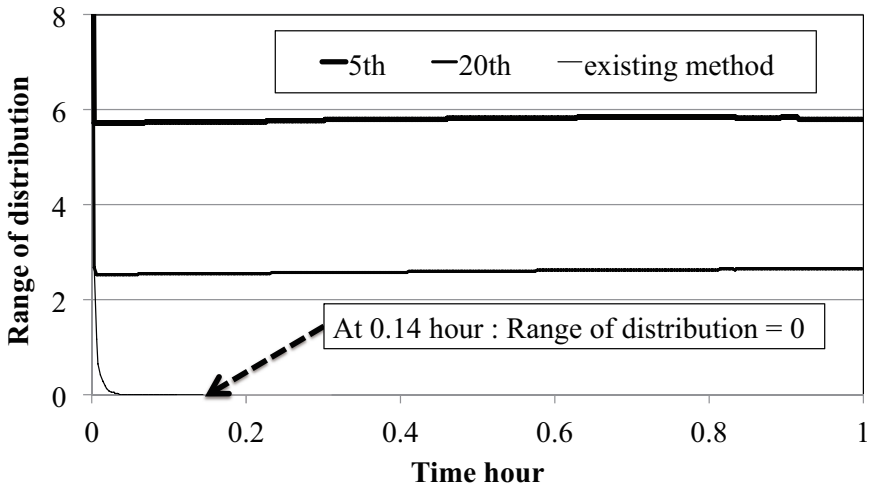

Figure 3.21: Temporal variation in the range of the distribution for the 5th and 20th components of $\boldsymbol{Q}(t_k)$ (Nodes move every 100 sec. Node mobility frequency is low.).

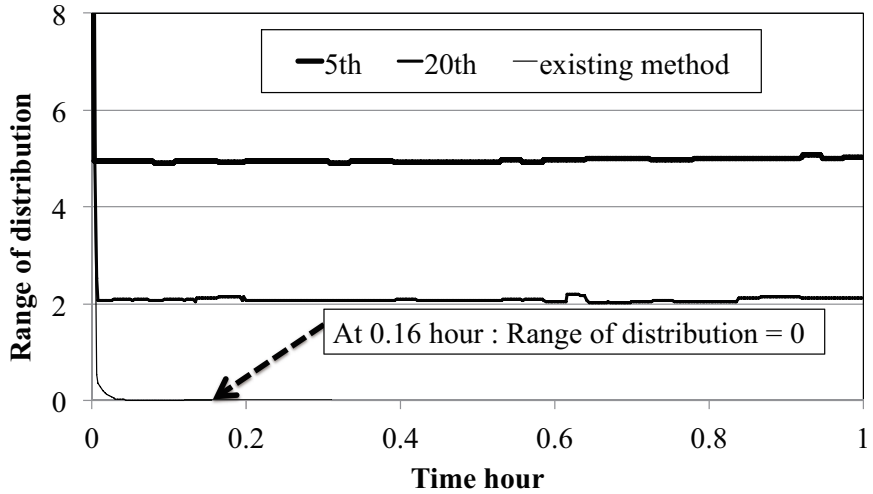

Figure 3.22: Temporal variation in the range of the distribution for the 5th and 20th components of $\boldsymbol{Q}(t_k)$ (Nodes move every 10 sec. Node mobility frequency is moderate.).

the value of b. This is because a large node mobility frequency leads to drastic changes of the network topology before the formation of the clusters converges.

Next, Fig.3.24, Fig.3.25, and Fig.3.26 show the time average of the number of clusters from $t = 20$ sec to $t = 3,600$ sec for the 5th and 20th components at each mobility frequency. The horizontal axis represents the vector component, and the vertical axis represents the number of clusters. The results show that the time average of the number of clusters yielded by the 20th component is smaller than that of the clusters formed by the 5th component. This indicates that the size of the configured cluster increases with the component number n. Thus, by changing the component number of the vector, the proposed clustering method cannot set strictly the number of clusters, but can decide the number of clusters to some (large or small) extent.

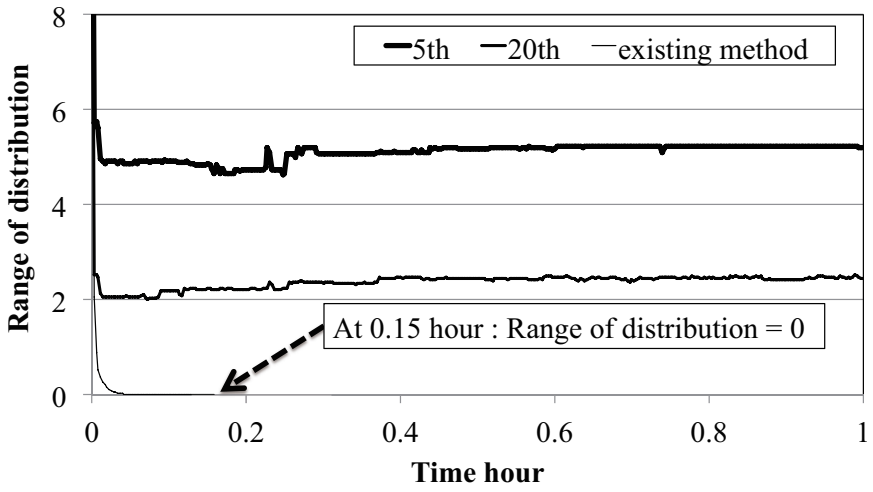

Figure 3.23: Temporal variation in the range of the distribution for the 5th and 20th components of $\boldsymbol{Q}(t_k)$ (Nodes move every 1 sec. Node mobility frequency is high.).

Table 3.5: The range of fluctuation b.

mobility frequency (Nodes move every f sec)	component number n	fluctuation b
small (f =100)	5	0.132
	20	0.124
moderate (f =10)	5	0.135
	20	0.128
large (f =1)	5	1.094
	20	0.531

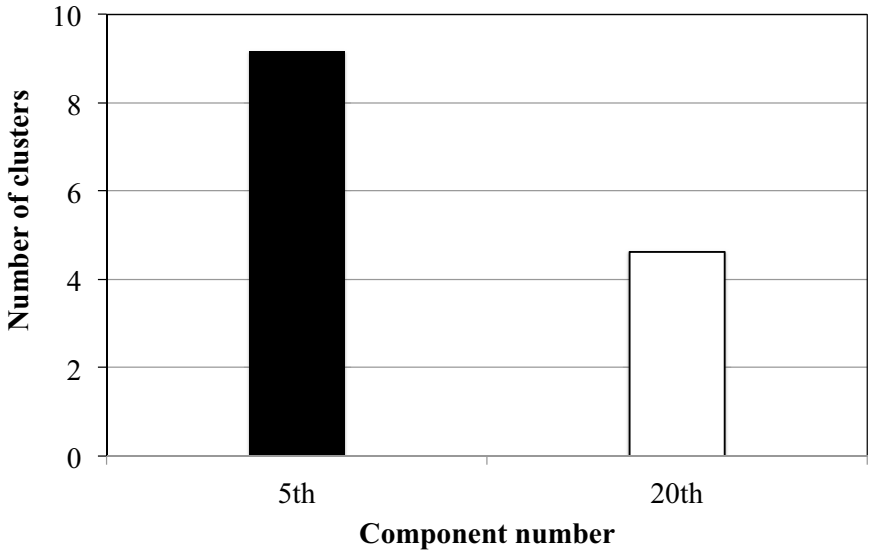

Figure 3.24: Time average of the number of clusters for the 5th and 20th components of $\boldsymbol{Q}(t_k)$ (Nodes move every 100 sec. Node mobility frequency is low.).

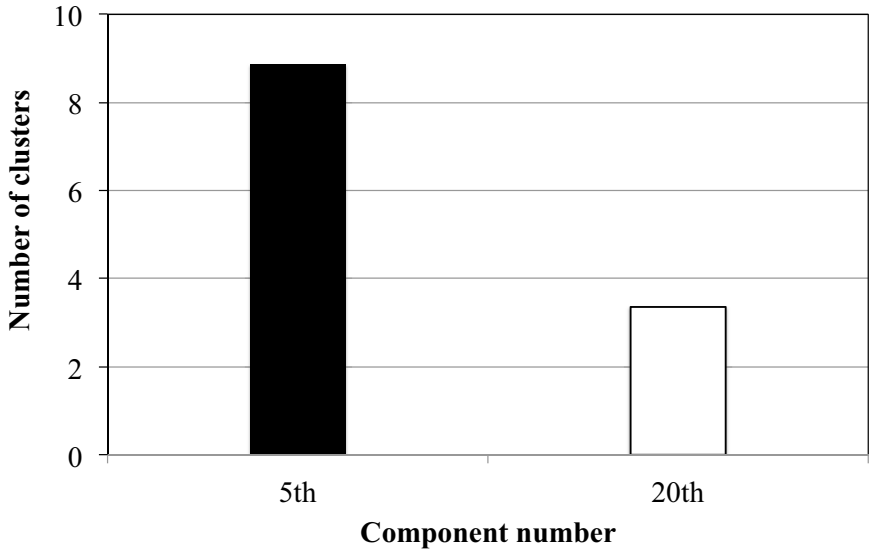

Figure 3.25: Time average of the number of clusters for the 5th and 20th components of $\boldsymbol{Q}(t_k)$ (Nodes move every 10 sec. Node mobility frequency is moderate.).

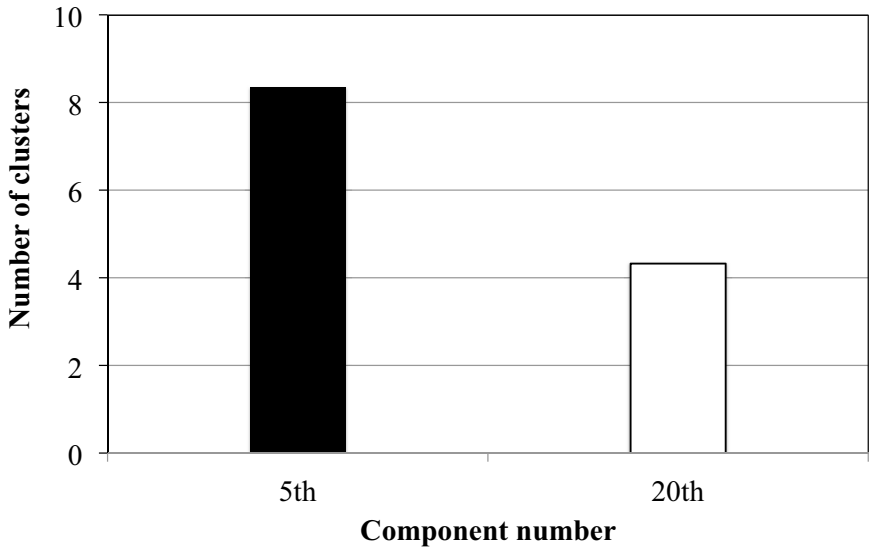

Figure 3.26: Time average of the number of clusters for the 5th and 20th components of $\boldsymbol{Q}(t_k)$ (Nodes move every 1 sec. Node mobility frequency is high.).

3.4 Evaluation of the effect which reflects the network condition for clusters

This section clarifies the effect which reflects the network condition for clusters from the point of view of both power consumption and data transfer efficiency while showing the results of a comparative evaluation of the temporal evolution of the live node percentage, the FND time, and the amount of data received by the destination node.

These evaluations do not take into account the physical layer and the MAC layer. This is because the aim of these evaluations are to evaluate the effect which reflects the network condition for clusters. In other words, this section evaluates the effect of the mismatch between the network condition and the configured clusters. Therefore, these evaluations focus on the importance of the clustering that reflects network conditions rather than evaluations of accurate power consumption. Power consumption and data transfer efficiency are merely metrics for the evaluation of the effect which reflects the network condition for clusters. Future research intends to evaluate the back-diffusion method by considering the effects of real environments, such as protocols and real battery models, using vector process [24–26].

3.4.1 Hierarchical routing Hi-TORA

This section describes *Hi-TORA* [68], a hierarchical routing algorithm which is applied to MANETs in this section.

Overview of Hi-TORA

Hi-TORA is a hierarchical routing (cluster-based routing) scheme used in MANETs. Hi-TORA has two phases according to the domain in which the routing algorithm operates: the intra-cluster (within a cluster) and the inter-cluster (among clusters) phases. The traditional link-state-type routes (shortest path routes) are provided for intra-cluster routing. For inter-cluster routing, on the other hand, Hi-TORA applies a TORA (Temporally Ordered Routing Algorithm) [76]. It regards one cluster as a virtual node in this case. In this way, Hi-TORA calculates the routing path from the source node to the destination node based on the two phases, when the destination node belongs to a different cluster from the source node. Next section briefly explains the routing algorithm for each phase.

Routing for the intra-cluster phase

For the intra-cluster phase, Hi-TORA executes the link-state routing algorithm, which finds the shortest path between the source node and the destination node using Dijkstra's algorithm. When the source node and the destination node are in the same cluster, the source node sends the data to the destination node through the shortest path. Otherwise, the source node sends the data to the boundary node adjoining the neighboring cluster on the path to the destination node. If two or more boundary nodes exist, the source node chooses as the boundary node the one that has the lower numerical node ID.

Table 3.6: Experimental environments (power consumption).

Network	Unit Disk Graph (UDG) of $1,000$ m $\times$ $1,000$ m
Number of nodes	101 (One of which is sink node)
Transmission range of node	125 m
Initial battery power of node	uniform random numbers in the range $[5, 15]$ $\times$1 J
Battery consumption [75]	1 μ J/bit (transmission) 0.1 μ J/s (processing of representative node)
Simulation time	$20,000$ sec
Number of Simulations	30

Routing for the inter-cluster phase

Hi-TORA adopts TORA to execute on-demand path calculations for the routing algorithm among the clusters because TORA is highly adaptable to node mobility. TORA establishes the DAG (directed acyclic graph) in which the destination node is regarded as the root. TORA then determines the logical direction of the links to the destination node by using the DAG, where the calculation of the direction of each link uses a metric called *height*. TORA controls the entire network to maintain multiple paths between the source and destination nodes. Thus, the overhead of the control packets for TORA inevitably increases with the number of nodes. The overhead can be reduced by assuming that each cluster is a virtual node, so that *height* can be set not to each link but to each cluster.

When a source node wants to communicate with a destination node, the source node sends a request to send (RTS) packet to the destination node. The *height* is then set for all clusters that receive the packet. The destination cluster's *height* is set to 0. The closer a cluster is to the source node, the larger the value of *height* set for it. Thus, the *height* of the source cluster, to which the source node belongs, is the highest value in the network, and the *height* of the destination cluster, to which the destination node belongs, is the lowest value. The data packets generated by the source node are forwarded through the clusters with lower *height*.

Note that the clusters on which Hi-TORA in [68] operates are configured by the clustering method in [77]. The evaluations of this section compare the back-diffusion method and the bio-inspired method as clustering methods.

3.4.2 Characteristics of power consumption and data transfer efficiency

This section examines the power consumption characteristics of data transfer for each method in order to clarify the importance of clustering that reflects network conditions. The network is an UDG of $1,000$ m $\times$ $1,000$ m and is constructed by 101 nodes. The network model has a torus topology to exclude the influence of the boundary. In other words, each node emerges on the other side when it crosses the boundary. Note that this evaluation assumes mobile nodes in MANETs. Node movement is set by a random direction model every second, and the average velocity of each node is 1.3 m/s. This

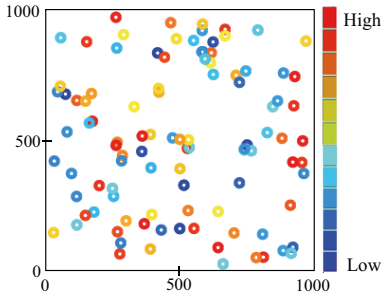

Figure 3.27: The distribution of initial battery power.

Table 3.7: Parameters of the back-diffusion method.

c	0.05
σ^2	0.5
γ	0.15

Table 3.8: Parameters of the bio-inspired method.

C	0.001
ι	0.05
υ	0.1
ρ_0	0.04
ρ_1	0.02
D_A	0.00122273
D_H	0.00180619

model is used for the simulating the movement of users in a mobile wireless networks.

One of the nodes is taken to be a sink node (destination node) and is set at the center of the network. The position of the sink node is (500 m, 500 m). Note that the sink node is fixed. It assumes that the sink node is a server or a base station. The established servers and base stations can secure battery supply. Therefore, the sink node does not consume its own battery. If the sink node consumes battery, it may become immediately unusable by the mobility pattern of each node. This is because the number of nodes adjacent to the sink node may suddenly increase. As a result, maximum data transfer efficiency cannot be measured, and the analysis of results becomes difficult.

Figure 3.27 shows an example of the distribution for initial battery power of each node. In Fig.3.27, the color represents the battery power of each node. This evaluation assumes that the initial distribution of each node is identical to the random initial battery power. Other conditions are shown in Table 3.6. Note that this evaluation assumes that the user carries its terminal, so that node movement does not increase battery consumption, and the battery consumption for each node occurs by packet transfer and the constant processing of each representative node. Therefore, the battery model of this evaluation does not capture its nonlinear characteristics. Furthermore, this study assumes a simplified power consumption model. Specifically, the condition that the same amount of power is consumed for transmitting packets and for receiving them is assumed. Naturally, considering a more realistic power consumption model is a very important issue. However, this is a basic study about whether the effect of the clustering reflects the network condition or not, and a future work will evaluate the characteristics of a network given a realistic power consumption model. Note that clusters are formed from $t = 0$ sec using each method, and the transmission of data packets using Hi-TORA starts at $t = 1,001$ sec. In addition, the results show the average of 30 simulations.

The thesis now describes the routing procedures. First, each node generates data packets (1 pkt = 1.5 kB) with time intervals that obey an exponential distribution with $\lambda = 0.005$. The value of λ is set according to [78]. The source node sends data packets to the sink node through the multi-hop path computed by Hi-TORA. Once established, the routing path is maintained until the transmission of packets is completed. For simplicity, this evaluation assumes that the sink node can receive multiple packets simultaneously; that is, packet collision is not considered. If the path to the sink node cannot be found, the source node cancels packet transmission. Only the sink node has a main power supply, and thus its battery power is never exhausted. The parame-

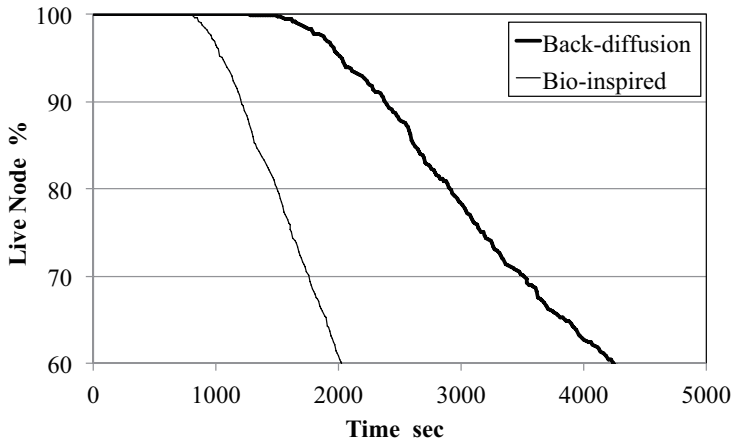

Figure 3.28: Temporal evolution of percentage of live nodes.

ters of the back-diffusion method and the bio-inspired method are shown in Tables 3.7 and 3.8, respectively. The parameters of the back-diffusion method are adjusted so that it yields the same number of clusters as the bio-inspired method at $t = 1,000$ s. For cluster formation, adjacent nodes exchange one control packet per second (1 pkt = 8 Bytes). Note that each node sends control parameters for adjacent nodes at the same time. Routing-control packets (1 pkt = 8 Bytes) are used in inter-cluster communication through Hi-TORA to set the *height* of each cluster on the path.

Figure 3.28 shows the temporal evolution of the percentage of live nodes for both methods. The horizontal axis represents time and the vertical axis is the percentage of live nodes. Figure 3.28 shows that the back-diffusion method offers a longer survival time than the bio-inspired method. One reason is the difference in the amount of control information used when configuring the cluster. Another is that the back-diffusion method forms clusters according to the distribution of initial battery power. On the other hand, clusters formed by the bio-inspired method are arranged at equal intervals regardless of the distribution of initial battery power. This increases the number of nodes with exhausted batteries and the live node percentage decreases with time.

Table 3.9 and Table 3.10 show the FND times of each method and the standard deviation of the results respectively. From the result, clusters configured by the back-diffusion method have a longer FND time, by 534s, than those configured by the bio-inspired method. Moreover, the standard deviation of the back-diffusion method is greater than that of the bio-inspired method, by 52 sec. The difference in the shape of the configured cluster and the number of control packets used influences these results for the same reasons as in the case of live nodes.

Table 3.11 and Table 3.12 show the amount of data received by the sink node and its standard deviation for the back-diffusion method and the bio-inspired method, respectively. The results show that the sink node can gather more information, by 1,168 packets, in clusters configured using the back-diffusion method than in those configured by the bio-inspired method. However, the standard deviation of data received by the sink node in the cluster configured by the back-diffusion method is greater than that of

Table 3.9: FND time.

back-diffusion	bio-inspired
1,565 sec	1,031 sec

Table 3.10: Standard deviation of FND time.

back-diffusion	bio-inspired
159 sec	107 sec

Table 3.11: Amount of total received data.

back-diffusion	bio-inspired
1,978 pkt	810 pkt

Table 3.12: Standard deviation of total received data by the sink node.

back-diffusion	bio-inspired
99 pkt	84 pkt

the bio-inspired method, as was the case with FND time. From these results that the back-diffusion method can reduce power consumption and permit the transmission of significantly more data than the bio-inspired method. The standard deviation of both the FND time and the amount of received packet for the back-diffusion method are greater than the one of the bio-inspired method, but the difference is small. Therefore, reflecting the network condition for clusters is effective from the point of view of both the power consumption and the data transfer efficiency.

3.4.3 Performance characteristics with varying number of nodes and node mobility

This section evaluates the characteristics of power consumption and data transfer efficiency when the number of nodes and their average mobility speed are changed. The network model, the routing procedures and the parameters of clustering are same as those in Sect. 3.4.2. The number of nodes and the mobility of nodes are set to (101, 201, 301, 401, 501) and (1 m/s, 5 m/s, 20 m/s), respectively. The outcome measures are the percentage of live nodes, FND time, and the number of packets received by the sink node.

Firstly, this section describes the behavior of the characteristics if the number of nodes is varied. Figure 3.29 and Fig.3.30 show the variation with time in the percentage of live nodes for varying number of nodes using the back-diffusion method and the bio-inspired method, respectively. In each figure, the horizontal axis represents time and the vertical axis represents the live node percentage. These figures show that as the number of nodes increases, the percentage of live nodes decreases more rapidly. This is because each node has more adjacent nodes in this case, thus leading to an increase in the number of control packets sent/received by each node. These results also show that the back-diffusion method reduces the rate at which the percentage of live nodes decreases compared to the bio-inspired method. This is because the back-diffusion method can configure clusters reflecting the network condition.

Secondly, FND time for each method is discussed. In Fig.3.31, the horizontal axis represents the number of nodes, and the vertical axis is time. This result shows that increase in the number of nodes decreases the FND time. This is for the same reason as

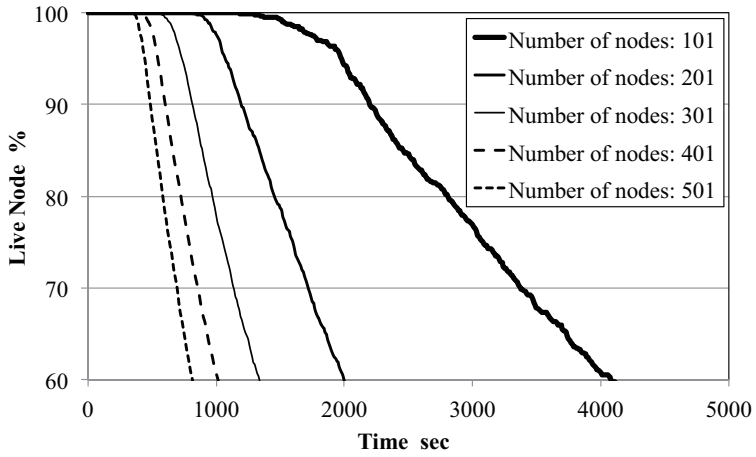

Figure 3.29: Relationship between the percentage of live nodes and the number of nodes (back-diffusion).

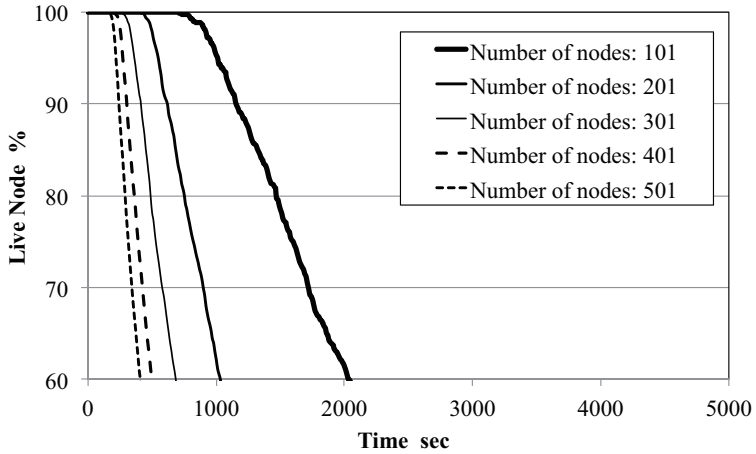

Figure 3.30: Relationship between the percentage of live nodes and the number of nodes (bio-inspired).

the decrease in the percentage of live nodes. The back-diffusion method yields longer FND times than the bio-inspired method regardless of the number of nodes. Moreover, Fig.3.32 shows the relationship between the number of nodes and the standard deviation of the FND time. This result shows an increase in the number of nodes decreases the standard deviation. This is because a node immediately runs out of battery regardless of its initial position when the number of nodes increases. From the above results, the back-diffusion method can better reduce power consumption than the bio-inspired method, even if the number of nodes varies.

Thirdly, Fig.3.33 and Fig.3.34 show the number of data packets received by the sink node and its standard deviation for varying numbers of nodes, respectively. These results show that increasing the number of nodes decreases the amount of data received by the sink node as well as its standard deviation for both methods. However, the back-diffusion method can transmit more data packets than the bio-inspired method. This is because the back-diffusion method allows nodes to live longer (the percentage of live nodes is high) and the route to the sink node is maintained in the network. From these

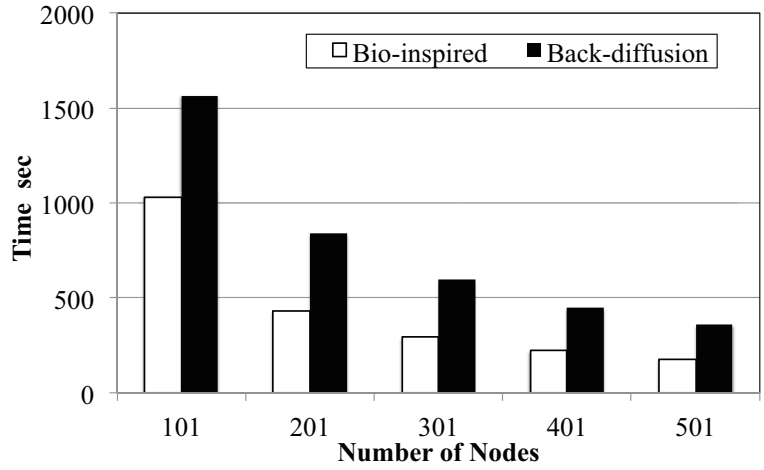

Figure 3.31: Relationship between the FND time and the number of nodes.

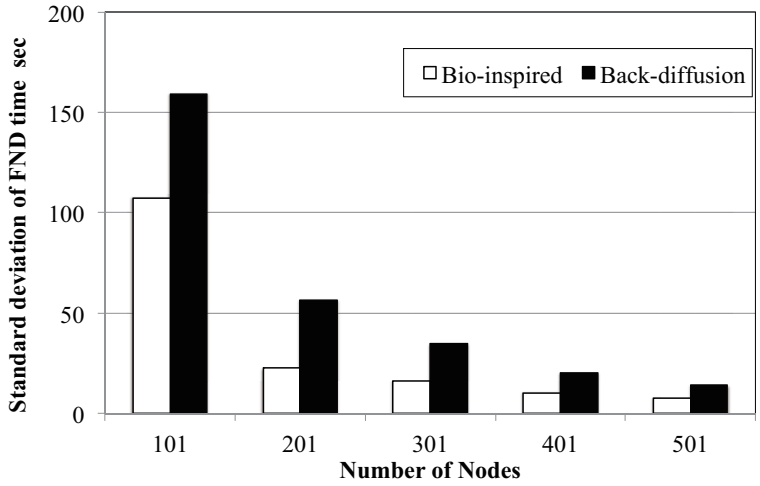

Figure 3.32: Relationship between the standard deviation of FND time and the number of nodes.

results, taking into account the network condition for clustering is very important from the viewpoint of power consumption and data transfer efficiency, even if the number of nodes increases.

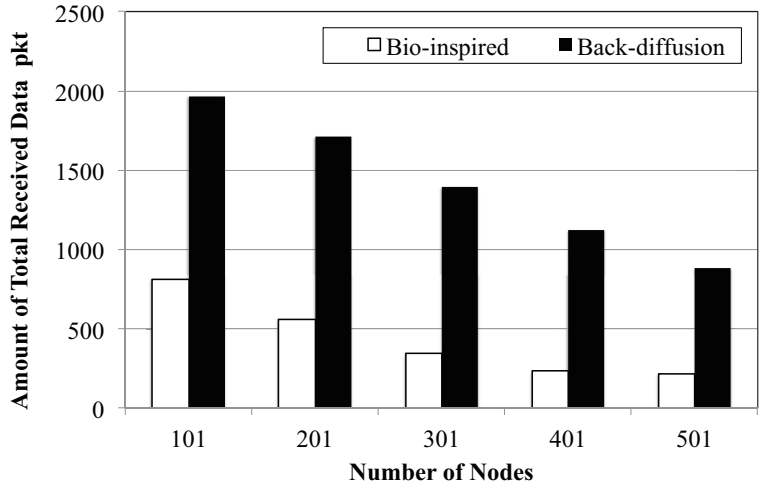

Figure 3.33: Relationship between the amount of received data and the number of nodes.

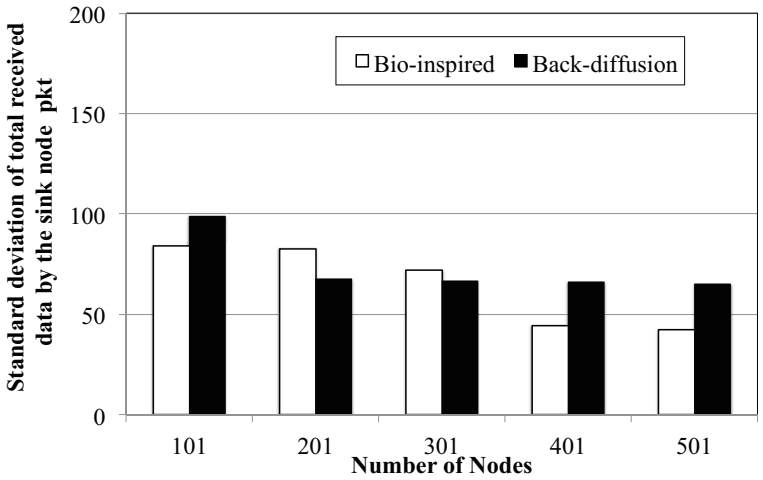

Figure 3.34: Relationship between the standard deviation of the amount of received data and the number of nodes.

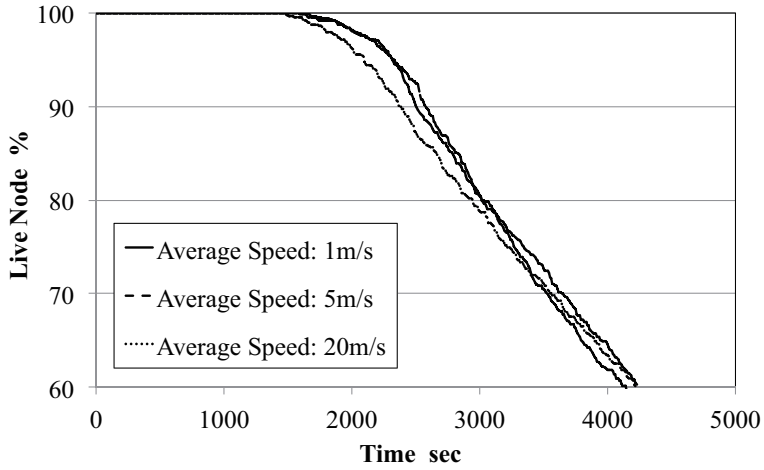

Figure 3.35: Relationship between the percentage of live nodes and the average node velocity (back-diffusion).

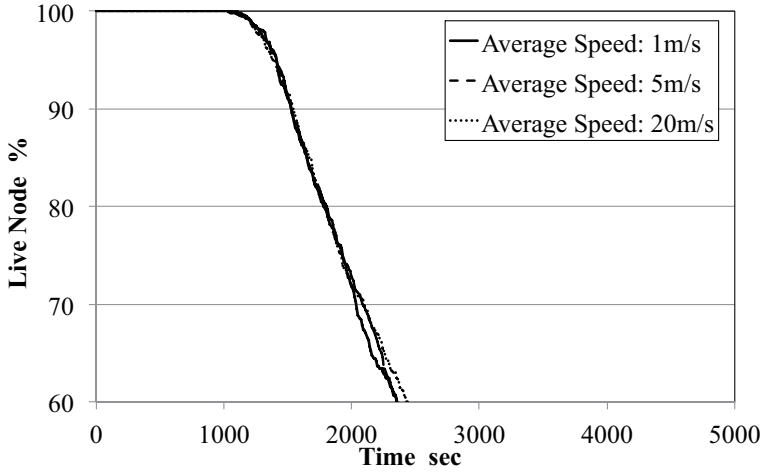

Figure 3.36: Relationship between the percentage of live nodes and the average node velocity (bio-inspired).

Next, this section now presents the experimental results of the relation between performance characteristics and node mobility. Figure 3.35 and Fig.3.36 show the temporal evolution of the percentage of live nodes for various node mobility values for each method. These results show that the rate at which the percentage of live nodes decreases is independent of average node mobility speed. This is because the number of adjacent nodes for each node changes little in the random direction model, even if the average node velocity increases. As a result, the number of control packets sent/received by each node does not so change. The back-diffusion method again yields a slower fall in the percentage of live nodes than the bio-inspired method.

Figure 3.37 shows the relationship between the FND time and average node velocity, and Fig.3.38 represents the standard deviation of the FND time for different average node velocities. These results show that the FND time and its standard deviation are not so dependent on average node velocity. From these results, the back-diffusion method yields longer FND times than the bio-inspired method, regardless of node velocity.

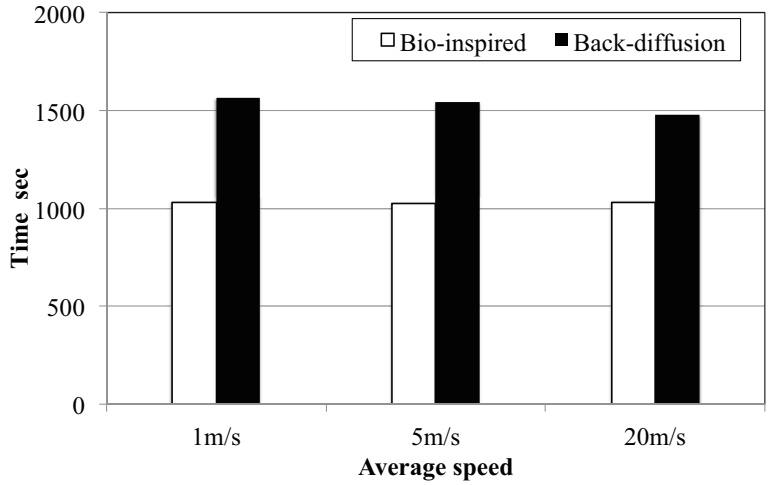

Figure 3.37: Relationship between the FND time and the average node velocity.

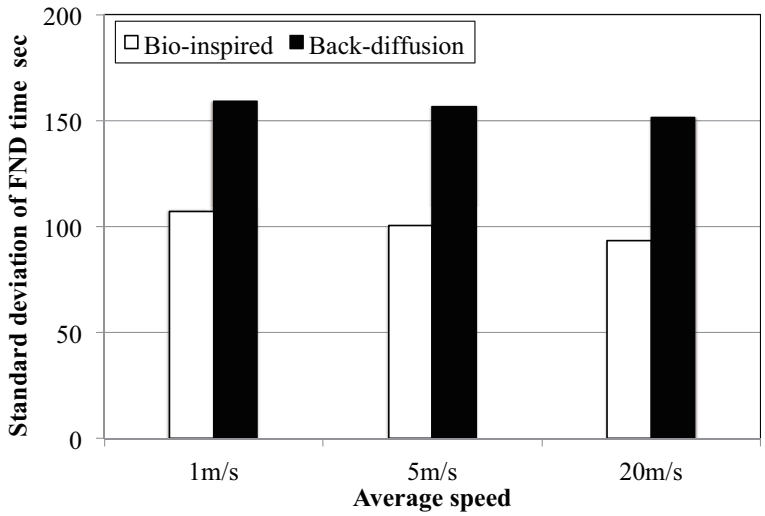

Figure 3.38: Relationship between the standard deviation of the FND time and the average node velocity.

Figure 3.39 shows the amount of data received by the sink node at different node velocities. From Fig.3.39, the number of data packets collected by the sink node does not change, even if average node velocity increases, because the number of live nodes changes only slightly as a consequence. Figure 3.40 shows the standard deviation of the amount of data received by the sink node. From Fig.3.40, the standard deviation is almost independent of average node velocity. Note that the back-diffusion method can transmit more data regardless of node velocity. These results show that reflecting the network condition for clusters is crucial, even if the node velocity increases.

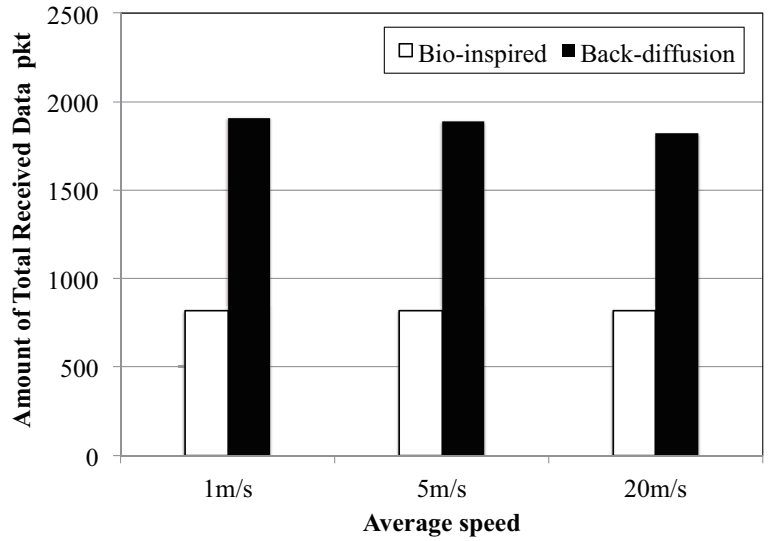

Figure 3.39: Relationship between the amount of received data and the average node velocity.

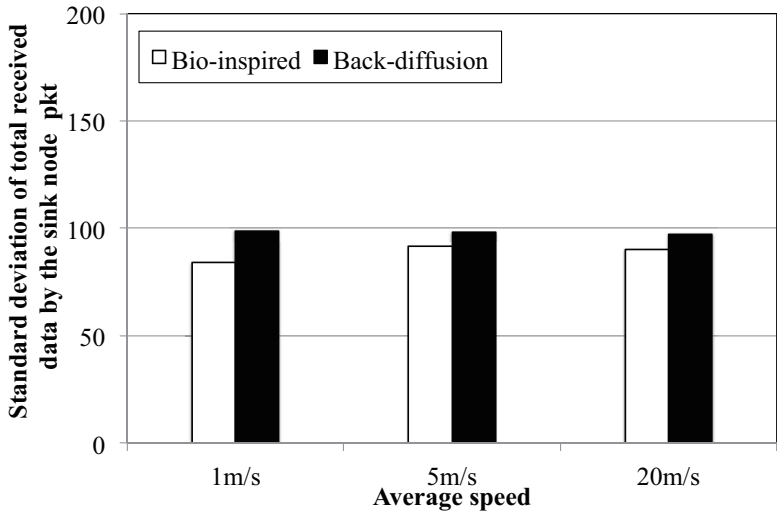

Figure 3.40: Relationship between the standard deviation of the amount of received data and the average node velocity.

3.5 Conclusion

In past research, an autonomous decentralized clustering technology based on local interaction (back-diffusion method) has been proposed and used it to realize clustering in MANETs. In this method, however, the number of clusters decreases with temporal evolution. Therefore, the hierarchical management of the network cannot be performed by this problem. This chapter provided a solution; a method that uses distribution vectors to preserve the distribution history and thus stabilize the range of the distribution of each node. Numerical simulations clarified that the back-diffusion method can guarantee the stability of the range of the distributions formed by the proposed method. In addition, by changing the components of the distribution vector, the back-diffusion method cannot set strictly the number of clusters, but can decide the number of clusters to some (large or small) extent. The issue for the proposed method is that a certain time is required to configure clusters.

Moreover, the effect of clusters that reflect the network condition has not been evaluated. To show the effectiveness, this chapter compared the back-diffusion method to a bio-inspired method based on the reaction-diffusion equation in order to evaluate the effect of clustering on network condition in terms of power consumption and data transfer efficiency. This evaluation used Hi-TORA as the routing algorithm, which offers one kind of cluster-based routing for ad hoc networks. Evaluations focused on the temporal change in the percentage of live nodes, the FND time, and the amount of the data received by the sink node. From evaluations, the clusters yielded by the back-diffusion method are superior in all respects to those generated by the bio-inspired method. This means that reflecting the network condition for clusters is effective from the point of view of both power consumption and data transfer efficiency. Therefore, the back-diffusion method can configure clusters that can operate for longer periods of time, and thus can help maintain communication after a disaster for longer periods.

Future research will involve investigating the compatibility of back-diffusion method with routing algorithms other than Hi-TORA, and enhancing the flexibility of the back-diffusion algorithm. Moreover, future works include that the evaluation of the back-diffusion method with vector processes in real environments.

Chapter 4

A Proposal of Design Method for Terminal Communication Range to Improve both Power Saving and Communication Reachability Based on Target Problem

This chapter proposes and evaluates a method for designing the communication range of wireless terminals in order to improve both power saving and communication reachability based on a target problem.

4.1 Introduction

In recent times, with the wide spread proliferation of wireless LANs based on the IEEE 802.11 standard [1], Internet connections through wireless LAN have become more common. An ad hoc network is a type of a utility form of a wireless LAN. Ad hoc networks [49] are very useful networks in various environments because they can construct networks autonomously without network infrastructure such as APs. As examples, ad hoc networks can be used to construct sensor networks [43], geocast communication systems [79], and V2V communication systems [44]. Therefore, ad hoc networks are useful during times of peace. On the other hand, wide-scale disasters may cause catastrophic damage to a geographic area, and consequently, considerable network infrastructure may suffer large-scale damage. In this situation, infrastructure mode wireless LANs are likely to be unable to communicate with other networks; however, ad hoc networks would be able to communicate because they are independent of network infrastructures [80].

In general, terminals in an ad hoc network such as smartphones and tablets are operated by battery powered systems. Here, the terminal in an ad hoc network is not only the source node of packets but also the relay node of packets. Therefore, considerable power consumption occurs compared to an infrastructure mode wireless LAN; this large amount of power consumption would need to be reduced else terminals composed of ad

hoc networks would shut down rapidly. Consequently, the network structure would become extremely sparse, which could result in a reduction of communication reachability of terminals. Therefore, extending the network lifetime through power saving at each terminal is an important issue in ad hoc networks. One solution for this issue is to reduce the power consumption of each terminal by reducing the radio transmission range of each terminal. However, the drawback to this solution is that the reachability of terminals may be adversely affected. To address this issue, various studies have already proposed and evaluated transmission range management methods [81–86]. However, these methods evaluated for a limited terminal distribution (terminal placement). For example, if terminal distribution follows a normal distribution, the aforementioned approaches may not work effectively. Note that if sensor nodes are vertically dropped from a certain point in midair, their spatial distribution could result in a two dimensional normal distribution [87, 88]. This chapter proposes a method for designing the radio transmission range considering a *Target Problem* [89–91] in order to improve both the power saving and reachability of each terminal in an ad hoc network where a terminal is normally distributed [30]. This chapter also evaluates the total goodput using two routing protocols (Destination-Sequenced Distance Vector: DSDV [92], Ad hoc On-demand Distance Vector: AODV [93]) and two MAC protocols (CSMA/CA, Time Division Multiple Access: TDMA [94]). Furthermore, this chapter clarifies the applicability of the proposed method to communication protocols. The main purpose of this chapter is to clarify the effectiveness of the proposed transmission range design method based on the target problem in a network where the terminal is normally distributed.

The remainder of this chapter is constructed as follows: Section 4.2 explains the related works. Section 4.3 describes the overview of the target problem and the method for designing the radio transmission range based on the target problem. Further, Sect. 4.4 evaluates the proposed method. Finally, Sect. 4.5 summarizes this chapter and discusses future works.

4.2 Related works

This section presents applications of ad hoc networks. Furthermore, this section discusses the power consumption and reachability issues of ad hoc networks. In addition, this section explains some existing radio transmission range management methods.

4.2.1 Applications of ad hoc network

Sensor networks [43] are examples of ad hoc networks. In a sensor network, sensor devices are distributed in an observation region to sense the surrounding environment, and send the sensing data to a sink node using wireless communication. Moreover, it is possible to collect a wide range of information by performing multi-hop communication via sensor nodes.

Another example of the ad hoc network is V2V communication systems [44]. The V2V communication system is a subset of the Intelligent Transportation System (ITS) [95]. In a V2V communication system, vehicles (nodes) communicate with each other through

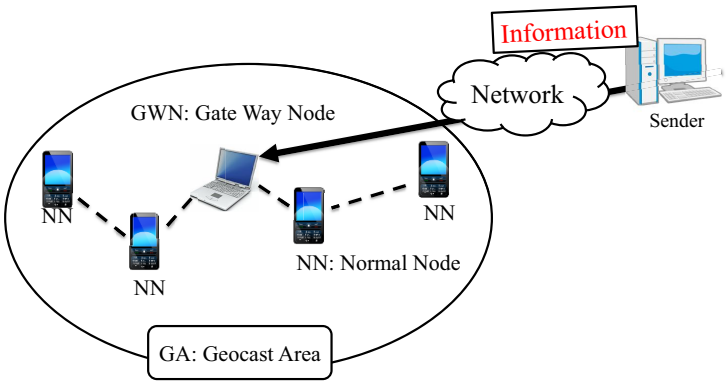

Figure 4.1: Overview of geocast communication.

information such as traffic information. Furthermore, the IEEE 802.11p [96] Physical layer and MAC layer is used for V2V.

Next, this section explain geocast communication, where in data is sent only to terminals in a specified area (referred to as the Geocast Area: GA) using the terminal's location information. Figure 4.1 shows components in a geocast communication system. Here, this section explains the geocast communication process, using Fig.4.1. First, there are two types of terminals in a GA, gateway nodes (GWNs) and normal nodes (NNs). The GWN is a terminal that connects the GA to other networks outside of the GA. Only the GWN receives information from outside networks; the received information is delivered to NNs in the GA by the GWN. In geocast communication, a terminal outside of the GA (Sender in Fig.4.1) sends information to the GWN of the GA, in order to communicate with an NN inside the GA. The GWN sends its received information to NNs in the transmission area of the GWN, and the NN can also send its received data to other NNs. Examples of geocast communication applications are shown as follows:

1. Transmission of warning messages in the event of a disaster
2. Delivery of traffic information such as traffic congestion and accidents using V2V
3. Delivery of information for residents in a specific area

4.2.2 Power consumption and reachability issues of ad hoc networks

This section describes the power consumption and reachability issues of ad hoc networks. Note that this section assumes that emergency evacuation information is required to be sent by the geocast during a disaster. In emergency situations, the information from a GWN must be received by all NNs that exist in the GA, because users are typically sending important and urgent information. That is, all NNs in a GA must be able to communicate with the GWN using single-hop or multi-hop communication. However, the transmission range of the terminals may be not sufficient if they were set haphazardly; in this case, an NN may not be able to connect to an NN that is communicating with the GWN. As a result, the NN is isolated from the GWN (isolated terminal). The

isolated terminal cannot receive information from the GWN, and cannot send information outside of the GA.

One solution for this issue is to extend the radio transmission range. Using this solution, it is possible to create an environment in which all NNs can transmit and receive information. However, terminals in an ad hoc network are, in general, battery powered. In addition to transmitting and receiving packets, terminals in an ad hoc network relay packets for other terminals. Thus, terminals consume more battery power; therefore, power consumption must be suppressed as much as possible, else, terminal batteries may be rapidly depleted, and network lifetime would be shortened (by increasing the number of terminals in which battery depletion occurs). In particular, having access to the latest information is essential during a disaster. Therefore, sufficient network lifetime is required to obtain the latest information. To extend a network's lifetime, its power consumption must be reduced. Consequently, there is a trade-off between creating an environment in which all terminals can transmit and receive information, and maintaining sufficient battery power. However, both *network power savings* and *communication reachability* are important goals in the management of geocast communications for ad hoc networks.

4.2.3 Existing methods for designing radio transmission range

To solve the issue of Sect. 4.2.2, various studies have been proposed that have evaluated transmission range management methods [81–86]. As a specific example, [81] shows the optimum transmission range in the chain topology network. Moreover, [82] suggests the radio transmission range designing method, and it evaluates the effectiveness in the ring topology network. In addition, [83, 84] propose and evaluate the methods in a network where node locations follow a uniform distribution. [85, 86] describes the setting method of the radio transmission range considering a realistic power consumption model. However, these methods do not consider a network where node locations follow a normal distribution. That is, if terminal distribution follows a normal distribution, these approaches may not work effectively. Note that an example of a network where node locations follow a normal distribution is shown in Sect. 4.3.

4.3 Setting the radio transmission range based on a target problem

This section provides an overview of the two-dimensional target problem [89–91]. Furthermore, this section describes the method for setting the radio transmission range based on the target problem, to improve power savings and terminal reachability in ad hoc networks.

4.3.1 Overview of the two-dimensional target problem and its application to single-hop communication

The nodes appear equivalent to the arrows that an archer shoots at a target. The hit points have a probabilistic characteristic. The two-dimensional target problem considers the distribution of hit points. Random variables X_i ($i = 1, 2, \cdots, n$) are independent of each other, and the normal distribution has variance σ_i^2 and average μ_i. Random variable Z is defined by Eq.(4.1):

$$Z = \sum_{i=1}^{n} \left(\frac{X_i - \mu_i}{\sigma_i} \right)^2 . \tag{4.1}$$

In Eq.(4.1), Z has χ^2 distribution whose flexibility is n. This indicates that the sum of the squares of independent random variables that follow standard normal distribution $N(0, 1)$ has a χ^2 distribution. In other words, the distribution of the squared sums of the distances between the hit points and the origin of the space has a χ^2 distribution. In the two-dimensional target problem, distribution of the distances is important. This section considers the χ distribution as the square root distribution of the χ^2 distribution. That is, the square root of the squared sum of distances from the origin to the hit point. Thus, the distribution of the distances from the origin indicates a χ distribution if flexibility n yields each component of the *Cartesian coordinates* (Fig.4.2). Therefore, in the two-dimensional target problem, the arrow's hit probability takes a χ distribution if the size of the target is known and the neighboring distribution of the hit points forms a normal distribution. As an example, this section assumes a target with a radius of R, whose origin is the center of a two-dimensional plane. Hit probability $F(R)$ has a χ distribution; its flexibility is 2 when the neighboring distribution of hit points follows a two-dimensional $N(0, \sigma^2)$. In other words, it follows a *Rayleigh distribution* as follows:

$$F(R) = 1 - \exp\left(-\frac{R^2}{2\sigma^2} \right). \tag{4.2}$$

Moreover, the probability that the hit point is outside of the target (miss probability) $Y(R)$ is expressed by the complementary distribution of Eq.(4.2) ($1 - F(R)$):

$$Y(R) = \exp\left(-\frac{R^2}{2\sigma^2} \right). \tag{4.3}$$

Next, this section explains the application of the target problem in geocast communication systems. This section assumes that the GWN's transmission range (unit distance) is the radius of the target, and that the GWN is located at the center of a GA (origin $(0, 0)$). The probability $Y(R)$ that an NN in the GA cannot connect to the GWN with a single-hop is estimated by Eq.(4.3). Therefore, NNs are placed according to a two-dimensional normal distribution and the GWN is placed in the center of a geocast area, and the miss probability $Y(R)$ that the NN cannot connect to the GWN with a single-hop follows the complementary distribution of a Rayleigh distribution. In a two-dimensional normal distribution, the NNs are concentrated near the GWN (the GWN is placed where NN density is high). As a specific example, the GWN may be placed

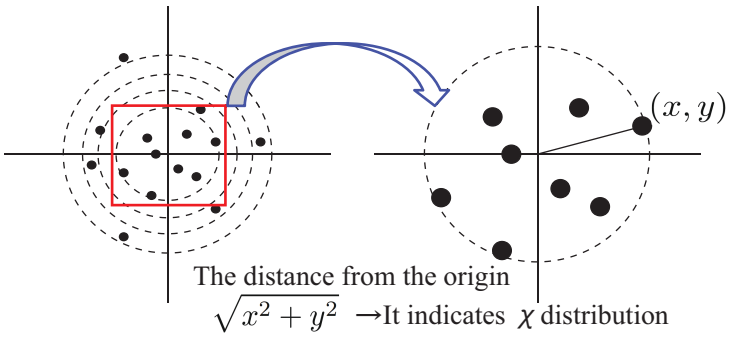

Figure 4.2: Relationship between the distance from the origin and the χ distribution in the two-dimensional target problem.

in an evacuation center when a disaster occurs. Moreover, when the GWN is placed in a location that will be used as a landmark for users, such as an aircraft [9], many users can observe the GWN move towards them. As a result, the distribution of the users may follow a normal distribution. Furthermore, it is known that if sensor nodes are vertically dropped from a certain point in midair, their spatial distribution will result in a two-dimensional normal distribution [87, 88].

4.3.2 Miss probability estimation method in multi-hop communication

To facilitate geocast communication in an ad hoc network, it is preferable for the NNs and the GWN to be connected using multi-hop, in order to reduce network power requirements. Based on the results from the single-hop environment in the previous section, this section models the existence probability of an isolated node (miss probability) in the communication area of the GWN for a multi-hop environment. This is a type of connectivity problem [97]. Note that the network model is an UDG, which is a type of intersection graph containing equal-radius circles. Moreover, the GWN is the nearest terminal from the origin. As a preliminary experiment, this section investigates the relationship between multi-hop miss probability and transmission range, for varying numbers of terminals. This experiment assumes a two-dimensional plane, and terminals are distributed according to two-dimensional $N(0, \sigma^2)$. The numbers of terminals N is set to $(1,000,\ 2,000,\ 4,000,\ 6,000,\ 8,000,\ 10,000)$. This section shows the results of $\sigma = 1.0$ as an example. Experimental results contain an average of 30 trials.

Figure 4.3 shows the relationship between the transmission range of each terminal in the multi-hop environment r and the miss probability of terminal $Y(r)$, and Fig.4.3 also shows the relationship between r and the complementary Rayleigh distribution. In Fig.4.3, the vertical axis denotes $Y(r)$ and the horizontal axis denotes r. From Fig.4.3, $Y(r)$ does not indicate the complementary Rayleigh distribution, regardless of the number of terminals N.

Next, this section investigates the relationship between the effective radius R_{ef} and transmission range of each terminal r. R_{ef} can be obtained by adding r and the distance of the farthest terminal that the GWN can connect with using multi-hop. That is, r meets $R_{ef} \geq r$. The relationship between R_{ef} and r is obtained as follows. First, the

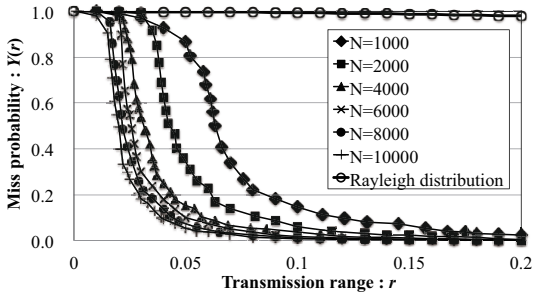

Figure 4.3: Relationship between the transmission range r and miss probability for each N ($\sigma = 1.0$).

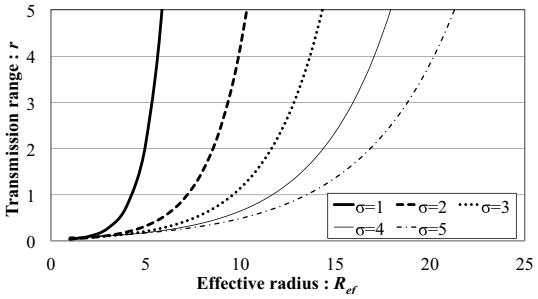

Figure 4.4: Relationship between the transmission range r and effective radius R_{ef} for each σ ($N = 1,000$).

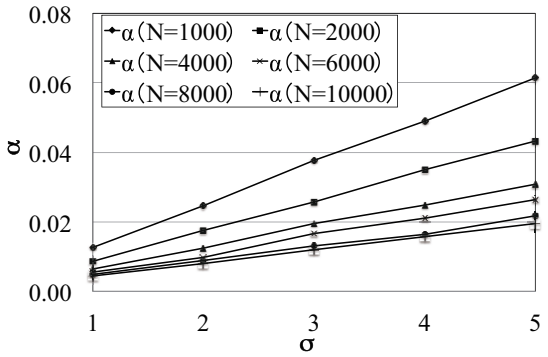

Figure 4.5: Relationship between α and σ.

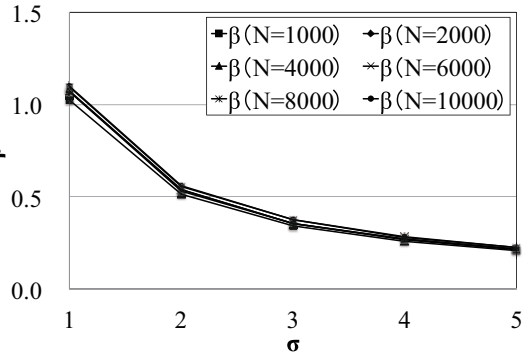

Figure 4.6: Relationship between β and σ.

transmission range of the GWN in the single-hop environment R as R_{ef} is established. Next, the miss probability of r in the multi-hop environment and the miss probability of R in the single-hop environment are compared. Then, the relationship between R_{ef} and r, to determine if the miss probability has the same value is investigated. As an example, Fig.4.4 shows the relationship between R_{ef} and r when N is $1,000$. Note that σ was set to (1.0, 2.0, 3.0, 4.0, and 5.0). As shown in Fig.4.4, R_{ef} has an exponential relation with r by Eq.(4.4):

$$r = \alpha \exp(\beta R_{ef}). \tag{4.4}$$

Next, this section investigates the relationship between α and σ. Figure 4.5 is the relationship between α and σ. As shown in Fig.4.5, a proportionality relation exists between α and σ ($\alpha = \phi(N)\sigma$). Table 4.1 shows the value of $\phi(N)$. From Table 4.1, $\phi(N)$ is described as Eq.(4.5):

$$\phi(N) = \frac{0.3786}{\sqrt{N}}. \tag{4.5}$$

Thus, α can be represented as follows:

$$\alpha = \frac{0.3786\sigma}{\sqrt{N}}. \tag{4.6}$$

Table 4.1: Value of $\phi(N)$.

N	1,000	2,000	4,000	6,000	8,000	10,000
$\phi(n)$	0.0123	0.0087	0.0062	0.0053	0.0043	0.0039

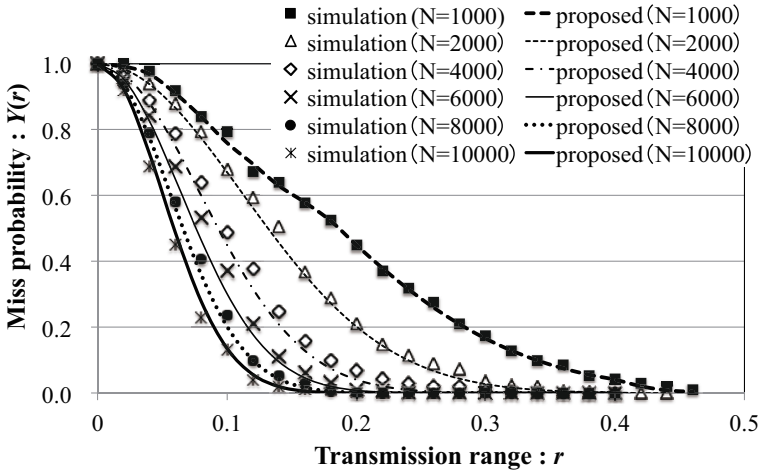

Figure 4.7: Comparison of the simulation value and the theoretical value Eq.(4.9) (σ = 1.0).

Next, Fig.4.6 shows the relationship between β and σ. As the figure shows, β is inversely proportional to the σ regardless of N. Moreover, β can be written using σ as follows:

$$\beta = \sigma^{-1}. \tag{4.7}$$

From Eq.(4.6) and Eq.(4.7), r is presented using R_{ef} as follows:

$$r = 0.3786 \frac{\sigma}{\sqrt{N}} \exp(R_{ef}\sigma^{-1}). \tag{4.8}$$

By substituting R_{ef}, which was obtained from Eq.(4.8) for Eq.(4.3), the existence probability of an isolated terminal (miss probability) in a multi-hop environment for each r can be obtained as follows:

$$Y(R_{ef}(r)) = \exp\left(-\frac{(\log(\sqrt{N}r\sigma^{-1}) + 1)^2}{2}\right). \tag{4.9}$$

In other words, the minimum transmission range that satisfies the existence probability of an isolated terminal P can be estimated by Eq.(4.9). Note that evaluations refer to P as an *acceptable miss probability* in Sec. 4.4.

Subsequently, the theoretical formula Eq.(4.9) and the simulated miss probability values in the multi-hop environment are compared. Figure 4.7 shows the relationship between r and the miss probability in the multi-hop environment. Note that the values of N and σ are the same as they were in the preliminary experiment. In Fig.4.7, the vertical

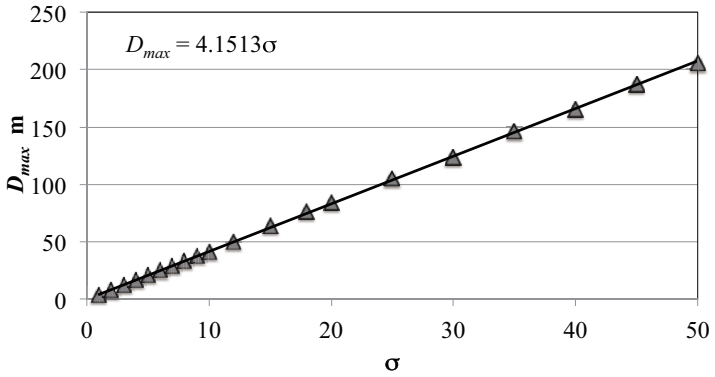

Figure 4.8: Relationship between σ and the distance of the node farthest from the GWN.

axis shows the miss probability and the horizontal axis shows r. As shown in Fig.4.7, Eq.(4.9) outputs almost the same miss probability as the simulation value. Therefore, Eq.(4.9) can estimate the miss probability in a multi-hop environment for each r. Here, Fig.4.8 shows the relationship between σ and the distance D_{max} between the GWN and the node farthest from the GWN. As shown in Fig.4.8, the relationship between σ and D_{max} is approximately obtained as follows:

$$D_{max} = 4\sigma. \tag{4.10}$$

Therefore, σ can be obtained by Eq.(4.10).

4.4 Evaluation

This section describes the evaluations of the proposed method using network simulator ns2 [98]. Evaluations focus on the total goodput and total power consumption. Note that the main purpose of the evaluations is to show the effectiveness of the proposed model equation (Eq.(4.9)). Therefore, both the number of terminals and σ are known by the terminals in the evaluations.

4.4.1 Simulation environment

This evaluation assumed a two-dimensional plane. The sink node is placed at $(0, 0)$, and wireless terminals (senders) are distributed according to two-dimensional $N(0, \sigma^2)$; the number of senders is 100. This network uses the IEEE802.11b (PHY) wireless LAN environment, and User Datagram Protocol (UDP) (with a segment size of 128 byte) for the transport protocol [78]. Moreover, each sender generates 60 seconds of Constant Bit Rate (CBR) traffic (1 Kbps). The routing protocol uses DSDV [92] and AODV [93]. In addition, the MAC protocol uses CSMA/CA and TDMA. This evaluation assumes that none of the terminals move.

In this evaluation, terminals consume battery power when they are connected to the GWN in the multi-hop environment, and power consumption is a normalized value for simplification. In the power consumption model for the evaluation, the amount of electricity uses by the terminal for the transmission range r is proportional to the square of

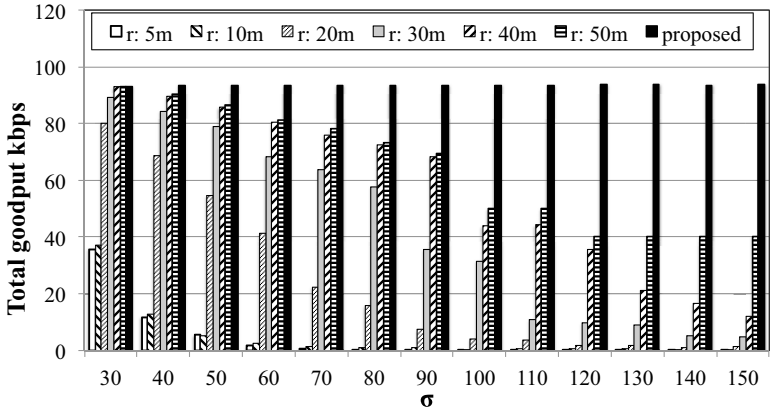

Figure 4.9: Total goodput for each σ (N = 100, DSDV, CSMA/CA).

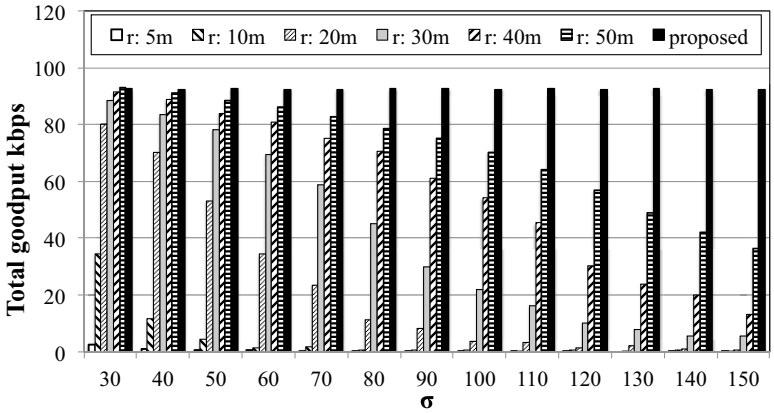

Figure 4.10: Total goodput for each σ (N = 100, DSDV, TDMA).

r [99], and terminals use electricity equal to 0.001 when r was 0.01. That is, terminal power consumption is increased by four times when r is doubled. Moreover, total power consumption is the sum of the power consumption for terminals that could communicate with the GWN, using multi-hop in one unit time. In addition, the acceptable miss probability P is 0.1% (to obtain r which satisfies P, $Y(R_{ef}(r)) = 0.001$ is calculated); the simulation results contain the averages of 20 tests.

4.4.2 Results

Total goodput characteristics with varying σ

First, this section shows the results when DSDV is used as the routing protocol. Figure 4.9 shows the relationship between σ and the total goodput for each r when the DSDV routing protocol was used. Moreover, Fig.4.10 shows the result when the TDMA is used for MAC protocol. In Fig.4.9 and Fig.4.10, the vertical and horizontal axes represent the total goodput and σ, respectively. Note that *proposed* in Fig.4.9 and Fig.4.10 is the transmission range set by Eq.(4.9), and proposed meets P. From Fig.4.9 and Fig.4.10, when r m was fixed, the total goodput decreased if σ increased. This occurred because terminals were widely distributed across the area when σ increased. Therefore,

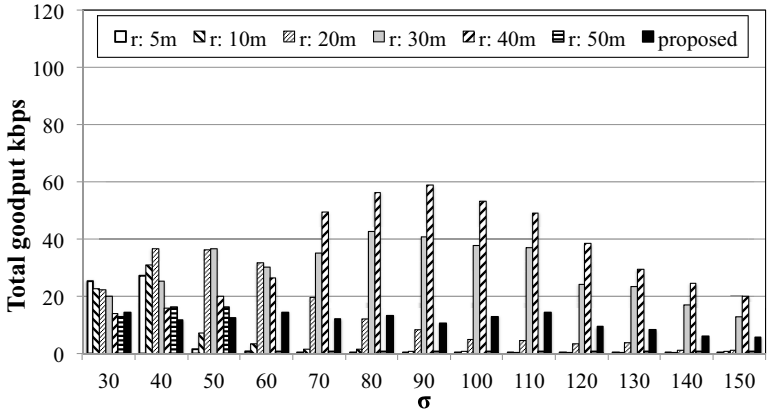

Figure 4.11: Total goodput for each σ (N = 100, AODV, CSMA/CA).

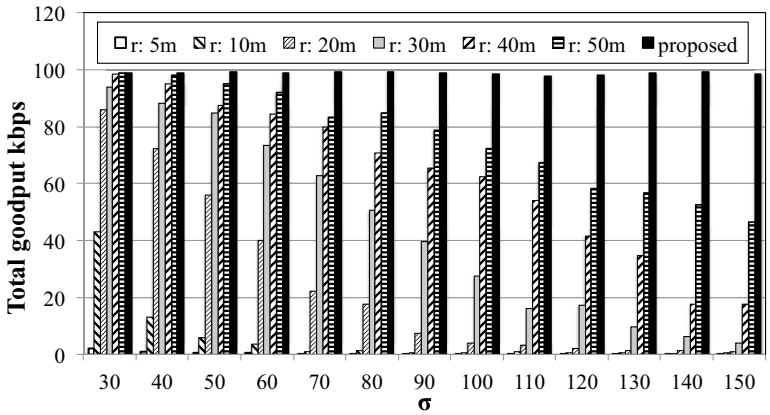

Figure 4.12: Total goodput for each σ (N = 100, AODV, TDMA).

the number of terminals that could not connect to the GWN increased if r was fixed. On the other hand, total goodput in each σ was the highest when r was set to the proposed m. The proposal sets the transmission range for each σ in order to meet P. As a result, the proposed method improved communication reachability when DSDV was used as the routing protocol.

Secondly, this section shows the results when AODV is used as the routing protocol. Figure 4.11 shows the relationship between σ and the total goodput for each r when CSMA/CA was used as the MAC protocol. Moreover, Fig.4.12 shows the result when TDMA is used. In Fig.4.11 and Fig.4.12, the vertical and horizontal axes represent total goodput and σ, respectively. Fig.4.11 and Fig.4.12 also represent the proposed transmission range, which is set by Eq.(4.9). From Fig.4.11, total goodput is lower than the results produced using DSDV when CSMA/CA is used. This decrease was caused by the placement of terminals, and the fact that AODV is a reactive protocol. In the evaluations, terminals were distributed according to a two-dimensional $N(0, \sigma^2)$. That is, terminals were concentrated near the sink node. Here, a path for the sink node was generated according to the routing table, which was constructed by exchanging distance vectors with broadcasts in DSDV. Moreover, the topology near the sink node was constructed in a manner similar to a mesh network. Even if a node near the sink loses in-

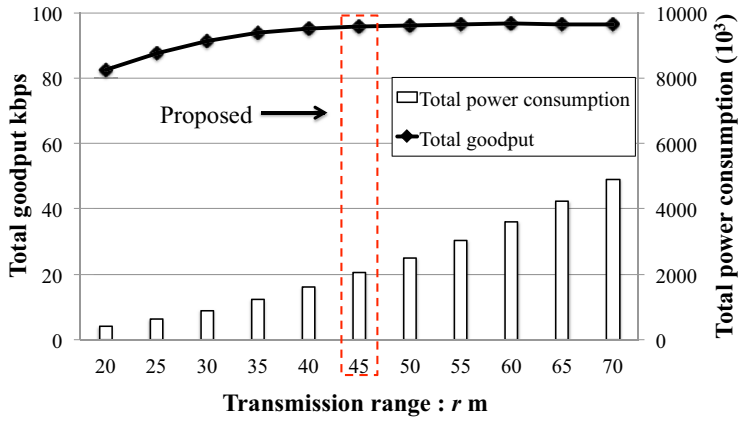

Figure 4.13: Relationship between the transmission range r and the total power consumption and total goodput (σ = 30.0, DSDV, CSMA/CA).

formation it receives from a node, it is possible to obtain that information from another neighboring node. Conversely, in AODV, a sender broadcasts a route request (RREQ) packet and receives a route reply (RREP) packet from the sink or other terminals that have already found a path to the sink during the routing path configuration process. In the evaluations, however, terminals were distributed according to a two-dimensional $N(0, \sigma^2)$. Therefore, frame collisions that included AODV control packets occurred frequently near the sink. Moreover, CSMA/CA congestion frequently occurred when terminals were densely located, and a significant amount of time was required to exchange AODV control packets. As a result, goodput decreased when AODV was used as the routing protocol. For this reason, network performance decreases when the transmission range is expanded and terminals are densely distributed (similar to a normal distribution), and reactive routing protocols such as AODV are used. When the network size is large and the density of nodes is high, the packet arrival rate of AODV drastically reduces [100]. This is known as a type of exposed node problem [101]. This problem occurs in a contention based MAC protocol (i.e. CSMA/CA). On the other hand, the result of TDMA (Fig.4.12) shows the high goodput when the proposed method is used. This is because TDMA can avoid the exposed node problem. Therefore, TDMA can achieve high goodput if terminals are densely distributed like in a normal distribution. From the above discussion, it is evident that AODV is suitable for the proposal if TDMA is used.

Total power consumption and total goodput vs. transmission range

Figure 4.13 and Fig.4.14 are the relationship between r and both the total power consumption and the total goodput when σ is set to 30 and DSDV is used as the routing protocol. Note that Fig.4.13 shows the result of CSMA/CA, and Fig.4.14 indicates the result of TDMA. In Fig.4.13 and Fig.4.14, r is investigated before and after 25 m of that proposed (about 45.4 m). From Fig.4.13 and Fig.4.14, the total goodput is improved along with an increase in the power consumption until that proposed. However, total goodput is not improved so much that if the transmission range is expanding more than that proposed, and only the total power consumption is increasing. Therefore, the

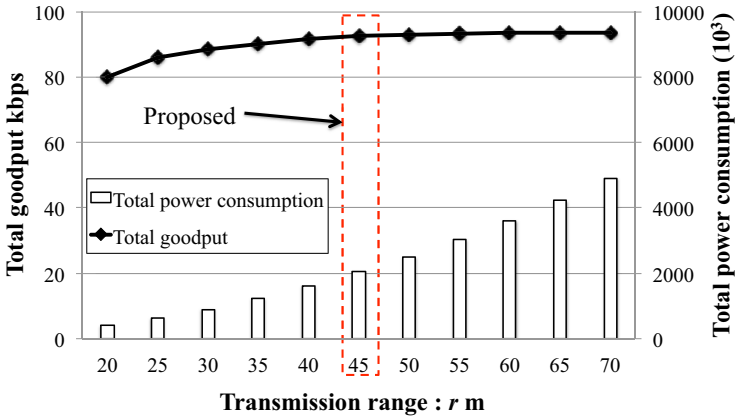

Figure 4.14: Relationship between the transmission range r and the total power consumption and total goodput (σ = 30.0, DSDV, TDMA).

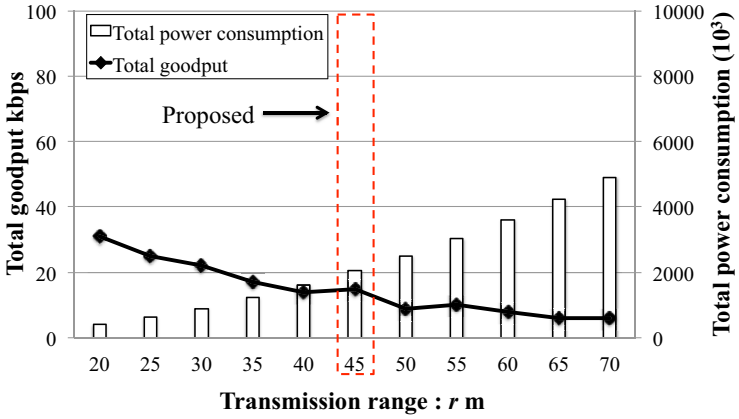

Figure 4.15: Relationship between the transmission range r and the total power consumption and total goodput (σ = 30.0, AODV, CSMA/CA).

transmission range that is obtained by the proposed method can achieve both high communication reachability and power saving of terminals if the routing protocol is DSDV. Fig.4.15 shows the result of similar experiments when AODV is used as the routing protocol and CSMA/CA is used as the MAC protocol. From Fig.4.15, goodput is improved by narrowing the transmission range more than that proposed. This is because the exposed node problem is restrained when reducing the number of adjacent terminals for each node, which is achieved by narrowing the communication radius. As a result, the exchange of AODV control packets is achieved easily. On the other hand, when TDMA is used for the MAC protocol, the exposed node problem can be avoided, and the transmission range that is obtained by the proposed method can achieve both high communication reachability and power saving of terminals even if AODV is used as the routing protocol (Fig.4.16).

Finally, Table 4.2 summarizes the applicability of the proposed method to each MAC protocol and routing protocol. From Table 4.2, TDMA and DSDV are suitable for the MAC protocol and the routing protocol, respectively, when the transmission range is set

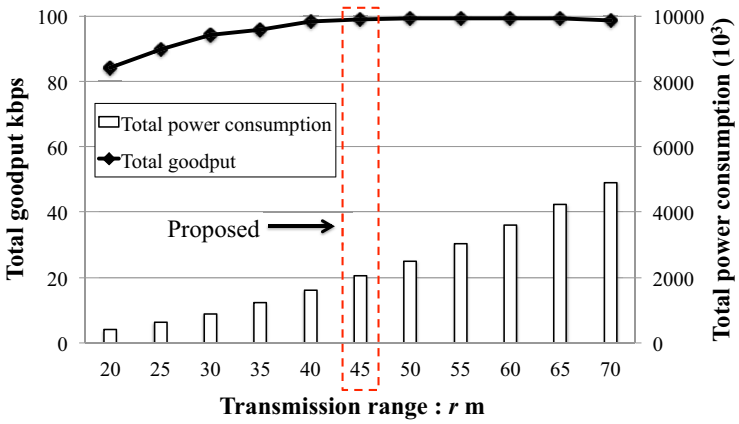

Figure 4.16: Relationship between the transmission range r and the total power consumption and total goodput (σ = 30.0, AODV, TDMA).

Table 4.2: Applicability of the proposed method.

MAC \ Routing	DSDV	AODV
CSMA/CA	○	×
TDMA	○	○

by the proposed method.

From the viewpoint of increasing ad hoc network uptime, setting the terminal transmission range using the target problem was very effective. Further, by using simulation experiments, the proposed method can improve communication reachability when DSDV and TDMA are used for the routing protocol and MAC protocol, respectively.

4.5 Conclusion

This chapter proposed a method to set the radio transmission range using a target problem, in order to improve both communication reachability and power savings for each terminal. This chapter evaluated the proposed method using network simulator ns2, from the viewpoint of both total goodput and total power consumption. Moreover, this chapter compared the results obtained by the proposed method and results obtained by setting a fixed value for the communication range. Simulation results demonstrated that setting the communication range using the proposed method can provide significant improvements in goodput and power savings when DSDV and TDMA are used as the routing protocol and the MAC protocol. Furthermore, when both AODV and CSMA/CA were used as the routing protocol, the proposal resulted in a drastic reduction of total goodput. Future works will include the following evaluations.

1. Evaluations considering the joining and leaving of terminals
2. Evaluations considering a more realistic power consumption model
3. Proposal for a setting method of radio transmission range for each terminal considering the condition of terminal

Chapter 5

An Acceleration of Throughput Prediction Method for Access Point in Multi-rate Wireless LAN Considering Terminal Distribution

This chapter explains an acceleration of throughput prediction method for an access point in multi-rate wireless LAN considering a terminal distribution.

5.1 Introduction

Wireless LANs based on the IEEE 802.11 standard have become increasingly common [1]. The number of public wireless LAN service areas has been increasing as more and more APs are being set up everywhere [102]. Moreover, even a smartphone can be used as an AP through tethering technology. Therefore, the Internet connections through wireless LANs have become common.

In wireless LANs based on the IEEE 802.11 standard, the AP and the terminal use multi-rate transmission for effective communication, because each terminal has a different communication environment. Note that in multi-rate transmission set, the transmission rate is set to match the electric wave environment between the AP and the wireless terminal. In this method, a terminal with a good electric wave environment can achieve high transmission rates, while those with poor environments only achieve low transmission rates (see Sect. 2.2). That is, throughput is optimal for the electric wave environment. Here, predicting the throughput of an AP in a multi-rate environment (quantity of data that an AP can receive including retransmission packets) is a very important issue in network design and network management. For example, it impacts the AP enlargement problem and the AP placement problem [103–105]. Furthermore, selecting an appropriate AP in an wireless LAN environment leads to assurance of communication QoS (throughput) when a terminal uses streaming communication. In this situation, the AP throughput can be used for the metric of an AP selection [34,106]. In addition, some studies [107–110] have evaluated characteristics of the throughput of terminals and APs in multi-rate transmission environments. In the future, more large-scale wireless LAN

networks constructed of a large number of terminals and APs are expected [111]. In such situations, APs are shared by many wireless terminals in the network. Depending on circumstances, however, uneven AP loading is caused, wherein wireless terminals are disproportionately connected to an AP. It results in a drastic decrease of QoS for all terminals connected to the AP. To solve this issue, the decision of acceptance for the connection of a terminal is necessary in order to ensure load balancing of the AP. The AP's throughput can be used for the threshold of the decision. Here, to provide service quickly for users, it is necessary to estimate the throughput of an AP quickly and accurately even if many terminals require access to the AP.

[48] explains that, in a multi-rate environment, AP throughput is equal to the harmonic average of transmission rates of the terminals connected to the AP (see Sect. 2.2). Moreover, an analytic proof that the harmonic average of the transmission rate is the upper limit of the throughput of the AP has been published [48]. Additionally, the predicted value of [48] almost equals the simulation value (true value) according to NS-2 [98]. Here, the throughput of one AP is calculated by assuming the transmission rate steps of the distance between an AP and the terminal [32–34, 106, 107]. That is, AP throughput is predicted by the distance between the AP and all terminals. Thus, the computational complexity is linear order against the number of terminals. Since the transmission rates of all terminals are known, the existing method can predict AP throughput with high precision. Reference of the field of the transmission rate in a frame is an example of realization for [48]. However, an exchange of a frame between the terminal and the AP is necessary. Here, it is known that the average time for exchanging a frame is about 1 ms, and the maximum time is about 100 ms. In current wireless LAN environments, a dozen or so terminals are connected to the AP. Therefore, even if the computational complexity is linear order, a second order time is required to estimate the throughput in the worst case. Additionally, battery operated APs such as smartphones will be more common in the future. To ensure power saving by reducing the processing time of an AP, it is desirable that the computational complexity of the estimation is of a constant order. Furthermore, some throughput prediction methods [112, 113] over wireless LAN have been proposed, but these methods do not consider multi-rate transmission.

This chapter proposes an acceleration of throughput prediction for access point in multi-rate wireless LAN considering terminal distribution [31]. The estimation method is based on the target problem [89] or area ratio of the system field wherein the terminal exists and the circular area that is determined by the transmission rate. The proposed method can reduce the calculation cost to $O(1)$. This chapter compares the throughput estimated by the proposal with the output of a previous work, and confirms the performance of the proposed method. Furthermore, this chapter compares the proposed method with an existing prediction method from the point of view of the calculation cost.

Table 5.1: Relationship between distance and transmission rate (IEEE 802.11a/g).

Index i	1	2	3	4	5	6	7	8
Threshold of distance d_i m from AP	5	7	9	20	25	40	50	60
Transmission rate b_i Mbps	54	48	36	24	18	12	9	6
Effective transmission rate b_{ei} Mbps	26.1	24.4	20.4	15.3	11.9	8.5	5.8	4.7

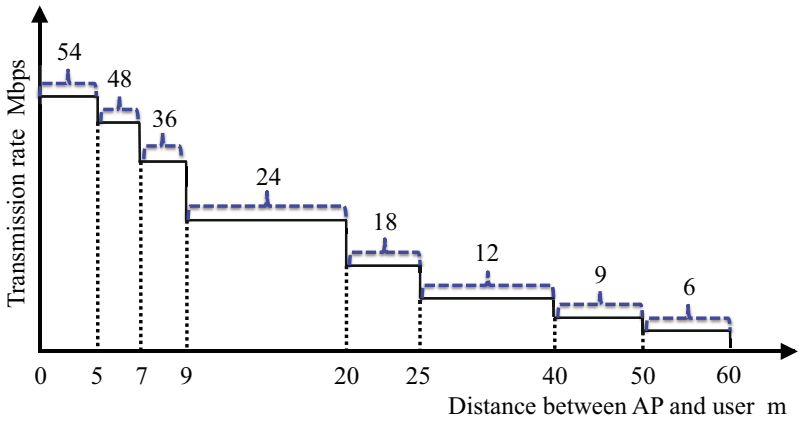

Figure 5.1: Stepped transmission rate.

5.2 Transmission rate of IEEE802.11 and an existing throughput prediction method

Firstly, this section explains the assumption of transmission rate for terminals. In [106], one of the stepped transmission rates is selected as per the distance (Table 5.1). Table 5.1 summarizes the distance, d_i, which is the maximum distance between each terminal and the AP without bit error, transmission rate b_i, which is selected by the AP as per IEEE802.11 a/g (theoretical value), and effective transmission rate b_{ei}, which is the effective transmission rate in a real environment due to the existence of events like collision. Note that index i ($i = 1, 2, \cdots, 8$) is allocated in decreasing order of distance from the AP. If the distance between the AP and the terminal is less than 5 m, the transmission rate of $i = 1$ is selected. If the distance between the AP and the terminal is greater than 60 m, the terminal cannot connect to the AP. In this study, this stepped effective transmission rate according to the distance [106] is used for evaluations (Fig.5.1).

Next, this section explains the issue of the existing throughput prediction method [48]. From Sect. 2.2, it is known that the throughput of the AP can be estimated by Eq.(2.2) in a multi-rate environment [48]. Algorithm 1 shows the procedure of the existing method which is proposed by [48]. Note that the positional information of each terminal is known by the AP. This study calls the AP throughput predicted by Eq.(2.2) the existing throughput value (Th_{exist}). From Eq.(2.2), as the number of the terminals increases, the computational complexity in terms of the sum in the denominator increases linearly. When real-time response is a requirement, complexity has a big impact on throughput

Algorithm 1 An existing method.

Require: $N \geq 0$
Ensure: Th_{exist}
1: $n_{cnt} \Leftarrow 0$
2: $bsum \Leftarrow 0$
3: **for** $j = 1$ to N **do**
4: calculate distance $Dist_j$ between AP and terminal$_j$
5: **if** $Dist_j \leq 60$ **then**
6: select b_j from Table 5.1 according to $Dist_j$
7: $bsum \Leftarrow bsum + (b_j)^{-1}$
8: $n_{cnt} \Leftarrow n_{cnt} + 1$
9: **end if**
10: **end for**
11: **if** $n_{cnt} > 0$ **then**
12: $Th_{exist} \Leftarrow n_{cnt} \times (bsum)^{-1}$
13: **else**
14: $Th_{exist} \Leftarrow 0$
15: **end if**

predictions. For example, when a terminal uses real-time transfer, it must be able to check that the bandwidth is sufficient for the application. Moreover, the processor of a portable AP is low in performance compared to a processor of smartphones. In this situation, even if the calculation cost is linear order, the processing time of the CPU is greatly influenced. However, the predicted value of [48] almost equals the true value.

5.3 High speed throughput prediction method considering terminal distribution

This section is an overview of a throughput prediction method that uses estimates of terminal distribution and details a terminal distribution estimation method. Note that the AP occupies the center of a circular radio transmission area.

5.3.1 Overview of throughput prediction method based on terminal distribution

First, this section defines n_i as the number of terminals communicating at transmission rate b_i ($i = 1, 2, \cdots, 8$) following Table 5.1. By using n_i, Eq.(2.2) can be rewritten as Eq.(5.1):

$$\frac{n_{cnt}}{\sum_{\{j|1\leq j\leq N,\ b_j>0\}} (b_j)^{-1}} = n_{cnt}\left(\sum_{i=1}^{8} n_i b_i^{-1}\right)^{-1}. \tag{5.1}$$

From Eq.(5.1), the computational complexity of the proposed method is $O(1)$ if n_i can be estimated at the cost of $O(1)$. Thus, the time required for throughput prediction is constant regardless of the number of terminals. In Eq.(5.1), n_i and n_{cnt} can be represented as follows:

$$n_i = p_i N, \tag{5.2}$$

$$n_{cnt} = \sum_{i=1}^{8} p_i N. \tag{5.3}$$

In Eq.(5.2) and Eq.(5.3), p_i implies the ratio of terminals whose transmission rate is b_i. In other words, p_i is the probability that the terminal uses b_i. Thus, Eq.(5.1) can be rewritten as follows:

$$Th_{proposed} = \sum_{i=1}^{8} p_i \left(\sum_{i=1}^{8} p_i b_i^{-1} \right)^{-1}. \tag{5.4}$$

From Eq.(5.4), the proposed method can predict the throughput from p_i with cost of $O(1)$. This study refers to the throughput predicted by Eq.(5.4) the proposed throughput value ($Th_{proposed}$). Next, a method to predict p_i with cost of $O(1)$ is discussed. This study assumes that the terminals are placed according to a two-dimensional normal distribution or a uniform distribution. The two-dimensional normal distribution has terminals concentrated near the AP. When the AP is placed in a landmark location, such as an airborne balloon used as an AP in an emergency communication network when a large-scale natural disaster occurs [9], the AP will attract many users. As a result, the distribution of the users follows a normal distribution. Further, as was mentioned before, if nodes are vertically dropped from a certain point in midair, their spatial distribution will result in a two-dimensional normal distribution [87, 88]. Furthermore, a uniform distribution assumes that terminals are widely distributed in an area.

5.3.2 Throughput prediction based on target problem

This section explains the overview of the two-dimensional target problem [89, 90]. Moreover, this section describes the throughput prediction method based on the target problem. The overview of the target problem is described in Chapter 4.

The proposed estimation method uses the miss probability $Y(r)$ (Eq.(4.3)), where r is the radius of the target. From Eq.(4.3), the number of terminals using each transmission rate can be estimated. As a result, this method can predict the throughput with $O(1)$. This study assumes that the AP is placed at the origin of the system field, and the terminals are distributed according to two-dimensional $N(0, \sigma^2)$. This section considers the probability of a terminal that lies outside the area of radius d_{i-1} (d_i is the threshold of the distance at which the transmission rate changes, $d_0 = 0$)), but within the area of radius d_i ($> d_{i-1}$). In Fig.5.2, this probability means the probability that the terminal lies in the colored area. From Eq.(4.3), the probability that a terminal lies outside the area of radius d_{i-1} and d_i are $Y(d_{i-1})$ and $Y(d_i)$, respectively. Thus, the ratio of the number of terminals, p_i, whose transmission rate is b_i, is defined as follows:

$$p_i = Y(d_{i-1}) - Y(d_i) \qquad (i = 1, 2, \cdots, 8). \tag{5.5}$$

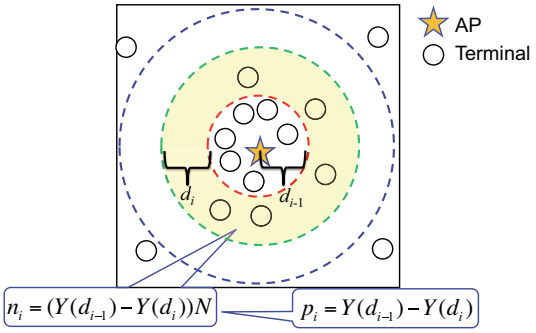

Figure 5.2: Throughput prediction using target problem.

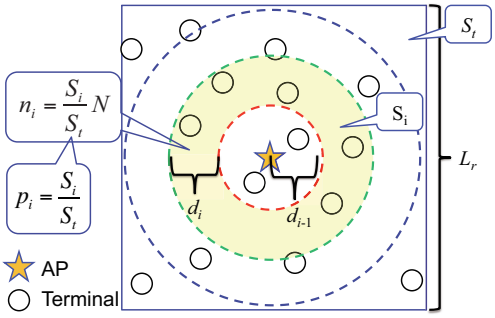

Figure 5.3: Throughput prediction using area ratio.

By substituting p_i for Eq.(5.4), the method can predict the throughput. In addition, this calculation can be performed using $O(1)$.

5.3.3 Throughput prediction based on area ratio

This section describes a throughput prediction method based on the area ratio of the system field wherein the terminal exists. This method uses a circular area whose radius is defined by the transmission rate. In this method, network structure is limited to a uniform distribution. To simplify, this section assumes that the AP is located in the center of the system field (the origin of the field) wherein the terminals exist, and the system field is a square with sides of L_r. In this method, S_t $(= L_r^2)$ denotes the area wherein terminals exist. Moreover, S_i means the area beyond radius d_{i-1}, but within radius d_i $(> d_{i-1})$. In Fig.5.3, this area means that the terminal exists in the colored area. S_i can be obtained by Eq.(5.6):

$$S_i = \pi(d_i^2 - d_{i-1}^2) \qquad (i = 1, 2, \cdots, 8). \tag{5.6}$$

Thus, the ratio of the number of terminals, p_i, whose transmission rate is b_i, is described as follows:

$$p_i = S_i(S_t)^{-1} \qquad (i = 1, 2, \cdots, 8). \tag{5.7}$$

By substituting p_i for Eq.(5.4), the method can predict the throughput. In addition, this calculation can be performed using $O(1)$.

5.3.4 Algorithm of the proposed method

This section explains the algorithm of the proposed method. From the above description, the proposed method uses a target problem for throughput prediction if the terminals are placed according to a two-dimensional normal distribution. If the target problem is used for the prediction, the input of the proposed method is σ. On the other hand, the proposal uses the area ratio for the throughput prediction if the terminals are placed according to a uniform distribution. In this situation, the input of the proposed method is S_t. An estimation method for σ is proposed in Chapter 4 (Eq.(4.10)). Moreover, this study

Algorithm 2 Throughput prediction method of the proposed method.

Require: $\sigma \geq 0$ or $S_t \geq 0$
Ensure: $Th_{proposed}$
1: $psum \Leftarrow 0$
2: $pbsum \Leftarrow 0$
3: **for** $i = 1$ to 8 **do**
4: calculate p_i by Eq.(5.5) or Eq.(5.7)
5: select b_i from Table 5.1
6: $psum \Leftarrow psum + p_i$
7: $pbsum \Leftarrow pbsum + p_i \times (b_i)^{-1}$
8: **end for**
9: **if** $psum > 0$ **then**
10: $Th_{proposed} \Leftarrow psum \times (pbsum)^{-1}$
11: **else**
12: $Th_{proposed} \Leftarrow 0$
13: **end if**

Algorithm 3 A selection mechanism of prediction formulas.

Require: $N \geq 0, \sigma \geq 0, S_t \geq 0$
Ensure: Using formula for the throughput prediction
1: Count n_1, which is the number of terminals that use the maximum transmission rate
2: $P_{max} \Leftarrow n_1 N^{-1}$
3: **if** $|P_{max} - (p_1$ of Eq.(5.5)$)| < |P_{max} - (p_1$ of Eq.(5.7)$)|$ **then**
4: Use Eq.(5.5) for the throughput prediction
5: **else**
6: Use Eq.(5.7) for the throughput prediction
7: **end if**

assumes that S_t can be measured in advance. The output is the prediction throughput $Th_{proposed}$. Based on the above, Algorithm 2 summarizes the procedure of the proposed throughput prediction method.

5.3.5 Adaptive selection mechanism of prediction formulas

The proposed method is necessary to appropriately change the p_i according to the terminal distribution. That is, it is necessary to change the throughput prediction formula according to the terminal distribution. This section discusses the adaptive selection mechanism of prediction formula using the estimation method of the terminal distribution [114]. Note that the estimation method of terminal distribution predicts the terminal distribution using the information that AP can easily obtained. In particular, the estimation method of a terminal distribution uses a ratio of the terminal communicating with a maximum transmission rate (From Table 5.1, it is 26.1 Mbps.) P_{max}. Note that the transmission rate of the terminal can be obtained through a field of the transmission rate that exists in a frame. Here, Fig.5.4 shows the numerical results of P_{max} in each L_r. P_{max} is obtained by substituting $i = 1$ for Eqs.(5.5) and (5.7). In the normal distribution, the

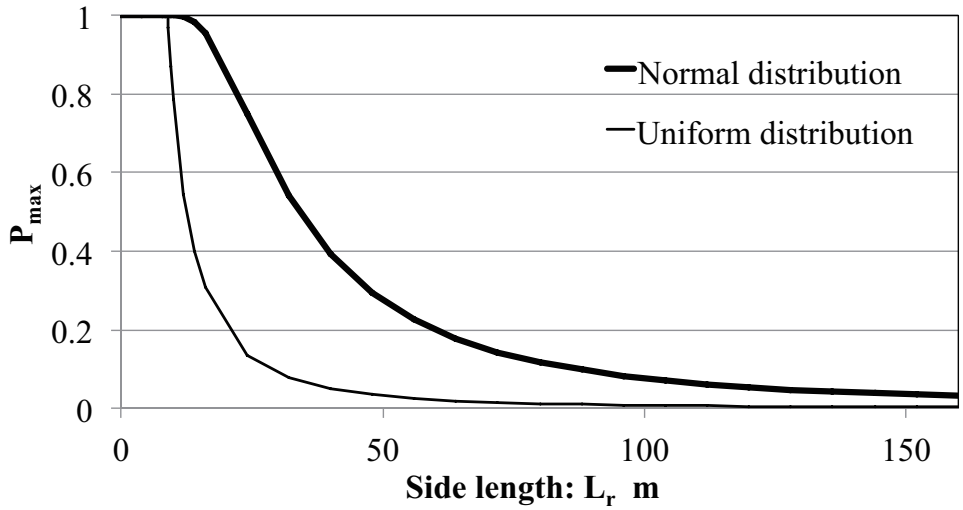

Figure 5.4: Ratio of terminals that use the maximum transmission rate.

value of σ equals to $L_r/8$ [31]. From Fig.5.4, the value of P_{max} for normal distribution and that for uniform distribution in each L_r differ greatly. Thus, a prediction formula can be selected using P_{max}.

Next, the procedure of selection mechanism of the prediction formula is discussed. In this study, the number of all the terminals N is known by the AP. First, the AP counts the number of terminals that are communicating at a maximum transmission rate n_1. Specifically, the AP transmits a beacon for terminals in a modulation scheme whose transmission rate is maximized. If a terminal receives the beacon, the terminal sends a reply such as a connection request for the AP. By counting the received replies, the AP can obtain n_1. Here, the beacon whose transmission rate is maximized can be received only neighbor terminals of the AP. An effective transmission rate, which is assumed in this study, can be achieved only at a terminal within 5 m from the AP. That is, neighboring terminals from the AP can only send the reply. Therefore, the AP can calculate n_i. The issue of this method is that the worst calculation cost is $O(N)$. However, the method of [48] requires the distance between the AP and all terminals for the estimation of terminal distribution. The proposed method can predict terminal distribution by investigating less than or equal to the number of terminals compared to [48][1)]. Future work discusses the prediction method of terminal distribution in a constant order. Secondly, the AP calculate P_{max} using n_1. Then, the absolute difference between P_{max} and p_1 of Eq.(5.5) and Eq.(5.7) are compared. The AP's throughput is predicted using the equation that the absolute difference is smaller. Algorithm 3 shows the procedure of the estimation method of the terminal distribution.

[1)]If $n_1 = N$, the calculation cost of the proposed method equals to that of [48].

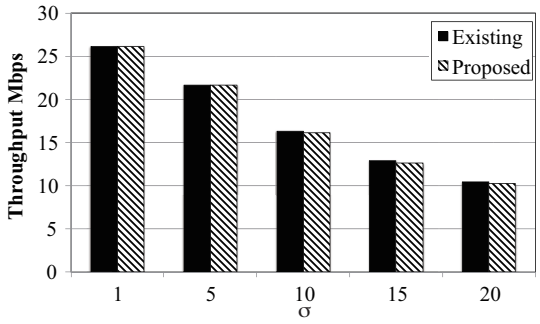

Figure 5.5: Throughput of an AP that is predicted by each method (normal distribution, 10 terminals).

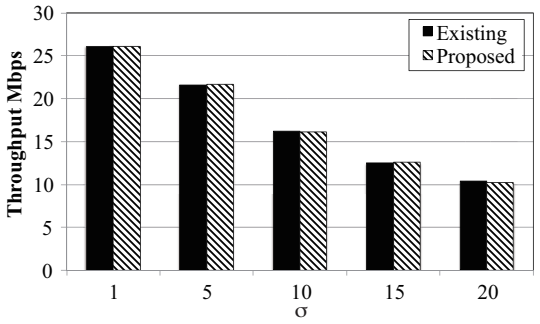

Figure 5.6: Throughput of an AP that is predicted by each method (normal distribution, 20 terminals).

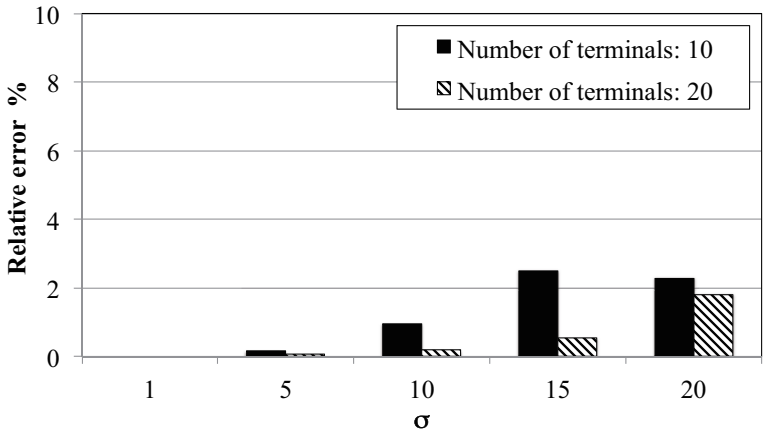

Figure 5.7: Relative error between the proposed method and the existing method in each σ.

5.4 Evaluation

This section compares the proposed method with the existing method [48] in terms of their predicted distances between the AP and each terminal. Moreover, this section evaluates the relative error between the existing method and the proposed method. This evaluation uses the effective transmission rates in Table 5.1. Terminal distribution follows a two-dimensional normal distribution (Sect. 5.4.1) and a uniform distribution (Sect. 5.4.2), and the AP is aware of the number of terminals and σ, or the field size S_t. Furthermore, Sect. 5.4.3 evaluates the effectiveness of the adaptive selection mechanism of predicting formulas. Sect. 5.4.4 shows the evaluation of a calculation cost of the proposal. Note that the calculation cost means the number of the steps of the algorithm.

5.4.1 Results of normal distribution

This evaluation assumes a two-dimensional plane. The AP is placed at $(0, 0)$, and the terminals are distributed according to two-dimensional $N(0, \sigma^2)$; the number of termi-

nals is 10 or 20. Note that in practice, the highest number of terminals that can connect to one AP is 20 [115]. This distribution reproduces an environment wherein many terminals congregate around the AP, because the terminals know that the communication quality improves, and thus the transmission rate rises, closer to the AP. Additionally, if the distance between the AP and the terminal is greater than 60 m, the transmission rate of the terminal is 0 bps (the terminal cannot communicate with the AP). In this evaluation, σ, which is the parameter of the normal distribution is set to 1, 5, 10, 15, and 20, and the AP is aware of σ and the number of terminals N. Experimental results are the averages of 60 trials. From chapter 4, the relationship between σ and the distance D_{max} between the AP and the terminal farthest from the AP is obtained by Eq.(4.10). Therefore, the system field can be regarded as a square, and the side length of the system field L_r is 8σ for all values of σ. Here, the relative error, E_r, in throughput estimates between the existing method and the proposed method is determined as Eq.(5.8):

$$E_r = |Th_{proposed} - Th_{exist}|(Th_{exist})^{-1}. \tag{5.8}$$

Note that this evaluation uses as throughput that on the UDP level.

Figure 5.5 and Fig.5.6 show the prediction throughput estimate outputs for both methods for terminal numbers of 10 and 20, respectively. In Fig.5.5 and Fig.5.6, the horizontal axis plots σ, and the vertical axis plots the throughput. These simulations show that the proposed method outputs almost the same throughput estimates as the existing method. Moreover, the throughput decreases as σ increases. This is because many terminals become more widely distributed in the system field as σ increases. This may trigger the Performance Anomaly problem since some terminals will have a low transmission rate (see Sect. 2.2).

Next, Fig.5.7 shows the relative error between the proposed method and the existing method at each σ. In Fig.5.7, the horizontal axis plots σ, and the vertical axis plots the relative error. From this result, the maximum relative error of the proposal for all σ values examined is around 2.4 % and 1.9 % for terminal numbers of 10 and 20, respectively. Thus, the error of the proposed method is very small if σ is known. Moreover, the result gained with 20 terminals is better than that with 10 terminals. This is because the deviation of the terminal distribution occurs when the number of terminals is 10 compared with the case where the number of terminals is 20. As a result the error increases.

5.4.2 Results of uniform distribution

This evaluation assumes the same 2 dimensional plane for the evaluation environment. The AP is placed in $(0, 0)$, and the terminal distribution is uniform; the number of terminals is 10 or 20. Note that the system field is a square with side length of L_r. Therefore, $S_t = L_r^2$. Moreover, the range of uniform distribution is $[-L_r/2, L_r/2]$. The evaluation in this section considers L_r values of 5, 10, 30, 50, 70, 90, and 120 m. The AP knows S_t and the number of terminals. The following results are the averages of 60 trials.

Figure 5.8 and Fig.5.9 show the throughput predicted by both methods for terminal numbers of 10 and 20, respectively. In Fig.5.8 and Fig.5.9, the horizontal axis plots L_r, and the vertical axis plots the throughput. From this simulation results, the proposed method almost matches the performance of the existing method.

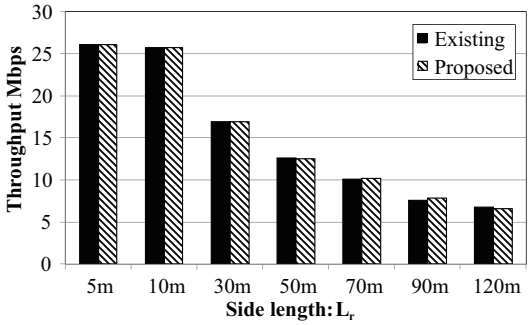

Figure 5.8: Throughput of an AP that is predicted by each method (uniform distribution, 10 terminals).

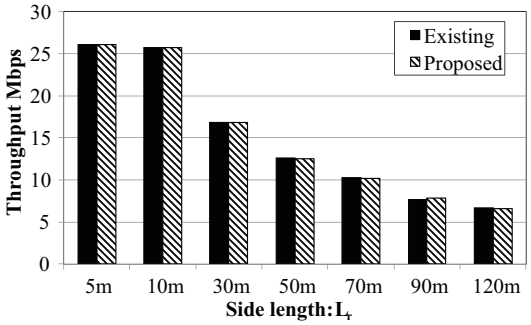

Figure 5.9: Throughput of an AP that is predicted by each method (uniform distribution, 20 terminals).

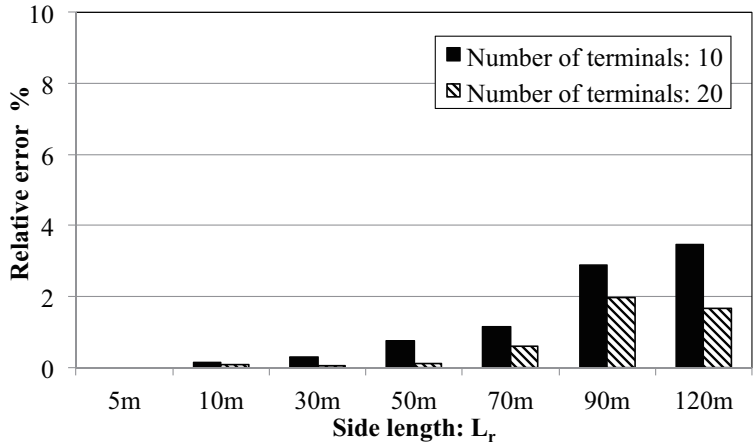

Figure 5.10: Relative error between the proposed method and the existing method in each L_r.

Figure 5.10 shows the relative error between the proposed method and the existing method at each L_r value. In Fig.5.10, the horizontal axis plots L_r, and the vertical axis plots the relative error. This result shows that the maximum relative error of the proposed method, for all L_r values examined, is around 3.7 % and 2.0 % for terminal numbers of 10 and 20, respectively. Moreover, the difference at 10 terminals is bigger than that at 20 terminals. The reason is same as the case of normal distribution. In addition, the relative error tends to increase when L_r increases. In other words, the prediction error tends to increase if the terminals are widely dispersed. However, multiple APs in the system field if the system field size is large. It may be possible to reduce the error by applying a prediction equation for each AP.

5.4.3 Evaluation for adaptive selection mechanism of prediction formulas

In this section, the adaptive selection mechanism of prediction formulas that is proposed in Sect. 5.3.5 is evaluated. The terminal distribution is two-dimensional $N(0, \sigma^2)$

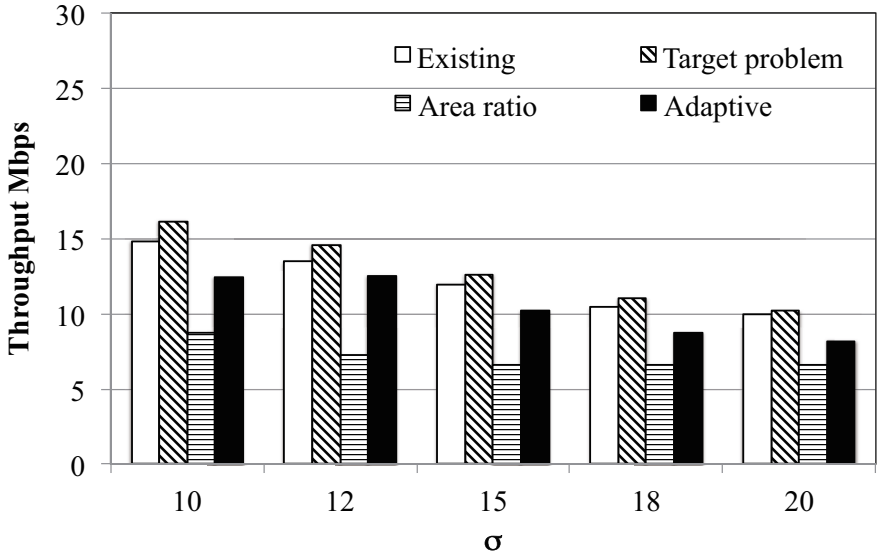

Figure 5.11: Throughput of an AP that is predicted by each method in each σ using the adaptive selection mechanism of the prediction formulas (normal distribution, v = 1.0 m/s).

Table 5.2: Relative error between the proposed method and the existing method in each σ using the adaptive selection mechanism of the prediction formulas (v = 1.0 m/s).

σ	Target problem %	Area ratio %	Adaptive %
10	8.9	41.2	16.2
12	8.3	46.2	7.1
15	5.2	45.0	14.4
18	5.7	36.9	16.6
20	2.6	34.0	17.7

/ uniform; the number of terminals is 20. The aim of this evaluation is to clarify the effectiveness of the adaptive selection mechanism of prediction formulas. Therefore, the AP knows the number of terminals that use the maximum transmission rate for communication. This evaluation assumes mobile terminals. Terminal movement is set by a random waypoint model every second, and the average velocity of each terminal v is 1 m/s. The simulation time is 180 sec and the throughput of the AP is predicted every second. The number of trials of the simulation is 60 in each σ and L_r. The system and other simulation parameters are the same as the previous evaluations. This evaluation compares the throughput obtained from the proposed method with the one obtained from the existing method [48] (*Existing*). This evaluation also shows the results when only the target problem is used for the prediction (*Target problem*) and only the area ratio is used for the one (*Area ratio*).

Figure 5.11 shows the average throughput in 180 sec estimated by each methods when the initial terminal distribution is according to the normal distribution. In Fig.5.11,

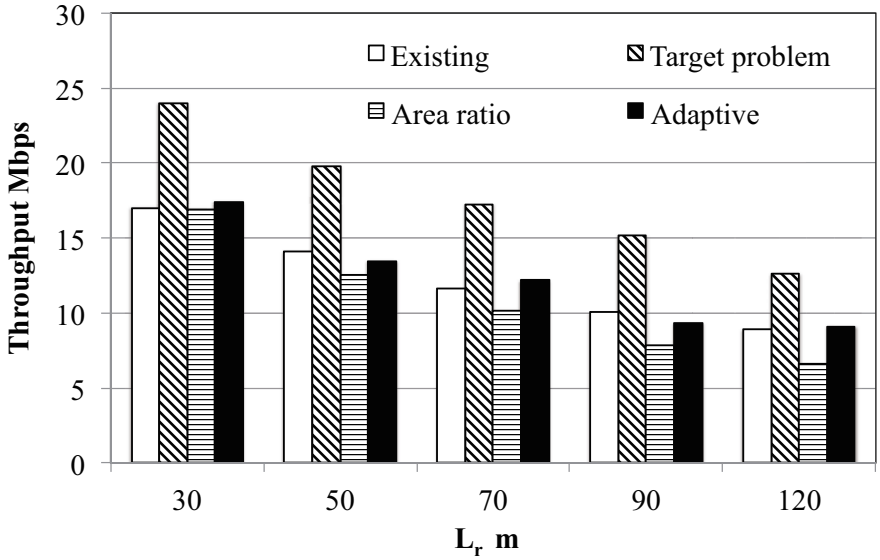

Figure 5.12: Throughput of an AP that is predicted by each method in each L_r using the adaptive selection mechanism of the prediction formulas (uniform distribution, v = 1.0 m/s).

Table 5.3: Relative error between the proposed method and the existing method in each L_r using the adaptive selection mechanism of the prediction formulas (v = 1.0 m/s).

L_rm	Target problem %	Area ratio %	Adaptive %
30	40.9	0.5	2.5
50	40.5	10.9	4.6
70	48.6	12.3	4.9
90	50.8	22.2	6.9
120	41.1	26.3	2.1

the horizontal axis and the vertical axis mean σ and the throughput, respectively. From Fig.5.11, the throughput of the adaptive selection mechanism (*Adaptive*) is almost the same as that of the Existing. Furthermore, the result of Adaptive is almost the same as that of the Target problem, and a more accurate result can be obtained compared to the result of Area ratio. That is, if the terminal distribution is not known, the proposal almost matches the performance of the existing method when using adaptive selection mechanism.

Next, Table 5.2 shows the relative error between the Existing and other methods at each σ. From Table 5.2, the value of the relative error between the Existing and the Adaptive is greater than the result between the Existing and the Target problem. However, the relative error of the Adaptive is less than that of the Area ratio. In particular, the maximum relative error is 46.2 % if the area ratio is only used for the throughput prediction, but the maximum relative error is 17.7 % when the adaptive selection mechanism is used. In addition, the maximum relative error is 8.9 % when the target problem

is only used. This is because the position of terminals does not collapse immediately by the movement of terminals after the simulation starts. In this situation, the relative error is large when the area ratio is only used for the prediction. However, the Adaptive can reduce the relative error by selecting the prediction equation. Table 5.2 also shows that the relative error in Area ratio decrease when the value of σ increases, because the ratio of the terminal communicating with a maximum transmission rate for the Area ratio is almost the same as that of the Target problem (Fig.5.4).

Next, Fig.5.12 shows the average throughput in 180 sec estimated by each methods when the initial terminal distribution is according to the uniform distribution. In Fig.5.12, the horizontal axis and the vertical axis are L_r and the throughput, respectively. From Fig.5.12, Adaptive is almost the same as the one of the Existing. Furthermore, the result of Adaptive yields more accurate results compared to the result of the Target problem. This is because Target problem estimates large amount of the number of high transmission rate terminal. As a result, the result of Target problem is greater than the one of the Existing. Moreover, the result of Adaptive yields more accurate results compared to the result of Area ratio, because the prediction value is lower than that of Existing if the terminals are gathered locally in the center of the area by the movement. From these discussion, Adaptive can overcome these issues.

Finally, Table 5.3 shows the relative error between the Existing and other methods in each L_r. From Table 5.3, the maximum relative error is 26.3 % if the area ratio is only used for the throughput prediction, and the maximum relative error is 50.8 % when the Target problem is only used. On the other hand, the maximum relative error is 6.9 % for the Adaptive.

From these result, the adaptive selection mechanism of prediction formulas is effective. If the terminal distribution is not known, a more accurate throughput of the AP can be predicted using this proposal.

5.4.4 Evaluation of calculation cost

This section evaluates the calculation cost of the proposal. In this chapter, the mean of the calculation cost is the number of steps required to realize the algorithm. The algorithm of the existing method is shown in Algorithm 1, and that of the proposal is shown in Algorithm 2. Note that this evaluation assumes that both the distance between the AP and each terminal and the terminal distribution is known. In other words, the 4-th step of Algorithm 1 and Algorithm 3 are not operated. From Sect. 5.3.2 and Sect. 5.3.3, p_i can be obtained by one operation (Eq.(5.5) or Eq.(5.7)).

Figure 5.13 shows the relationship between the number of all terminals in the system N and the number of steps of each algorithm for one prediction. In Fig.5.13, the vertical axis and horizontal axis indicate the number of steps and the number of terminals, respectively. From Fig.5.13, if the number of terminals is less than 8, the number of steps of the existing method is less than that of the proposal, but the number of steps is more than 8, the number of steps of the proposal is less than that of the existing method. Nowadays, many devices such as smartphones, tablet PCs, AV devices, and consumer electronics correspond to the wireless LAN [116]. Thus, typically more than 8 devices are connected to one AP.

Next, Fig.5.14 shows the relationship between the number of terminals N and the

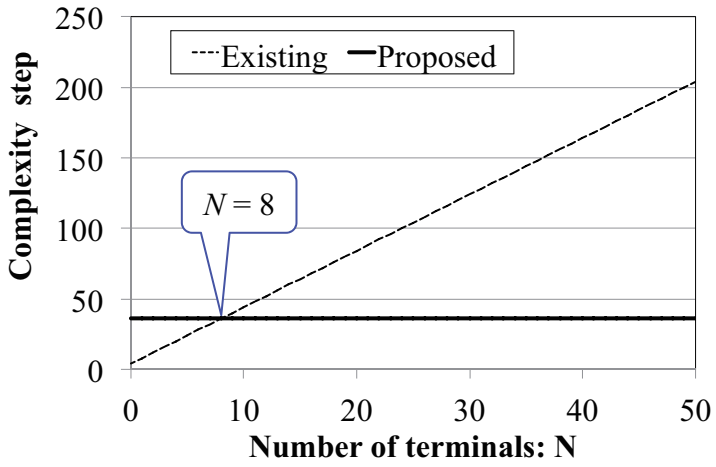

Figure 5.13: Number of terminals v.s. complexity.

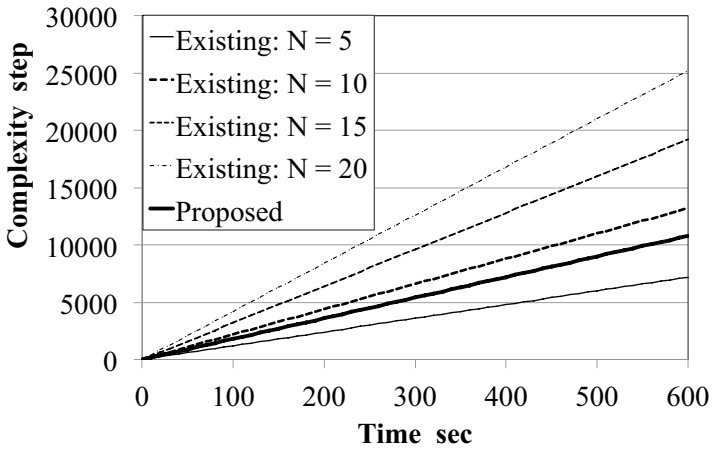

Figure 5.14: Accumulated complexity.

number of accumulated steps of each algorithm when the throughput prediction is operated in each Δt sec. In this section, Δt equals to 2 sec [117]. In Fig.5.14, the horizontal axis indicates the time and the vertical axis shows the accumulated steps. From Fig.5.14, if the number of terminals equals to 5, increasing the accumulated steps of the proposed method is faster than that of the exiting method. However, if the number of terminals is more than 10, increasing the accumulated steps of the existing method is faster than that of the proposal.

From these discussion, if the number of terminals is more than 8, the number of steps for the proposal is less than the one of the existing method. From Sect. 5.4.1 and Sect. 5.4.2, the relative error increases if the number of terminals is small. Therefore, in order to reduce the relative error and the number of steps, if the number of terminals is more than 8, the proposed method is used for throughput prediction. Furthermore, the existing method is used when the number of the terminals is less than 8.

5.5 Conclusion

This chapter proposed a rapid AP throughput prediction method in multi-rate wireless LAN environments that uses a new method of estimating terminal distribution. This chapter showed that the proposed method can reduce the calculation cost to $O(1)$. Moreover, this chapter compared the proposed method to an existing method that determines the harmonic average of terminal transmission rates. In addition, this chapter evaluated two situations where terminal locations follow a normal distribution and a uniform distribution in the system field. Simulations showed that the proposed method can output almost the same predicted values as the existing method but at low calculation cost of $O(1)$; the relative error increases when terminals are distributed widely in the system field. Additionally, this chapter compared the calculation cost of the proposed method and the existing method. Note that the calculation cost refers to the number of steps of each algorithm. From evaluations, the number of steps of the proposed method is less than that of the existing method if the number of terminals connected to the AP is greater than 8. Future works include the following evaluations:

- Evaluation considering real environments such as TCP flow case and CSMA/CA
- Evaluation of the proposal by using a network simulator [118]
- Evaluation considering bidirectional flow
- Evaluation considering other terminal distribution
- Application for the load balancing method for APs

Chapter 6

A Proposal of Access Point Selection Method Based on Cooperative Movement of Both Access Points and Users

This chapter proposes and evaluates an AP selection method based on cooperative movement of both APs and users.

6.1 Introduction

Recently, wireless LANs based on the IEEE 802.11 standard [1] have been spreading rapidly, and connecting to the Internet using this technology has become more common. In addition, the number of public wireless LAN service areas, such as train stations, hotels, and airports, are increasing. A more recent trend is the popularity of portable APs, such as mobile Wi-Fi routers. In addition, the tethering technology has enabled smartphones to act as AP. Consequently, multiple APs can exist in the same area. In this situation, wireless terminal users must select one of many APs.

The standard wireless LAN protocol based on IEEE 802.11 usually selects the AP with the highest Received Signal Strength Indicator (RSSI) [2]. However, even if there are multiple APs, this AP selection method causes uneven AP loading when wireless terminals are disproportionately distributed to a single AP. It causes traffic congestion and AP overload, which greatly reduces communication quality. [102] shows that an AP selection method that considers the highest RSSI value may not provide fair bandwidth allocation or effective bandwidth utilization in environments such as train stations and hotel lobbies. Furthermore, multi-rate wireless LAN environments where terminals use multiple transmission rates suffer from a performance anomaly [47, 119]. This performance anomaly causes throughput degradation because the AP is connected to a terminal with an extremely low transmission rate. As a result, the communication quality decreases drastically.

To solve this problem, various AP selection methods [106, 120–130] have been proposed and evaluated. In particular, [106] proposed an AP selection method based on

cooperative movement of a new joining user and demonstrated that it improves system throughput (User-Only-Mobility Method: UOMM). Note that the system throughput means the sum of the throughput of all APs in the system. The proposed AP selection method [32] is based on the aforementioned study [106]. Other studies [131–135] have shown the effectiveness of cooperative mobility of users. For example, [131] proposed a traffic control method based on user collaboration, and [132] introduced a mechanism to increase the spectral efficiency of cellular OFDMA systems through the cooperation of users accessing wireless cellular networks. In addition, [133–135] revealed the relationship between route selection of the device user and communication quality.

Previous studies have not considered AP mobility; however, AP mobility will become more common in the future. Here, it is expected that the throughput can be improved dramatically by considering the cooperative movements of both APs and users. Note that this study primarily assumes a mobile AP (3G/LTE equipped portable Wi-Fi AP) that can move easily rather than a fixed AP. The example of AP movement is that the device owner moves a mobile Wi-Fi router to a more convenient location in a conference room. This chapter proposes an AP selection method based on cooperative movements of both APs and users (User-AP-Cooperative-Mobility Method: UACMM) [32]. Furthermore, this chapter evaluates the characteristics of UACMM [33]. Additionally, this chapter evaluates the system throughput under the assumptions that the movable distance of both users and APs are discrete values or continuous values [34]. The main purpose of this chapter is to clarify the effectiveness of cooperative movement of both the user and the AP. Essentially, this chapter attempts to clarify the relationship between the cost (sum of the distance between an AP and users) and the improvement of system throughput by numerical simulations.

The remainder of this chapter is organized as follows. Section 6.2 describes the overview of UOMM. Next, Sect. 6.3 introduces the UACMM. This chapter then evaluates the UACMM in Sect. 6.4. Finally, Sect. 6.5 provides conclusions and suggestions for future work.

6.2 UOMM: AP selection method based on user cooperative movement

This section provides an overview of the AP selection method based on user cooperative movement [106]. Note that this chapter calls this method User-Only-Mobility Method (UOMM). This chapter uses the UOMM as a baseline in comparative evaluations. The UOMM maximizes the system throughput Θ by cooperative actions of a new joining terminal (new user). Note that Θ indicates the sum of the throughput of all APs in the system. The action is to move the new user to the AP within an acceptable area (distance) before establishing connection.

The new user has movable distance d_{th}, and the new user attempts to connect to the AP that can maximize Θ. To improve the user and system throughput, the new user is assumed to be willing to move up to d_{th}. From chapter 5, [106] investigated the relationship between the transmission rate of the terminal and the distance between the AP and the terminal (Table 5.1). Furthermore, [106] used the stepped transmission

rates (Fig.5.1) based on the Table 5.1 for their evaluations. This chapter uses the same stepped transmission rate as [106] for evaluations (see Sect. 6.4).

Here, the AP selection of UOMM is performed as follows. First, throughput for all APs in the system is calculated assuming that the new user moves to an AP within d_{th}. If several APs offer the same maximum throughput value, the AP with the shortest move distance is selected. According to the above consideration, the UOMM is defined as an optimization problem; identifying AP a^* that offers the maximum Θ and minimum move distance $\mathbf{m}^*$ with a new user connection. Note that the maximum movable distance of the user is d_{th}. In this chapter, the mean of *move distance* is the distance which users have actually moved. Furthermore, the mean of *movable distance* is the distance which users may move. That is, the user move distance is less than d_{th}.

6.3 UACMM: AP selection method based on user-AP-cooperative-mobility

This section describes the proposed AP selection method based on cooperation of both the AP and the user movement, and this chapter calls this method User-AP-Cooperative-Mobility Method (UACMM). For simplicity, this section explains the procedure for selecting a single AP.

6.3.1 Overview of UACMM

The UACMM is illustrated in Fig.6.1. This method is an extension of [106], in which movable distance is set for both users and APs. The UACMM defines the movable distance of a new user and that of the ith AP as d_{th} and $e_{i,th}$, respectively. n_a denotes the number of users connected to the ath AP. The new user and AP can move freely within the specified distance in the system area. The new user selects the AP to maximize system throughput Θ. Here, Θ has the same meaning as above. The new user moves to the position where system throughput can be maximized. The AP moves to maximize Θ while minimizing the reduction in the transmission rates of users already connected to the AP. If there are several APs that can maximize Θ, this method selects the combination that has the shortest move distance for the AP and user. The UOMM is the same as the UACMM if $e_{i,th} = 0$.

To define the UACMM as an optimization problem, an objective function and constraints are defined as follows. The objective function maximizes Θ by connecting the new user to the AP. Θ depends on the selected AP a^*, the move distance of new user to the AP $\mathbf{m}^*$, and move distance of the AP $\mathbf{l}^*_{a^*}$. The constraint conditions are the movable distances of the user and the AP. The maximum movable distance of a new user and maximum movable distance of the ith AP are denoted d_{th} and $e_{i,th}$, respectively. In real environments, the number of users is usually limited by provider policies and AP specifications; thus, in this chapter, the maximum number of users that can connect to any one AP is $N(\geq n_a)$.

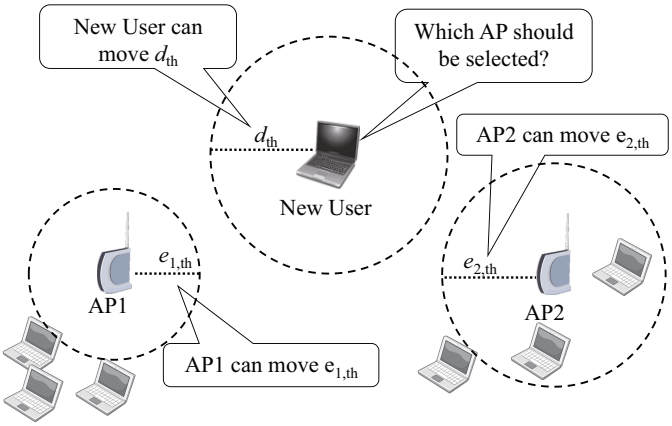

Figure 6.1: AP selection method based on AP cooperative movement of both the AP and the user.

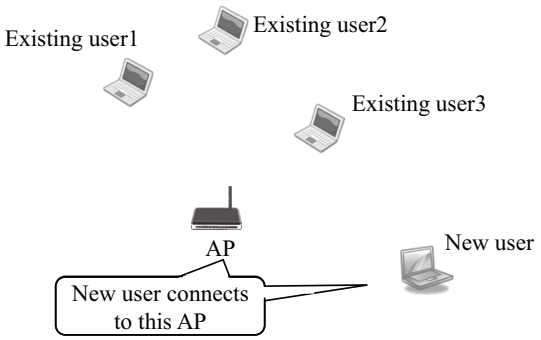

Figure 6.2: Initial position of APs and users.

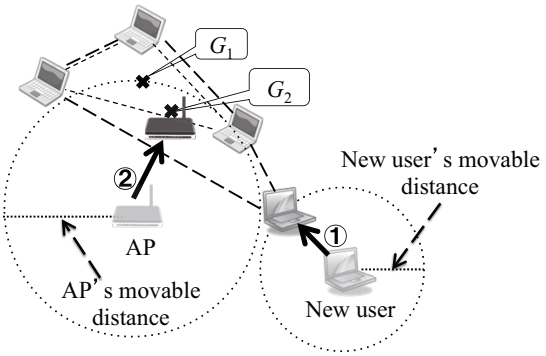

Figure 6.3: Determination of communication position of APs and new users.

6.3.2 Determination of communication position of APs and users to maximize system throughput

This section describes a method that yields the communication positions of APs and users to maximize system throughput. Figure 6.2 illustrates initial positions of the AP and users. In Fig.6.2, three users are currently connected to the AP and one new user intends to connect to this AP. The UACMM assume that each AP and user can determine position information (coordinates) of each terminal using appropriate tools, such as GPS technology. Furthermore, the AP maintains the coordinates of all terminals connected to the AP and instructs the destination for a new joining user in UACMM. Note that the new joining user notifies all APs of its position when the user joins. This control can be operated in an environment where IEEE802.11k [136] is implemented generally. Additionally this system assumes movement on a two-dimensional surface. In other words, users and APs exist on the same plane.

First, the new user moves toward the gravity point (G_1) of the plane formed by all existing users connected to the AP within the new user's movable distance (d_{th}) (Fig.6.3 ①). If the new user can reach G_1, it stops at G_1. If the new user cannot reach G_1, it

stops at the point that minimizes the distance between G_1 and themselves. Here, the gravity point of the plane is defined as the point that minimizes the sum of the squares of the distances from each vertex constituting the plane. By this procedure, throughput will improve for the new and existing users after the AP moves. If there are no existing users, the new user moves to the position of the AP. If only one user is connected to the AP, the new user moves to the position of the existing user. If only two users are connected to the AP, the new user moves to the midpoint of the line connecting both existing users. Next, the AP moves to the gravity point (G_2) of the plane formed by both the new user and all existing connected users. The AP moves up to its movable distance ($e_{AP,th}$) (Fig.6.3 ②). If the AP can reach G_2, it stops at G_2. If the AP cannot reach G_2, it stops at the point that minimizes the distance between G_2 and the AP. In addition, if there is no existing user, the AP moves to the position of the new user. If only one user is connected to the AP, the AP moves to the midpoint of the line connecting the new and existing user. Through movement of the AP and the new user, all existing users and the new user can minimize the distance to the AP without exceeding the movable distance upper limit. Thus, users can communicate at a higher transmission rate because the distance between users and the AP is decreased. As a result, these procedures can maximize system throughput. This strategy uses [137] as a reference. Note that the UACMM performs the above procedures for all APs and only the AP with the maximum Θ value among all APs moves. Algorithm 4 shows the series of actions for the proposed method. In addition, the UACMM can be performed using $O(N_{STA} \cdot N_{AP})$, where N_{STA} is the number of terminals and N_{AP} denotes the number of APs.

Note that this study includes the AP selection problem and the AP placement problem. In addition, improvement of throughput by cooperative movement of both APs and users is demonstrated. These results are useful for AP selection and AP placement. Furthermore, each terminal uses saturated traffic, and this study considers the performance anomaly in the evaluation (see Sect. 6.4). The effect of the performance anomaly depends on the distance between AP and users; therefore, if both AP and users move cooperatively, throughput can be improved effectively. A method for distributing required load information for autonomic load balancing has been investigated [138,139]. Future works include investigation of the distribution of required load information to achieve autonomic load balancing.

Algorithm 4 An algorithm of UACMM.

new user u arrives
user u notifies all AP of both d_{th} and the position of u
$a \Leftarrow 1$
$a^* \Leftarrow 1$
$|\boldsymbol{m}^*| \Leftarrow d_{th}$
$|\boldsymbol{l}_{a^*}| \Leftarrow e_{1,th}$
$\Theta_{a^*} \Leftarrow 0$
while All AP **do**
    AP a calculates G_1, which is the gravity point of the plane formed by all existing users connected to the AP a
    AP a calculates the position of new user and move distance of new user $|\boldsymbol{m}|$
    AP a calculates G_2, which is the gravity point of the plane formed by both all existing users connected to the AP a and new user u
    AP a calculates the next position and move distance $|\boldsymbol{l}_a|$
    AP a calculates system throughput Θ
    if $\Theta_{a^*} == \Theta$ **then**
        if $|\boldsymbol{m}^*| + |\boldsymbol{l}_{a^*}| > |\boldsymbol{m}| + |\boldsymbol{l}_a|$ **then**
            $a^* \Leftarrow a$
            $|\boldsymbol{m}^*| \Leftarrow |\boldsymbol{m}|$
            $|\boldsymbol{l}_{a^*}| \Leftarrow |\boldsymbol{l}_a|$
            $\Theta_{a^*} \Leftarrow \Theta$
            $G_1^* \Leftarrow G_1$
            $G_2^* \Leftarrow G_2$
        end if
    end if
    if $\Theta_{a^*} < \Theta$ **then**
        $a^* \Leftarrow a$
        $|\boldsymbol{m}^*| \Leftarrow |\boldsymbol{m}|$
        $|\boldsymbol{l}_{a^*}| \Leftarrow |\boldsymbol{l}_a|$
        $\Theta_{a^*} \Leftarrow \Theta$
        $G_1^* \Leftarrow G_1$
        $G_2^* \Leftarrow G_2$
    end if
    $a \Leftarrow a + 1$
end while
user u moves toward the G_1
AP a^* moves toward the G_2
user u connects to AP a^*

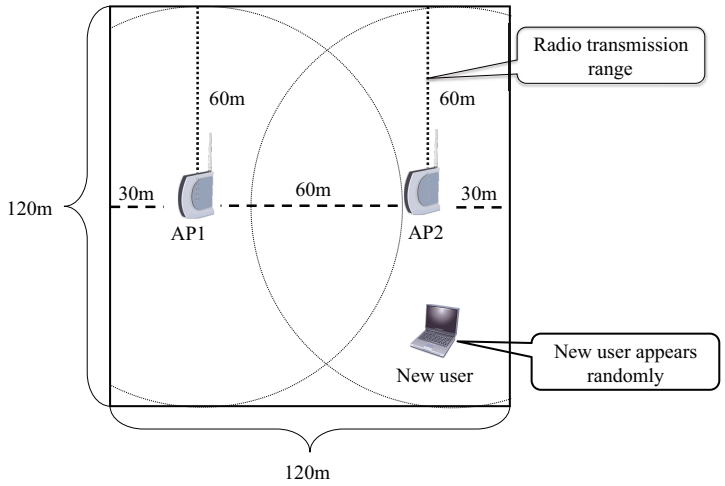

Figure 6.4: Initial configuration of system (1).

6.4 Throughput evaluations

This section evaluates the UACMM using a simulator written in C language. This section focuses on system throughput and average AP throughput. Moreover, this section evaluates the following four characteristics:

I Impact of movable distance of APs on system throughput performance

II Impact of the number of APs on AP throughput performance

III Throughput evaluation when joining and leaving users exist

IV Throughput evaluation considering disconnection methods of a user

Characteristic I shows the effectiveness of AP movement, a key idea of the UACMM. Characteristic II indicates the effectiveness of AP movement in terms of the throughput of each AP. Characteristic III assumes a typical wireless communication environment. Characteristic IV indicates a case when a user who affects communication quality negatively is disconnected to guarantee communication quality. In addition, this section evaluates system throughput under the assumptions that the move distances of both users and APs are discrete or continuous values. Note that AP throughput is calculated by Eq.(2.2). Here, the radio property of the physical layer changes drastically if the communication environment changes. In this situation, MAC characteristics also change because MAC depends on the physical layer. If the physical layer and MAC are assumed, it is expected that the potential effect of cooperative movement becomes unclear. Therefore, this study does not consider the physical layer and MAC in the evaluations. Future work evaluates the UACMM using a network simulator to consider real environment characteristics, such as control overhead and interference between APs.

6.4.1 Movable distance of APs and throughput performance

First, this section evaluates the relationship between system throughput and AP movable distance. Figure 6.4 shows the system configuration used in the evaluation. In a

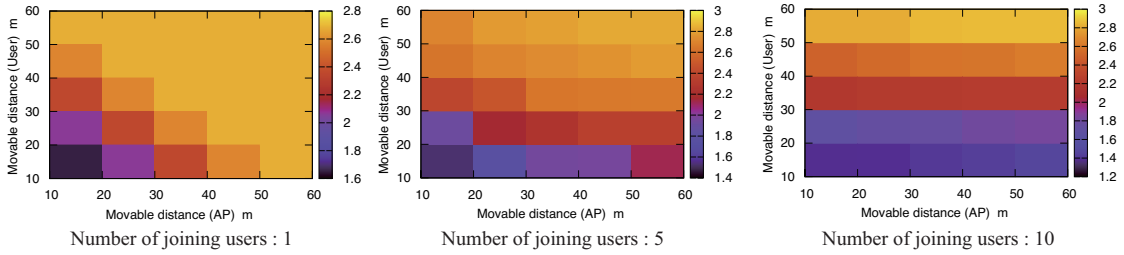

Figure 6.5: Relationship between system throughput and movable distance of both the AP and new user (vs. minimum distance selection method).

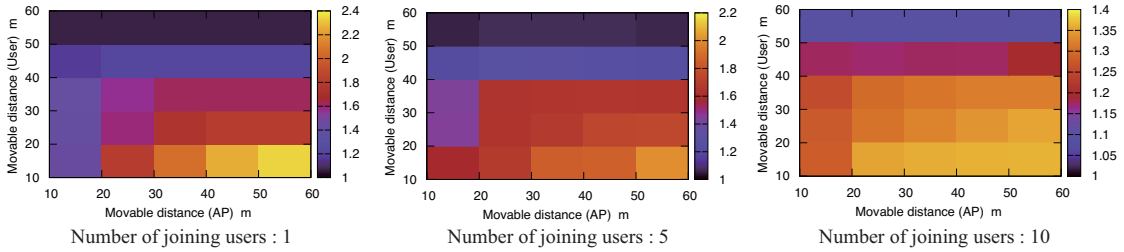

Figure 6.6: Relationship between system throughput and movable distance for both the AP and new user (vs. UOMM).

120 m $\times$ 120 m area, there are APs at coordinates (30 m, 60 m) and (90 m, 60 m). This system configuration follows a previous study [106]. In the initial state, only APs are present. Next, both a x-coordination and a y-coordination of a user is set by continuous uniform random numbers which range is $[0, 120]$. Here, 120 indicates the side length of the system area (see Fig.6.4). Then, the users appear at the position that is decided by the random value in a moment. Also, the users can move to the specified position calculated by the Algorithm 4 in a moment. That is, this evaluation assumes that each user turns on the terminal at two points in the system area, where the initial position of user and destination point calculated by the Algorithm 4. In the evaluations of UACMM and UOMM, the appearance position of users for ith ($1 \leq i \leq 30$) trial is same. All users connect to the AP that offers the highest system throughput. In this situation, the UACMM improves system throughput compared to two existing methods, a minimum distance selection method and UOMM. In the minimum distance selection method, the user connects to the nearest AP without moving. This method is similar to the AP selection method using RSSI values as the metric, which is a common approach. Table 5.1 shows the user transmission rate employed in previous studies, and this study uses the stepped effective transmission rate b_{ei} as the transmission rate. This evaluation assumes saturated UDP flow (the user always has data to send). Each simulation ran for 30 trials, and the results are the averages of the 30 trials. The position of the user changed in each simulation.

Figure 6.5 and Fig.6.6 show the throughput improvement ratio of the UACMM compared to the minimum distance selection method and UOMM, respectively. This section defines the throughput improvement ratio as follows:

$$\text{Improvement ratio} = \frac{Th_{UACMM}}{Th_{existing}}. \tag{6.1}$$

In Eq.(6.1), $Th_{existing}$ is the system throughput of minimum distance selection method or UOMM, and Th_{UACMM} is the system throughput of UACMM. In Fig.6.5 and Fig.6.6, the number of joining users is 1, 5, and 10. In Fig.6.5 and Fig.6.6, the horizontal and vertical axes represent the movable distance of the AP and the movable distance of a new user, respectively. The movable distance of both the AP and the user changes every 10 m. Here, the aim of this study is to clarify the effectiveness of cooperative movement of both the APs and the users, which greatly contributes to the system throughput improvement. Therefore, more detailed evaluation is considered as a future work. In Figs.6.5 and 6.6, the color of the square area ($\eta \leq e_{i,th} < \eta + 10$, $\psi \leq d_{th} < \psi + 10$)($\eta = \{10, 20, 30, 40, 50\}$, $\psi = \{10, 20, 30, 40, 50\}$) means the system throughput improvement ratio where $e_{i,th}$ and d_{th} mean the movable distance of ith AP and the user, respectively. Note that the system throughput improvement ratio of one square includes the boundary of bottom and left side. From Fig.6.5, if the number of joining users is 1, the system throughput for the UACMM is 2.8 times greater than that of the minimum distance selection method when the UACMM can obtain the highest values. In addition, with 5 and 10 users, the UACMM can triple system throughput compared to the minimum distance selection method. However, compared to the minimum distance selection method, when the number of joining users is high and user movement distance becomes short, the UACMM does not improve throughput significantly even if AP movable distance increases because it is difficult to improve throughput by an AP movement due to the large number of users. Therefore, throughput improvement is best achieved by increasing the movable distance of users rather than that of the AP.

Figure 6.6 shows the improvement ratio of system throughput compared to the UOMM. For the UACMM, the movable distance of both APs and new users is 10 m to 60 m. When the number of joining users is 1, the UACMM improves system throughput by up to 2.4 times that of UOMM. If there are 5 and 10 users, system throughput is improved by up to 2.2 times and 1.4 times, respectively. Here, throughput does not improve significantly when user movable distance is greater than 60 m because users can reach a position where they can obtain a higher transmission rate when the user movable distance increases. Therefore, the system can obtain higher throughput without AP movement. In summary, the UACMM can improve throughput significantly compared to existing methods.

Here, this section evaluates the system throughput when the sum of the AP and user movable distance is fixed. The experimental environment is the same as that in the previous evaluations. Figure 6.7 shows the result when the total movable distance is 60 m. In Fig.6.7, the horizontal axis shows the number of joining users in the system, and the vertical axis shows system throughput. Note that the result of UOMM is for the same case when the AP movable distance is 0 m. From Fig.6.7, if the number of joining users is high, the cooperative movement of both APs and users is effective for the system throughput compared to the case when a AP or a user only moves. Furthermore, the UACMM improves system throughput by approximately 25 Mbps compared to results in the UOMM when the number of joining users is 10 and UACMM is (AP: 10 m, User: 50 m). In addition, Fig.6.7 shows that if the number of joining users is high, the system throughput can drastically improve when the movable distance of the user is greater than the one of the AP. This is because that it is difficult to improve the throughput by only using AP movement or user one when a large number of users are widely distributed

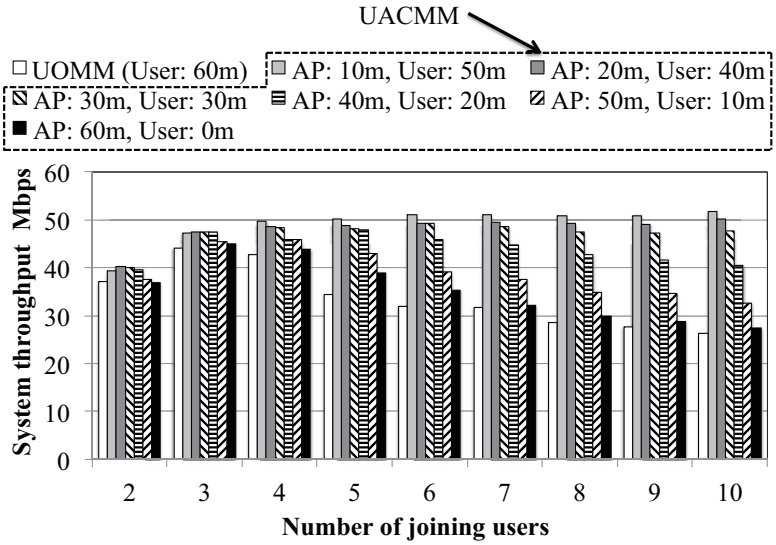

Figure 6.7: Relationship between system throughput and movable distance (total movable distance is 60 m).

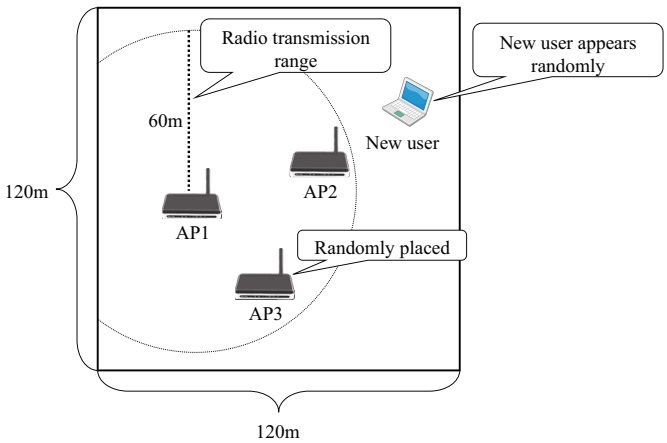

Figure 6.8: Initial configuration of system (2).

in the system area. From this result, if the AP and user movable distances are equal, cooperative movement (AP and user) is more effective than only user movement.

6.4.2 Throughput performance vs. number of APs

This section evaluates the average AP throughput when the number of APs in the system changes. For the evaluation, an area of 120 m × 120 m as in Sect. 6.4.1 is used. In the initial state, a specified number of APs are set in the area (Fig.6.8). Subsequently, users enter the area randomly until the number of users connected to the AP becomes greater than two. At that point, the average AP throughput are calculated. All APs have connected users since the number of user is greater than two. Furthermore, the performance anomaly may occur when at least two or more users connect one AP. The transmission rate, traffic type, and the number of trials of the simulation are the same as those in Sect. 6.4.1.

Figure 6.9 shows average AP throughput with the UOMM and the UACMM. The

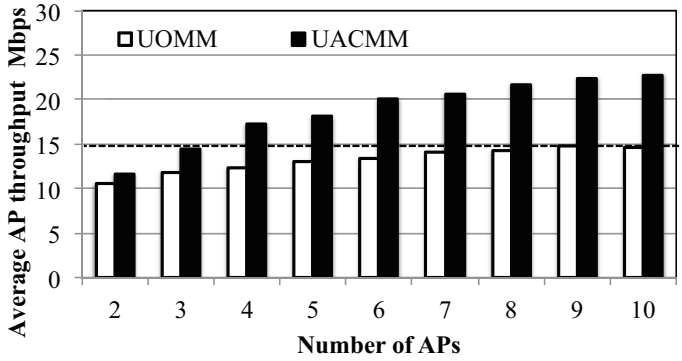

Figure 6.9: Throughput performance vs. the number of APs in the system (movable distance; AP 10 m, new user 10 m).

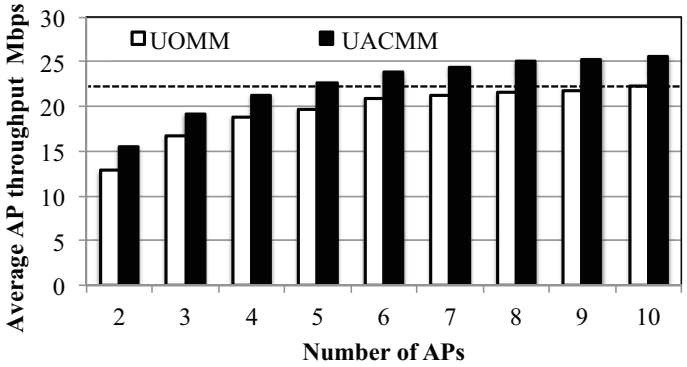

Figure 6.10: Throughput performance vs. number of APs in the system (movable distance; AP 30 m, new user 30 m).

user movable distance is 10 m in both methods, and AP movable distance is 10 m in the UACMM. From Fig.6.9, the maximum difference between the UACMM and the UOMM is approximately 8 Mbps when there are 10 APs. Moreover, with 3 APs, the UACMM attains the same average AP throughput as the UOMM with 10 APs (dotted line in Fig.6.9).

Next, this section discusses the results shown in Fig.6.10 when the user movable distance is 30 m in the UOMM and the movable distance of both users and APs is 30 m in the UACMM. Since the user and AP can move the same distance (30 m), the total movable distance is 60 m. This result shows that the maximum difference between the UACMM and the UOMM is approximately 4 Mbps when there are 9 APs. Moreover, with 5 APs, the UACMM can attain the same average throughput achieved by the UOMM with 10 APs (dotted line in Fig.6.10).

From the above results, it is clear that the UACMM can achieve higher average AP throughput with fewer APs than the UOMM.

6.4.3 Evaluation of throughput when joining and leaving users exist

Join and leave users can be modeled using a queuing model. Here, the M/M/1 queue model is used to model joining and leaving users. In this subsection, the relationships between the utilization rate ρ for M/M/1 join and leave user model and system through-

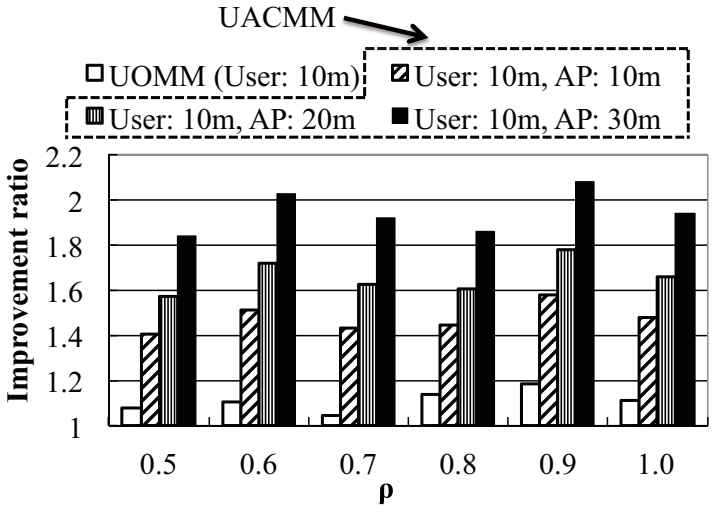

Figure 6.11: Utilization rate (ρ) vs. improvement ratio of system throughput (new user movable distance: 10 m).

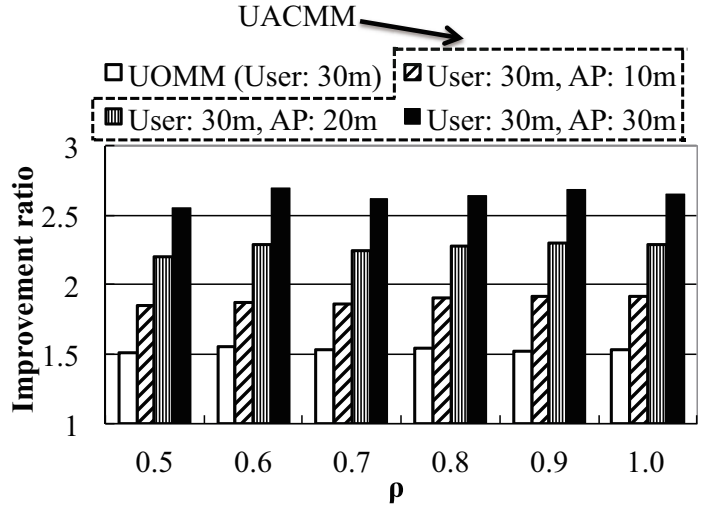

Figure 6.12: Utilization rate (ρ) vs. improvement ratio of system throughput (new user movable distance: 30 m).

put are evaluated. Note that the relationship among ρ, λ, and μ is defined as follows:

$$\rho = \frac{\lambda}{\mu}. \tag{6.2}$$

In Eq.(6.2), λ and μ indicate user arrival rate and service rate, respectively. The system configuration is the same as that in Sect. 6.4.1 (Fig.6.4). In the initial state, there are only APs in the system. Next, the specified number of users appears randomly. Then, all users connect to the AP with the highest system throughput. This evaluations calculates the average throughput until all users leave when ρ changes. Then, the UACMM is compared to the UOMM using throughput improvement ratio based on a minimum distance selection method. The transmission rate, number of trials of the simulation, and traffic type are the same as in Sect. 6.4.1. In this evaluation, the number of joining users is 100, and they have joining time and service time defined by an exponential distribution. The exponential distribution is yielded by a specified utilization rate ρ, user

arrival rate λ, and service rate μ. The service rate μ is 0.1 and the arrival rate λ is set to $\{0.05, 0.06, 0.07, 0.08, 0.09, 0.1\}$. Note that the aim of this section is to show the effectiveness of the cooperative movement of both users and APs for the system throughput. Thus, the more detailed characteristics about the relationship among the arrival rate, the service rate, and the system throughput are evaluated in the future. The number of users that can connect to AP N is 10. If the number of connected user is 10, a new user waits for connecting to an AP until a connected user leaves. Here, this evaluation assumes that a user joins and connects to the AP, and then the user communicates during the service time. When communication is finished, the user shutdowns its terminal and the user leaves the system. The user's terminal sends the saturated UDP flow when the user communicates with an AP.

If there is an upper limit of the connectable user number, the queue length becomes greater as ρ increases. Consequently, the number of users reaches the limit immediately, and the throughput becomes nearly stable, even if the queue length has increased to maximum capacity. Since the distance between an AP and users in the UACMM is less than the UOMM, a user can send data at a higher rate. In addition, the throughput of the UACMM improves.

Figure 6.11 shows the relationship between the throughput improvement ratio and ρ when the movable distance of a user is 10 m. The x-axis and y-axis show ρ and the throughput improvement ratio compared to the minimum distance selection method, respectively. From Fig.6.11, the average improvement ratio of the UOMM is 1.1 times. Conversely, even if ρ changes, the UACMM can improve 1.5 and 1.9 times when the AP movable distance is 10 m and 30 m, respectively.

Figure 6.12 shows similar results when the user movable distance is 30 m. From Fig.6.12, the average improvement ratio of the UOMM is 1.6 times. On the other hand, even if ρ changes, the UACMM can improve 1.9 and 2.6 times when the AP movable distance is 10 m and 30 m, respectively. Therefore, the UACMM can improve throughput dramatically compared with the UOMM even if the frequency of user's join and leave is high.

6.4.4 Evaluation of throughput considering disconnection methods of a user

Here, this section evaluates throughput when the number of connected users reaches the upper limit and one user is forced to disconnect due to a new joining user. In this situation, it is assumed that, given a network policy, the AP disconnects the user with the most negative impact on AP throughput in order to maintain communication quality. This evaluation considers three methods for disconnection and assume that the AP has no resources available for a new user. In the first method, one user is selected randomly (option 1). In the second method, the user furthest from the AP is selected (option 2). In the third method, all users return to their initial position and then move to the optimal position to connect to the AP. Then, the connected user furthest from AP is selected (option 3). The system configuration used in Sect. 6.4.1 is also used in this evaluation. Moreover, the AP has the acceptable number of users N. In this evaluation, there are two APs in the initial system. Then, the acceptable users join the system and they select the

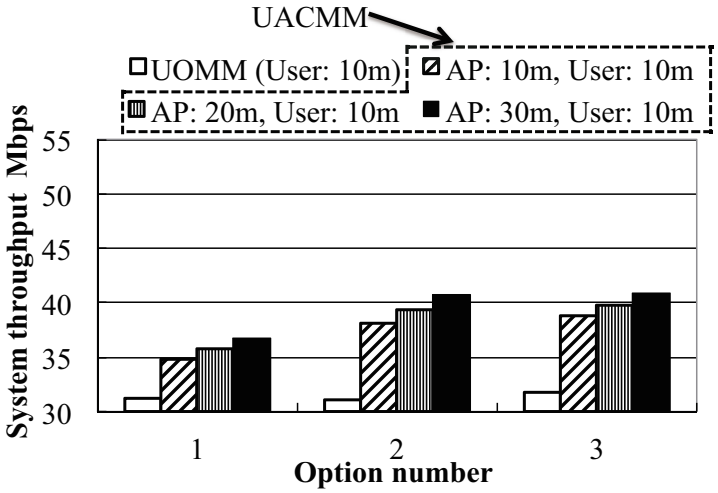

Figure 6.13: Relationship between system throughput and each option (AP capacity: 2, new user movable distance: 10 m).

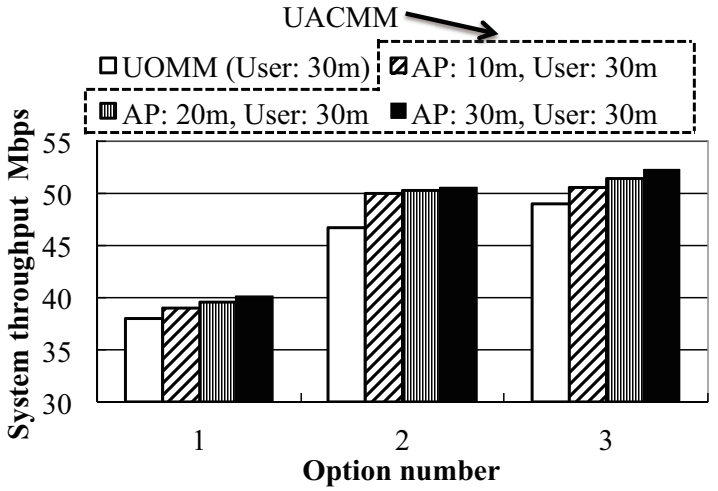

Figure 6.14: Relationship between system throughput and each options (AP capacity: 2, new user movable distance: 30 m).

AP. Furthermore, if one user joins the system, AP disconnects one user according to the option. This evaluation investigates the relationships between the acceptable number of users N and system throughput.

Here, it is expected that the effective selection of the user to be disconnected will affect system throughput. The user furthest from the AP that has the lowest transmission rate decreases system throughput. Thus, rather than selecting randomly, if the user furthest from the AP is selected for disconnection, system throughput can be reduced. In addition, the UACMM can maintain higher throughput compared to the UOMM because the distance between the AP and user in the UACMM is shorter.

Figure 6.13 and Fig.6.14 plot the relationships between each option and system throughput when the acceptable number of users is 2. The x-axis and y-axis show the option number and system throughput, respectively. Figure 6.13 and Fig.6.14 illustrate the case in which the user movable distance is 10 m and 30 m, respectively. The AP movable distance in each figure is set to 10 m, 20 m, and 30 m. From Fig.6.13, the

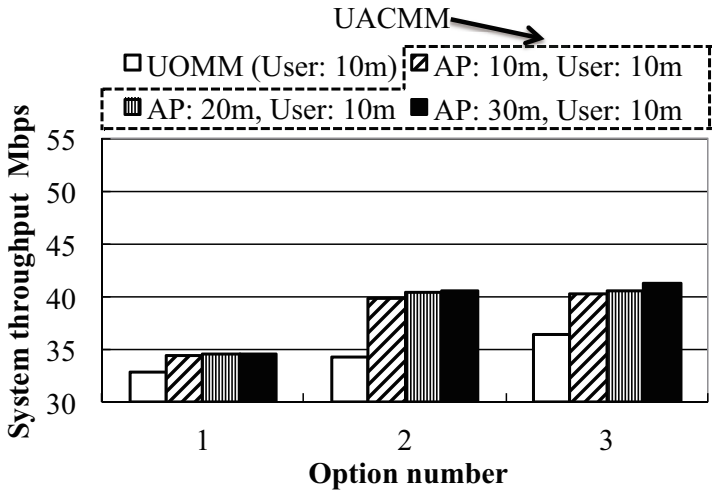

Figure 6.15: Relationship between system throughput and each option (AP capacity: 10, new user movable distance: 10 m).

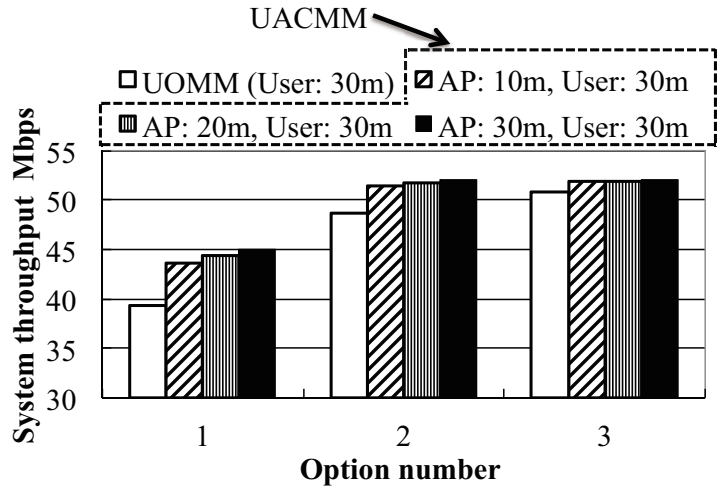

Figure 6.16: Relationship between system throughput and each option (AP capacity: 10, new user movable distance: 30 m).

system throughput of the UOMM for all options is approximately 30 Mbps. In contrast, for option 1, the UACMM can achieve 35 Mbps and 38 Mbps when the AP movable distance is 10 m and 30 m, respectively. Furthermore, if option 2 or 3 are used to disconnect the user that is affecting system throughput, throughput improves from 39 Mbps to 40 Mbps by increasing the AP movable distance in UACMM. Figure 6.14 indicates that the UACMM achieves nearly equal performance as the UOMM when the user movable distance is 30 m. This is because the UOMM can reduce the distance between a user and an AP when the movable distance is 30 m. Consequently, even if the AP disconnects any user, the difference between the UACMM and the UOMM becomes small. However, in the case of options 2 and, 3 the UACMM can achieve higher throughput (approximately 5 Mbps) than the UOMM. Therefore, the UACMM can improve throughput with any of the three disconnection methods.

Figure 6.15 and Fig.6.16 show results when the acceptable number of users increases (10 users). The results shown in Fig.6.15 and Fig.6.16 are similar to the results presented

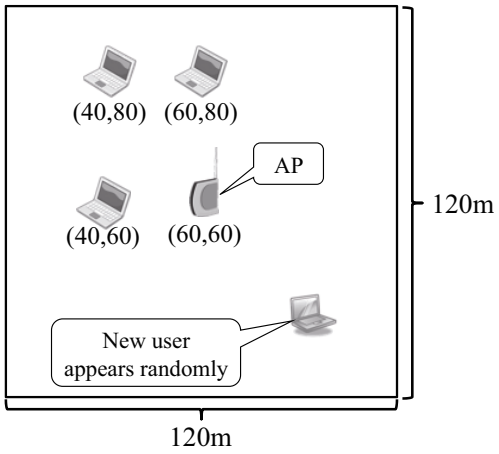

Figure 6.17: Initial configuration of system (3).

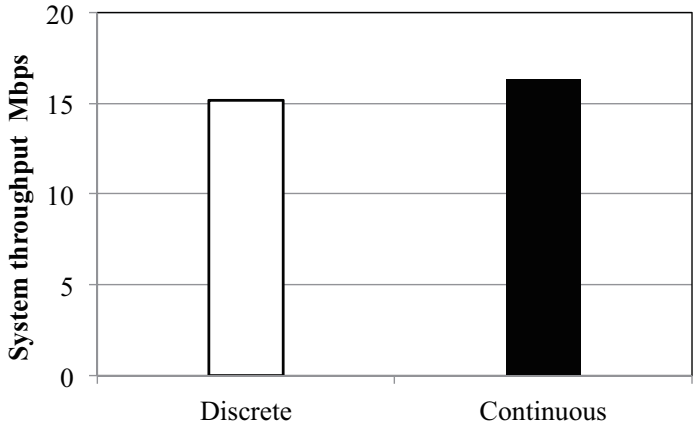

Figure 6.18: System throughput with discrete and continuous destination points.

in Fig.6.13 and Fig.6.14, respectively. It is evident from Fig.6.15 and Fig.6.16 that the difference of throughput between the UACMM and the UOMM is small compared with $N = 2$ because there are a significant number of users. However, the throughput of the UACMM is greater than that of the UOMM for all options. In summary, the UACMM can improve throughput compared to the UOMM regardless of the disconnection method used and when the acceptable number of users changes.

6.4.5 Realistic solution

Here, this section evaluates the UACMM's performance in a more realistic situation. In particular, this section evaluates system throughput under the assumption that the move distances of both users and APs are discrete or continuous values.

Discrete destination points

In the previous evaluations, the destination points of the user and the AP were taken to be continuous values. However, it is expected that discrete destination points will be common in actual environments. This section evaluates the system throughput under

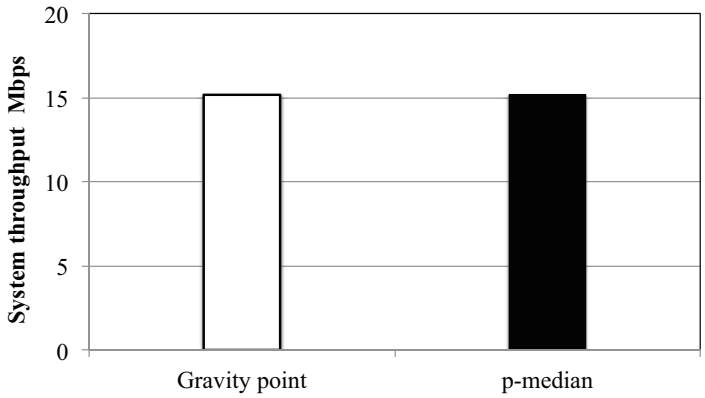

Figure 6.19: Comparing system throughput achieved with gravity point and p-median.

the assumption that the move distances of both users and APs are discrete or continuous values. If the difference of these system throughput becomes larger, the effectiveness of the proposal is not shown sufficiently. In order to clarify the difference, this section evaluated the performance over the simple model without AP selection.

Figure 6.17 shows the system configuration considered in this experiment. The two tuple shown in the bottom of the AP or each user show the coordinates (x-axis, y-axis) of the AP or each user in Fig.6.17. This system has one AP in a 120 m $\times$ 120 m area, and 3 existing users are connected to it. The movable distance of both the AP and a new user is 20 m. This emphasizes the difference between discrete and continuous destination points. If the destination points are discrete values, the region is divided by a mesh with an interval of 1 m, and both the AP and new users can be set only on the grid points. Thus, the AP and a new user move to the grid point that is the closest to the gravity point. Note that the aim of this chapter is to propose and to evaluate an AP selection method considering the cooperative moving of users and APs. Therefore, the evaluation considering methods to determine the realistic grid is the future work. The number of existing users is 3, and new users appear at randomly in the area same as subsection 6.4.1. The transmission rate, type of traffic, and number of trials in the simulation are the same as those of the simulation described in Sect. 6.4.1.

Figure 6.18 shows a comparison of the throughput. From Fig.6.18, continuous and discrete destination points yield nearly equal throughput; the difference is approximately 1.1 Mbps, and the relative error is approximately 5 %, which is very small. Therefore, since discrete destination points (realistic solution) yield nearly the same results as continuous destination points, it is confirmed that the UACMM yields realistic values.

Comparing gravity point and p-median

Next, this section discusses coordination of both APs and users to maximize system throughput. Note that this evaluation assumes discrete destination points. In this situation, the coordination is possible by techniques that are not based on the gravity point, such as the p-median technique [140]. Finding the p-median has been widely studied [141]. The p-median problem calls for finding the p facilities that minimize the total distance between the demands and the selected facilities. This study uses the p-median as the point at which total throughput is maximized. The p-median problem

is known to be NP-hard [142]. This experiment investigates how system throughput changes when coordination is realized by the gravity point or the p-median. The experimental environment is the same as that in Sect. 6.4.5.

Figure 6.19 shows a comparison of throughputs. From Fig.6.19, it is evident that the p-median approach yields nearly equal throughput as the gravity point approach because the transmission rate is given by a step function. However, even if the transmission rate is continuous, it is expected that the difference would remain minor because, in this experiment, the grid points (the destination points) are close to each to other. In other words, p-median position is nearly equal to the gravity point position. However, the gravity point can be found more quickly than the p-median. Thus, using the gravity point for AP selection is very effective in terms of time complexity.

6.5 Conclusion

This chapter has proposed an AP selection method that considers the movement of users and APs (UACMM). Further, this chapter evaluated the effectiveness of portable APs, such as mobile Wi-Fi routers, to increase system throughput in a multi-rate wireless LAN environment. The UACMM can improve system throughput and AP average throughput dramatically compared to the UOMM that only moves a new user because the AP can move to a position where existing users can obtain higher transmission rates. Furthermore, the system throughput under the assumption has been evaluated that the move distances of both users and APs are discrete or continuous values.

Future work will include the following evaluations:

- Evaluation of UACMM considering real environments (some MAC protocols and TCP flow case)
- Evaluation of UACMM considering QoS control method such as [143, 144]
- Evaluation considering the distribution of required load information to achieve autonomic load balancing
- Evaluation of UACMM considering methods to determine realistic grid

Chapter 7

A Media Access Control Method Based on the Synchronization Phenomena of Coupled Oscillators over Wireless LAN

In this chapter, to improve the total throughput, a novel media access control method, SP-MAC, which is based on the synchronization phenomena of coupled oscillators is proposed.

7.1 Introduction

The rapid spread of mobile terminals, such as smartphones and tablet devices, is increasing the usage of wireless LANs based on IEEE802.11 [1]. IEEE802.11 adopts CSMA/CA as the MAC. To avoid data frame collisions, CSMA/CA uses the random differing time (back-off time) derived using a random integer in the CW. However, if the number of wireless terminals connecting an AP increases, the back-off time derived by the initial CW tends to conflict among wireless terminals. Consequently, data frame collisions often occur, which causes the degradation of the total throughput in the transport layer protocols (UDP and TCP). This thesis assumes that the number of wireless LAN terminals dramatically increases. Therefore, to provide stable and tolerant wireless LAN services in the future, it is expected that the collision avoidance will become one of the critical problems to overcome in wireless LAN networks.

To avoid data frame collisions, several kinds of methods can be used such as point coordination function (PCF) methods [1, 145–149] and TDMA methods [94, 150–153]. However, these methods always need to control the access timing at the AP. Furthermore, some studies [154,155] use a method in which each terminal autonomously avoids data transmission conflicts. However, because the methods used in these studies [154, 155] always need to send the control packets to avoid the collision, it is expected that the overhead increases with the number of wireless terminals. Consequently, the total throughput decreases when there are numerous wireless terminals. In addition, there are several resource reservation methods [156–159] based on CSMA/CA [160]. Because these methods are based on CSMA/CA, they are compatible with the CSMA/CA terminals. However, these methods require that each wireless terminal needs extra pro-

cedures for reserving resources and avoiding collisions; for example, sending the current status and measuring the status of other terminals.

In this chapter, to improve the total throughput by avoiding data frame collisions, a novel MAC method, SP-MAC, which is based on the synchronization phenomena [161] of coupled oscillators is proposed and evaluated [35–38]. The key concept of the proposed method is to calculate the back-off time using the synchronized phase with phase shifting instead of the random integer in the original CSMA/CA method. Moreover, each terminal independently calculates the synchronized phase with phase shifting after receiving a control packet from the AP at the beginning of data transmission. Thus, all terminals can avoid data frame collisions. Next, this chapter evaluates the performance of SP-MAC using simulation experiments. The simulations show that SP-MAC can drastically decrease the probability of data frame collisions and improve the total throughput when compared with the original CSMA/CA method. Furthermore, this chapter clarifies that SP-MAC can effectively use the bandwidth by avoiding data frame collisions when the number of terminals increases.

The rest of this chapter is structured as follows. The synchronization phenomena of coupled oscillators, and existing methods are described in Sect. 7.2. Section 7.3 explains the proposed method (SP-MAC) based on the synchronization phenomena of coupled oscillators. Section 7.4 presents the evaluations and discussions of the results obtained from simulation experiments. Finally, this chapter is summarized in Sect. 7.5.

7.2 Related works

This section presents an overview of the model for the synchronization phenomena of coupled oscillators. Moreover, this section describes the existing methods for avoiding data frame collisions over wireless LAN.

7.2.1 Synchronization model of coupled oscillators

Synchronization indicates that the phenomena caused by multiple oscillators with different periods transform incoherent rhythms into synchronized ones with each interaction. This phenomena is also observed in nature such as the synchronous flashing of fireflies [162] and the synchronization of metronomes [163]. These synchronized oscillators are called coupled oscillators. During the synchronization, the phase differences and frequencies of all the coupled oscillators converge at certain values.

Several studies [164–166] discuss the synchronization phenomena, and have proposed mathematical models for this phenomena. Additionally, another study [167] has demonstrated the synchronization phenomena based on the synchronization model in a real environment. One of the typical models is the *Kuramoto model* [168]. This section explains the synchronization of N coupled oscillators using the Kuramoto model. In the Kuramoto model, the ith oscillator runs independently at its own natural frequency ω_i and interacts with all the others. Then, the ith oscillator's phase θ_i ($0 < \theta \leq 2\pi$) is

calculated using Eq.(7.1).

$$\frac{\mathrm{d}\theta_i}{\mathrm{d}t} = \omega_i + \frac{K}{N}\sum_{j=1}^{N}\sin(\theta_j - \theta_i) \quad (i = 1, 2, \cdots, N). \tag{7.1}$$

In Eq.(7.1), $K(> 0)$ indicates coupling strength. The second term is an interaction term, which is normalized by K/N to be independent from system size N.

In addition, a mathematical analysis [168] is performed using the mean field theory when numerous oscillators synchronize. The mean field is determined using Eq.(7.2).

$$MF = \frac{1}{N}\sum_{j=1}^{N}\exp(i\theta_j(t)) \equiv R\exp(i\bar{\theta}). \tag{7.2}$$

In Eq.(7.2), R $(0 \leq R \leq 1)$ and $\bar{\theta}$ $(0 < \bar{\theta} \leq 2\pi)$ indicate the amplitude and phase in the mean field, respectively. In addition, i denotes an imaginary unit in Eq.(7.2). The mean field MF is called an order parameter and is used as a synchronization index. If a collective synchronization occurs, the amplitude R has a constant value and the phase $\bar{\theta}$ describes a linear increase, such as $\bar{\theta} = \Omega t$. Ω is the collective frequency. When R is 0, synchronization does not occur. On the other hand, as R increases close to 1, the synchronization level is strong.

Next, in the Kuramoto model, Eq.(7.1), K has to satisfy Eq.(7.3) for collective synchronization.

$$\begin{aligned} K &> K_c\,, \\ K_c &= \frac{2}{\pi g(\omega_0)}. \end{aligned} \tag{7.3}$$

In Eq.(7.3), K_c and $g(\omega_0)$ are the critical coupling strength and density function of a natural frequency (i.e., the symmetric function with ω_0 as the center of all ω), respectively. For example, if the natural frequency ω has a uniform distribution in $[L, U]$, the density function is derived using $g(\omega_0) = (U - L)^{-1}$. In this case, the critical coupling strength is determined using Eq.(7.4).

$$K_c = \frac{2(U - L)}{\pi}. \tag{7.4}$$

Note that this is a theoretical threshold when there are infinitely oscillators. Therefore, this chapter has to carefully calculate K_c.

7.2.2 Existing media access controls for collision avoidance

This section explains the existing MAC methods for collision avoidance.

First, the typical collision avoidance methods are IEEE802.11 PCF and its modified method [145–149]. These methods can avoid data frame collisions because the AP controls the access timing of all wireless terminals using a polling frame. However, if multiple APs use the same channel, the transmission of polling frames can fail among APs because each AP does not synchronize the transmission timing of polling frames. In

this situation, the wireless terminal cannot send data. In addition, because IEEE802.11 PCF is the option function, DCF and PCF are alternately used. Therefore, the collision occurs in a DCF period even if PCF is used.

The other collision avoidance method is a TDMA-based method [94, 150–153]. In TDMA, each slot time is applied to the wireless terminal. Then, even if the number of wireless terminals increases, no collision occurs. However, the TDMA-based method needs to strictly synchronize the clock among all wireless terminals. Moreover, the central terminal always needs to maintain the detailed time slot of all wireless terminals, and this method cannot coexist with CSMA/CA terminals.

Some studies [154, 155] have proposed a Phase Diffusion Time Division (PDTD) method that autonomously avoids the conflict of data transmission timing. PDTD is developed for wireless sensor networks and is based on the dynamics of coupled phase oscillators among peripheral terminals. In PDTD, each terminal exchanges control information (including the coupled phase dynamics [155]) within two-hop neighbor terminals and calculates the communication timing using this information. Another study [169] has demonstrated the synchronization phenomena by implementing the PDTD in a real environment. However, PDTD always needs to send control packets between two-hop neighbor terminals to maintain a collision-free state. Therefore, the number of control packets (overhead) increases as the number of wireless terminals increases. The total throughput is expected to decrease as the number of terminals increases. Furthermore, this method cannot be used when CSMA/CA terminals coexist because CSMA/CA terminals do not transfer control packets.

Finally, some studies [156–159] have proposed a resource reservation method based on CSMA/CA [160]. First, [156] proposed a method using the modified RTS to reserve bandwidth. However, this method needs to overhear the modified RTS from other wireless terminals. Moreover, because RTS/CTS increases the overhead, the available bandwidth becomes smaller. Next, EBA [157] and CSMAC [158] try to reserve the time slot for a data frame transmission at the AP. In these methods, to avoid collision among the wireless terminals, the AP adjusts the CW for each wireless terminal based on the next CW value that is sent by each wireless terminal and notifies the terminal of the adjusted CW. Then, each wireless terminal uses the data frame using the adjusted CW. However, these methods need to send the next CW to all wireless terminals and the AP has to synchronize the clock with all the wireless terminals. Finally, [159] proposes a method, Semi-Random Backoff (SRB), that reuses a time slot in the consecutive back-off cycles. In this method, after successful transmission using the random value based on the CW, the successful wireless terminals use the deterministic value based on the previous random value for the next transmission. Thus, the wireless terminal sends a data frame using the deterministic back-off time based on the previous one that does not conflict with the other wireless terminals. However, this method needs to estimate the number of busy slots for setting the back-off time. Therefore, if the estimation fails, it is possible that this method would not work effectively. In summary, the existing resource reservation methods require that each wireless terminal needs extra procedures for reserving resources and avoiding collisions. Therefore, this chapter proposes a new method that does not require the wireless terminal to send the extra control frame and observe the transmission status.

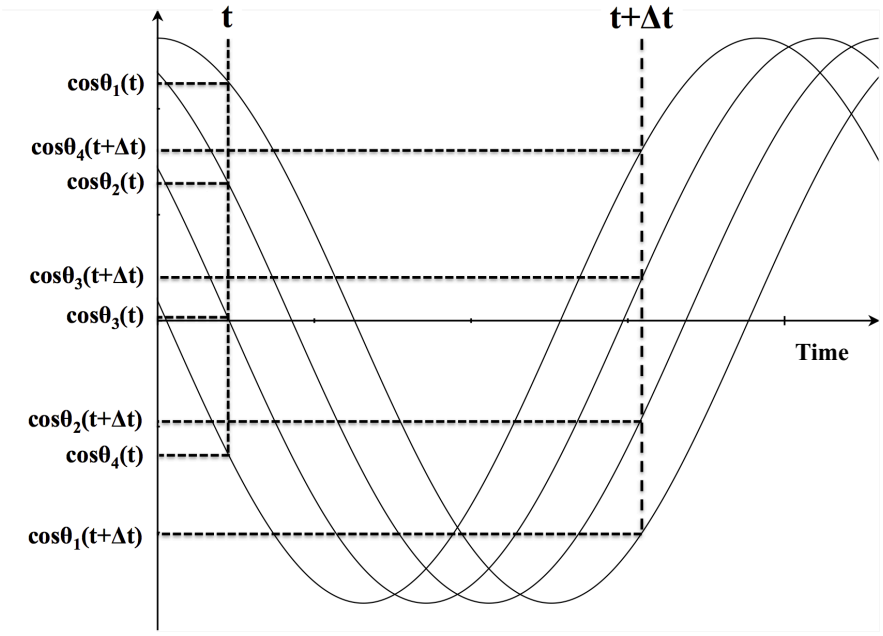

Figure 7.1: Example: cosine curves of synchronized oscillators with phase shifting.

7.3 SP-MAC: A media access control method based on the synchronization phenomena of coupled oscillators

This section explains the proposed MAC method (SP-MAC) based on the synchronization phenomena of coupled oscillators.

7.3.1 Overview of SP-MAC

As mentioned in Sect. 2.1, CSMA/CA in the IEEE802.11 standard calculates the back-off time using a random integer derived from the discrete uniform distribution [0, CW]. SP-MAC uses the synchronized phase based on Eq.(7.1) for setting the back-off time instead of using a random integer. It should be noted that all the oscillators synchronize with phase shifting. Fig.7.1 shows an example of cosine curves that result when four oscillators synchronize with phase shifting. Each cosine curve indicates the phase of each oscillator. When all the oscillators synchronize with phase shifting, each oscillator has a different $\cos\theta_i(t)$ at time t. After a certain time Δt passes $(t + \Delta t)$, the relationship of $\cos\theta_i(t)$ changes; for example, $\cos\theta_1(t) > \cos\theta_4(t)$ and $\cos\theta_1(t + \Delta t) < \cos\theta_4(t + \Delta t)$. Therefore, it is expected that SP-MAC can avoid the overlap of back-off time among terminals using these synchronized phases with phase shifting.

For this study, the following preconditions are set.

- The AP and all wireless terminals do not move.

- The AP and all wireless terminals stop using the RTS/CTS function (i.e., they do not send RTS/CTS).

7.3.2 Detailed procedures of SP-MAC

This section presents the details of the procedures for the AP and wireless terminals in SP-MAC.

Initially, the AP determines the control parameters in advance. Then, it sends the parameters to all wireless terminals at the beginning of the data transmission.

Procedures at AP

1. The AP determines the number of connected wireless terminals N based on the number of connection requests from wireless terminals.

2. The AP determines the natural frequency ω_i and coupling strength K, which satisfy the synchronizing condition according to N (see Sect. 7.2.1). To lead the condition that each oscillator synchronizes with phase shifting, the AP adopts a different ω_i for each wireless terminal (i.e., there is no overlap among all ω_i). Next, the AP sets an ID i ($1 \leq i \leq N$), which identifies each wireless terminal. Then, the AP applies ω_i and an initial phase $\theta_i(0)$ to the i-th wireless terminal. Each initial phase $\theta_i(0)$ has a different value to avoid the collision at the beginning of the data transmission.

3. Using a beacon, the AP sends the control parameters, which include i, $\theta_i(0)$, ω_i, K, a control interval Δt, and N for all wireless terminals.

4. After sending the beacon, if the AP receives a data frame from a wireless terminal, it sends an ack frame in the same manner as the original CSMA/CA method.

5. If the number of wireless terminals changes after each wireless terminal starts data transmission, the AP modifies the control parameters based on N and sends them using a beacon again.

Then, each wireless terminal works as follows after receiving the beacon.

Procedures at Wireless Terminal

1. After receiving the beacon, the wireless terminal immediately starts calculating the phase using the control parameters. Next, the wireless terminal calculates the phase $\theta_i(t)$ for all ID i using Eq.(7.1) for every Δt. The phase calculation continues, even if there is no data for transmission while connecting to the AP. If the wireless terminal receives a beacon including the control parameters from the AP again, it uses the control parameters in the latest beacon.

2. If data arrives from the upper layer at time t, the wireless terminal calculates the back-off time Backoff using Eq.(7.5) and the phase $\theta_i(t)$ for each ID i (see Fig,7.2). In Eq.(7.5), SlotTime and ξ show the slot time interval specified in IEEE802.11

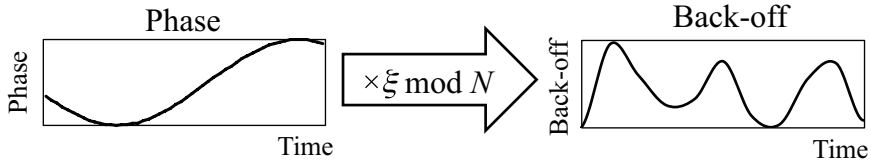

Figure 7.2: Relationship between the phase and back-off time of SP-MAC.

Algorithm 5 Procedures at AP.

Require: $N \geq 0$

1: Set K and ω_i based on N for a terminal i
2: Send $(i, \theta_i(0), \omega_i, K, \Delta t, N)$ by using beacon
3: **loop**
4: **if** Receive a data frame from the terminal **then**
5: Send an ack frame for the terminal
6: **end if**
7: **if** The number of wireless terminals changes **then**
8: goto 1 :
9: **end if**
10: **end loop**

and a coefficient for obtaining the normalized phase, respectively. This chapter sets ξ equal to 100[2)] [35, 36].

$$\text{Backoff} = ((|\cos\theta_i(t)| \times \xi) \bmod N) \times \text{SlotTime}. \tag{7.5}$$

3. When the channel remains idle after DIFS and the back-off time, the wireless terminal sends a data frame, which is the same as the one used in the original CSMA/CA method. If the wireless terminal detects data frame collisions, it calculates the new back-off time using Eq.(7.5) and the phase when the collision is detected again. Then, the wireless terminal retransmits the data frame.

The above-mentioned procedures are summarized in Algorithm 5 and Algorithm 6. If the AP needs to send data, i.e., there is a downlink flow from the AP to the wireless terminal, it uses one of the phases and repeats the same procedures at wireless terminals. Therefore, the downlink flow can coexist with the uplink flow.

SP-MAC only sends the control parameters for calculating the phase at the beginning of transmission. Hence, each wireless terminal works autonomously based on the model for the synchronization phenomena of coupled oscillators. Furthermore, because SP-MAC is based on the original CSMA/CA (i.e., only the calculation of back-off time at the wireless terminal is different), it can be used for an environment where both the SP-MAC terminals and the original CSMA/CA terminals exist [36]. The drawback of SP-MAC is to need the calculation of the Eq.(7.1) for every Δt.

[2)]This chapter adopts $\xi = 100$ for setting the time scale of the back-off time equal to the one used with the CSMA/CA method. Moreover, because this study focus on basic performance, the detailed discussion regarding ξ includes future work.

Algorithm 6 Procedures at wireless terminal.

Require: $i, \theta_i(0), \omega_i, K > K_c, \Delta t > 0, N \geq 0$

1: $time_{current} \Leftarrow 0$
2: $calc_{interval} \Leftarrow \Delta t$
3: **loop**
4: **if** $time_{current} > calc_{interval}$ **then**
5: **for all** i $(1 \leq i \leq N)$ **do**
6: Calculate $\theta_i(t)$ using Eq.(7.1)
7: **end for**
8: $calc_{interval} \Leftarrow calc_{interval} + \Delta t$
9: **end if**
10: **if** The terminal wants to send a data frame **then**
11: Calculate Back-off time using Eq.(7.5)
12: Send a data frame after DIFS and Back-off time
13: **end if**
14: **if** Detect collision at $time_{current}$ **then**
15: Calculate Back-off time using Eq.(7.5) at $time_{current}$
16: goto 12 :
17: **end if**
18: **if** Receives a beacon including the control parameters from the AP **then**
19: goto 1 :
20: **end if**
21: **end loop**

7.4 Simulation experiments

This section discusses the SP-MAC evaluations using the network simulator ns2 [98]. First, for basic evaluations, this section compares SP-MAC to the original CSMA/CA. Then, this section shows the comparative evaluations between SP-MAC and the typical existing methods for collision avoidance (PCF in IEEE802.11, TDMA, and SRB [159]). Next, this section presents the results under the scenario where both SP-MAC and CSMA/CA exist. Then, this section discusses the results when the joining and leaving terminals exist. Finally, this section shows the results considering a multi-rate wireless LAN environment.

7.4.1 Simulation settings

Table 7.1 and Fig.7.3 show simulation parameters and the simulation model. This network uses the IEEE802.11g (PHY) [40] for the wireless LAN environment, and SP-MAC is implemented in all wireless terminals. The evaluations assume that none of the terminals are moved. This model consideres the case in which wireless terminals are the senders and generated 60 seconds of traffic (each wireless terminal generated one flow). Next, UDP and TCP are used for the transport protocol and TCP-Reno with Sack (the basic control) and CUBIC-TCP (the standard of Linux and Android OS) for TCP version. All wireless terminals are always sending data, and the sending rate of

Table 7.1: Simulation parameters.

Simulator	ns2 (ver.2.34)
Wireless environment	IEEE802.11g
AP buffer size	250 packets
Transport protocols	UDP, TCP
Segment size	1000 byte
TCP receiver window size	128 Kbyte
Simulation time	60 sec

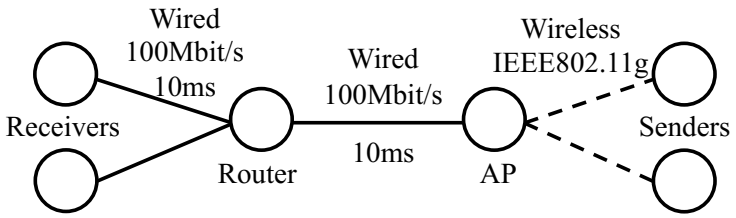

Figure 7.3: Simulation model.

UDP was 30 Mbps. Each TCP flow sends data using FTP. The simulation results show averages of 10 trials. This study evaluates the number of data frame collisions and the total throughput determined by receipt data at the receiver terminal.

SP-MAC sets the control parameters [35] as follows by considering the synchronization condition (see Sect. 7.2.1). First, the initial phase $\theta_i(0)$ and natural frequency ω_i are set to non-overlapped values in the range of $(0, 1.0)$ and $[0, 2.0]$, respectively. Then, these evaluations set the coupling strength K to 5 by considering Eq.(7.3) and Eq.(7.4), such that it is larger than the critical coupling strength K_c. The control interval Δt is set to 10 ms. In this condition, for $N = 20$, the convergent amplitude R and frequency Ω in the mean field are 0.993 and 1.05, respectively. Thus, using these parameters, all wireless terminals synchronize with phase shifting.

7.4.2 Basic performance evaluations

First, this section shows the number of data frame collisions. Tables 7.2, 7.3, and 7.4 show the results of UDP, TCP-Reno with Sack, and CUBIC-TCP when the number of flows changes from 5 to 20, respectively. From Tables 7.2, 7.3, and 7.4, the number of data frame collisions increases with the number of flows, as in the case of the original CSMA/CA. This occurs because the initial back-off time tends to conflict easily when the number of flows increases. In particular, because UDP always uses a higher transmission rate (30 Mbps) than that of TCP, it has the largest number of collisions. On the other hand, SP-MAC can drastically reduce the number of data frame collisions in all the transport protocols. In SP-MAC, the collisions only occur at the beginning of data transmission. For example, for 20 UDP flows, the collisions occur from 0 to 2 sec.

Table 7.2: The number of collisions for each flow (UDP).

The number of flows	CSMA/CA	SP-MAC
5	55234.9	1.0
10	94796.6	3.2
20	135802.5	10.2

Table 7.3: The number of collisions for each flow (TCP-Reno with Sack).

The number of flows	CSMA/CA	SP-MAC
5	17632.2	0
10	32554.5	0
20	42999.0	0

Table 7.4: The number of collisions for each flow (CUBIC-TCP).

The number of flows	CSMA/CA	SP-MAC
5	18446.9	0
10	56168.3	0
20	75248.9	1.4

The Kuramoto model requires a specific amount of time for synchronization, and the convergence time is around 2 sec in this environment. Consequently, if the transmission rate is always high as with UDP, the collisions occur at the beginning of data transmission. Moreover, in TCP-Reno with Sack and CUBIC-TCP, the collisions rarely happen, compared with UDP, because TCP controls the transmission rate. In addition, because TCP-Reno with Sack usually has a lower congestion window size than CUBIC-TCP, no collisions occur in this environment. Therefore, it is confirmed that collisions rarely happen using SP-MAC even when the number of flows increases.

Next, this section shows the total throughput. Figures 7.4, 7.5, and 7.6 plot the total throughput of UDP, TCP-Reno with Sack, and CUBIC-TCP when the number of flows changes from 5 to 20, respectively. From Figs.7.4, 7.5, and 7.6, SP-MAC can obtain higher throughput than the original CSMA/CA method. In the case of UDP and CUBIC-TCP, the throughput of the original CSMA/CA method tends to decrease as the number of flows increase. UDP uses a stable transmission rate of 30 Mbps because it does not have a rate control mechanism. Therefore, because the number of collisions increases with the number of flows, the number of received UDP segments at the receiver decreases. Consequently, the total throughput of UDP decreases. Next, CUBIC-TCP drastically increases the congestion window size at the beginning of data transmission. Therefore, if the number of flows increases, the number of transmitted data frames also drastically increases. In this situation, a TCP segment can be easily lost because a continuous collision of data frames occurs, as in the case of UDP. Therefore, the total throughput of CUBIC-TCP also decreases as the number of flows increases. In TCP-Reno with Sack, because the increment rate of the congestion window size is significantly smaller than that of CUBIC-TCP, the number of collisions is

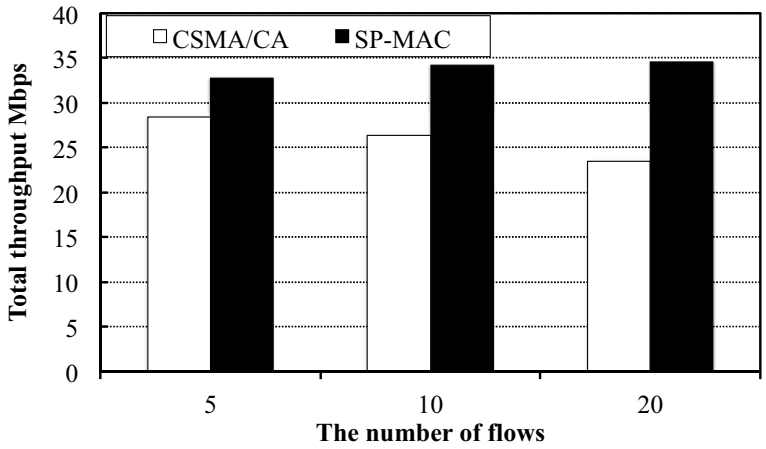

Figure 7.4: The total throughput for each flow (UDP).

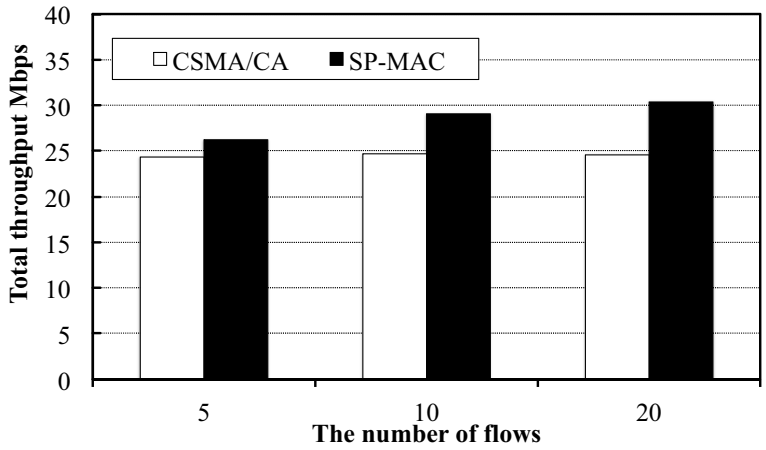

Figure 7.5: The total throughput for each flow (TCP-Reno with Sack).

also smaller than CUBIC-TCP. As a result, the total throughput of TCP-Reno with Sack does not decrease in this environment. On the other hand, SP-MAC increases the total throughput as the number of flows increases in UDP, CUBIC-TCP, and TCP-Reno with Sack cases. This is because SP-MAC can drastically decrease the number of collisions (see Table 7.2, Table 7.3, and Table 7.4), and the idle time of the channel decreases as the number of flows increases. In addition, because the AP sends data (TCP-ACK) in Figs.7.5 and 7.6, they show the case when the downlink flow coexists with the uplink flow. Therefore, these results indicate that SP-MAC can support the coexistence of both the uplink and downlink flow.

If the collision causes data loss, the difference of the congestion window size among TCP flows increases. Then, the throughput becomes unfair [170] among uplink (from the wireless terminal to AP) TCP flows in the wireless LAN (CSMA/CA). However, because SP-MAC can drastically reduce the number of collisions, it is possible to solve the throughput unfairness. Thus, this section evaluated the throughput of each flow and determined whether SP-MAC could obtain the fairness. Figure 7.7 shows the standard deviation of each flow when TCP version is CUBIC-TCP. As shown in Fig.7.7, the standard deviation of the original CSMA/CA method increases when the number of

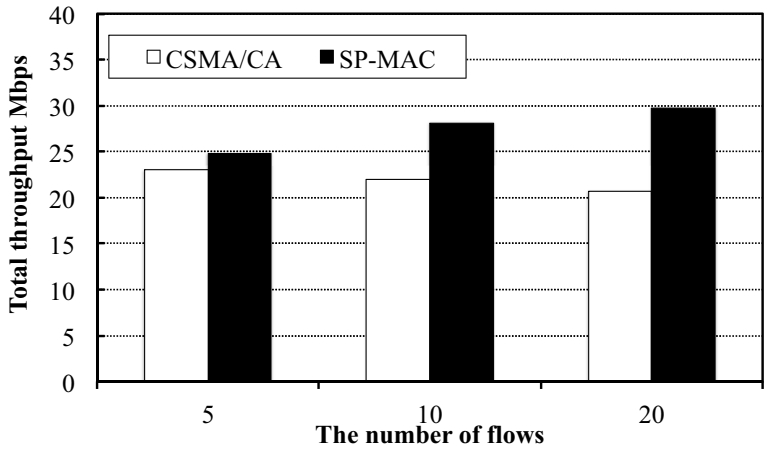

Figure 7.6: The total throughput for each flow (CUBIC-TCP).

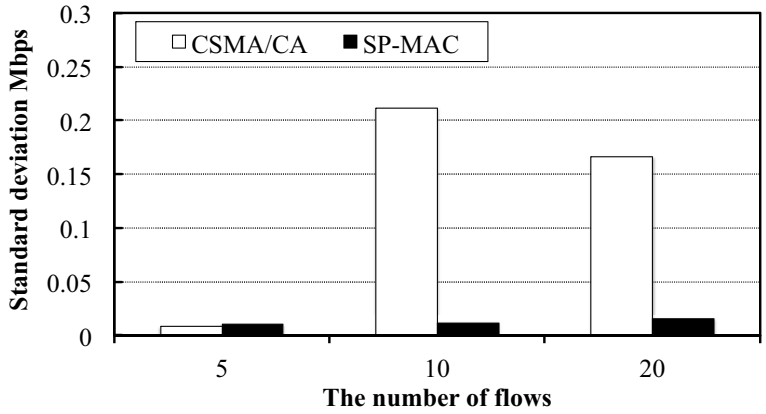

Figure 7.7: The standard deviation of each flow (CUBIC-TCP).

flows increases from 5 to 10. Therefore, the difference of throughput among TCP flows increases because the difference of the congestion window size between the collision terminal and collision-free terminal increases. On the other hand, as mentioned above, in SP-MAC, collisions hardly occur when all flows use the access interval based on the synchronized oscillators. Therefore, even if the number of flows increases, all flows can obtain almost the same congestion window size. Consequently, the throughput of all flows becomes almost the same. Therefore, it is clear that SP-MAC can obtain throughput with more TCP fairness than the original CSMA/CA method.

7.4.3 Comparative evaluation with existing method for collision avoidance

This section compares SP-MAC to the existing methods for collision avoidance. This evaluation uses PCF in IEEE802.11 because PCF can avoid collisions and coexist with CSMA/CA (DCF) in the same manner as SP-MAC. In addition, this study uses TDMA because it can completely avoid collisions and have lower overhead using the time scheduling. Furthermore, this evaluation uses SRB because it is based on CSMA/CA and can avoid collisions effectively.

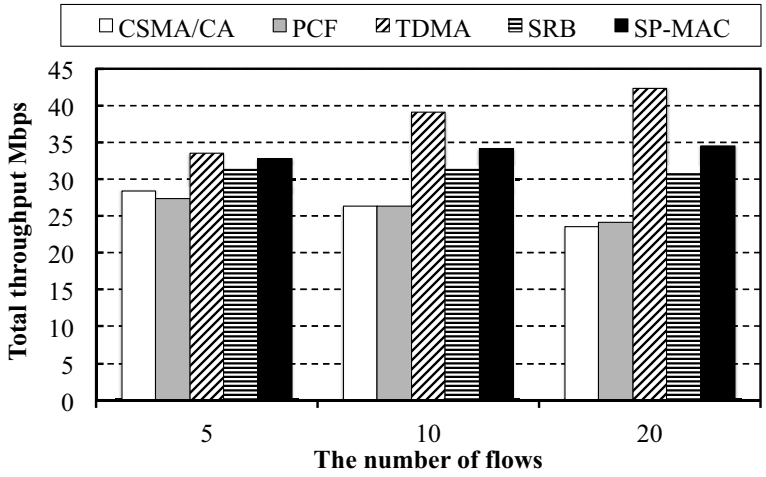

Figure 7.8: The total throughput of UDP for each flow when comparing SP-MAC to PCF, TDMA, and SRB.

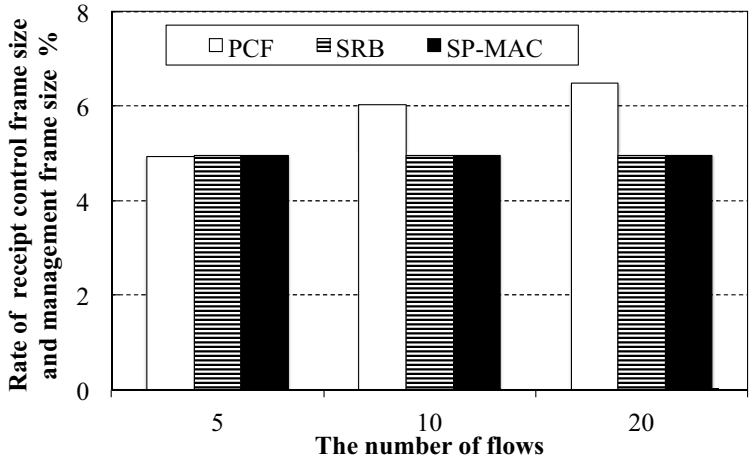

Figure 7.9: The rate of the sum of receipt control frame size and management frame size compared to total receipt frame size.

Figure 7.8 plots the total throughput of UDP for each flow. In TDMA, the slot time is allocated for all wireless terminals, including the AP, and one slot time is set equal to the time required for sending one data frame. As shown in Fig.7.8, PCF can obtain a higher total throughput than the CSMA/CA when the number of wireless terminals becomes larger than 10 (i.e., the collisions often occur) because it can avoid the collisions of data frames by polling. However, the total throughput of PCF decreases as the number of flows increases. Because PCF is the option function in IEEE802.11, the contention-free period of PCF and the contention period of DCF are continuously repeated. In the contention-free period, there are no collisions. On the other hand, the contention period has collisions. Therefore, the contention period decreases the total throughput of the PCF case as the number of flows increases. On the other hand, SP-MAC can drastically reduce collisions (see Table 7.2). Thus, the total throughput of SP-MAC is larger than that of PCF. Additionally, the total throughput of SRB is also larger than that of PCF and CSMA/CA because it can avoid collisions effectively. However, SP-

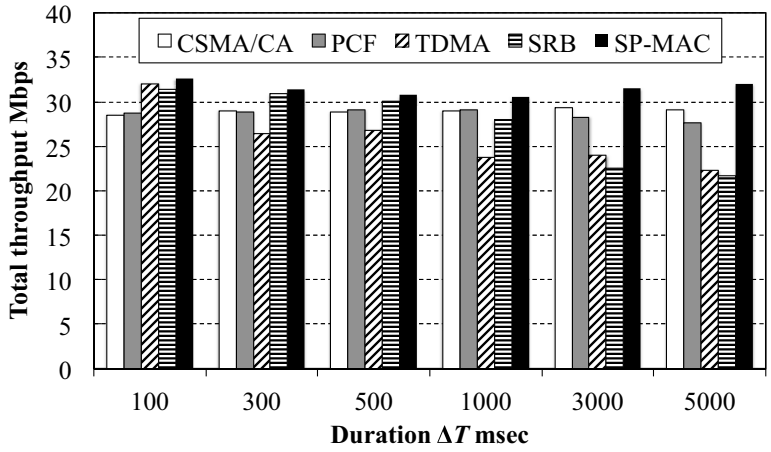

Figure 7.10: The total throughput of UDP for each flow in the unsaturated flow case.

MAC can obtain higher total throughput than SRB. This is because that the average back-off time of SRB is larger than that of SP-MAC. SRB uses the deterministic value for the back-off time after successful transmission using the random value. Therefore, because SRB uses a binary increase of CW after collisions, the average back-off time becomes larger when the deterministic value is set after collisions. On the other hand, SP-MAC does not use the binary increase even if the collisions occur. As a result, the total throughput of SP-MAC is larger than that of SRB. Next, TDMA has the highest throughput because there is no collision using the time scheduling and it does not require the ack frame transmission for confirming successful data transmission. Thus, TDMA result shows the maximum performance in this environment. In this case, SP-MAC can obtain higher throughput than CSMA/CA, PCF, and SRB. Therefore, SP-MAC can achieve the closest value against the maximum performance of TDMA.

Next, Fig.7.9 shows a rate of the sum of receipt control frame size (ack and poll) and management frame size (beacon) compared to total receipt frame size. That is, Fig.7.9 indicates the control overhead of each method. In Fig.7.9, because TDMA does not send control frame during the transmission, the SP-MAC, PCF, and SRB results were only shown. As shown in Fig.7.9, the SP-MAC rate is smaller than that of PCF when the number of flows is larger than 10. This occurs because the total receipt frame size of PCF decreases by collisions of data frames as the number of flows increases. Furthermore, the receipt control frame size and management frame size for polling (poll and beacon) does not decrease because collisions of control frames hardly occur using short IFS time. As a result, the rate of control frame size increases when the number of flows increases. On the other hand, SP-MAC does not increase collisions, even if the number of flows increases. In addition, SP-MAC does not send any control frames to avoid collisions during data transmission. Thus, because the number of receipt data frame is usually the same as that of an ack frame, the rate of receipt control frame size and management frame size does not increase even if the number of flows increases. Therefore, the rate of SP-MAC is smaller than that of PCF. Furthermore, the control overhead of SP-MAC is almost same as that of SRB.

The situation shown in Fig.7.8 assumed the saturated flow case; all wireless terminals always have data for transmission. However, it is expected that each flow does not

always send data (unsaturated flow). Therefore, this evaluation shows the throughput of an unsaturated flow case. Figure 7.10 plots the total throughput of UDP for each flow in the unsaturated flow case, where the number of flows is 5. In this evaluation, each wireless terminal has a data transmission time and an idle one, and these values have the exponential distribution with mean ΔT (in the range of [100, 5000]ms). In Fig.7.10, the x-axis duration indicates ΔT. As shown in Fig.7.10, SP-MAC can obtain the best throughput in the unsaturated flow scenario. Because SP-MAC has lower collisions than CSMA/CA and PCF, the throughput of SP-MAC is larger than that of CSMA/CA and PCF. In addition, because the average back-off time of SP-MAC is smaller than that of SRB, the total throughput of SP-MAC is lager than that of SRB. On the other hand, the throughput of TDMA decreases as the duration increases. This occurs because all wireless terminals do not always send data in this case. That is, if the duration increases, the unused time slot becomes larger because the wireless terminal does not always have transmission data. As a result, the throughput of TDMA decreases. Then, because SP-MAC can send data when the channel becomes idle, like CSMA/CA, SP-MAC can obtain higher throughput than TDMA. Furthermore, it is important to note that TDMA cannot simultaneously exist with CSMA/CA. On the other hand, SP-MAC can simultaneously exist with CSMA/CA. Thus, the next section will show the coexisting scenario.

7.4.4 Performance evaluation when both SP-MAC and CSMA/CA exist

This section evaluates the throughput (UDP case) when both the SP-MAC and CSMA/CA terminals exist in the same wireless LAN system. In this evaluation, the total number of wireless terminals is always set to 20 (and remained unchanged). However, the number of CSMA/CA (SP-MAC) terminals changes from 0 to 20.

Firstly, results of UDP flows are explained. Figure 7.11 shows the total throughput when the number of SP-MAC and CSMA/CA terminals changes. When the number of CSMA/CA terminals was zero, only SP-MAC terminals were present. Similarly, when the number of CSMA/CA terminals was 20, no SP-MAC terminals existed. As shown in Fig.7.11, the CSMA/CA terminals can achieve throughput even when the SP-MAC terminals exist because SP-MAC changes the mechanism of the back-off time calculation. Here, Fig.7.12 shows the average throughput for each method. As shown in Fig.7.12, the SP-MAC method can achieve higher throughput than the CSMA/CA method. This is due to the fact that SP-MAC does not use the binary increase, like CSMA/CA, when the collisions occur. That is, the back-off time of SP-MAC terminals is relatively lower than that of CSMA/CA terminals. As a result, the throughput of SP-MAC is higher than that of CSMA/CA.

Secondly, results of TCP flows are discussed. Figure 7.13 shows the total throughput of CUBIC-TCP and Compound-TCP, respectively. From Fig.7.11 and Fig.7.13, when the terminal sends data by TCP, the trend of throughput is almost the same as that in the UDP. The total throughput of TCP is slightly smaller than that of UDP because TCP needs to wait for TCP-ACK segments. Here, Fig.7.14 shows the average throughput of CUBIC-TCP in Fig.7.13. From the results in Fig.7.14, the average throughput of SP-MAC terminals with CUBIC-TCP is greater than that of CSMA/CA terminals same as

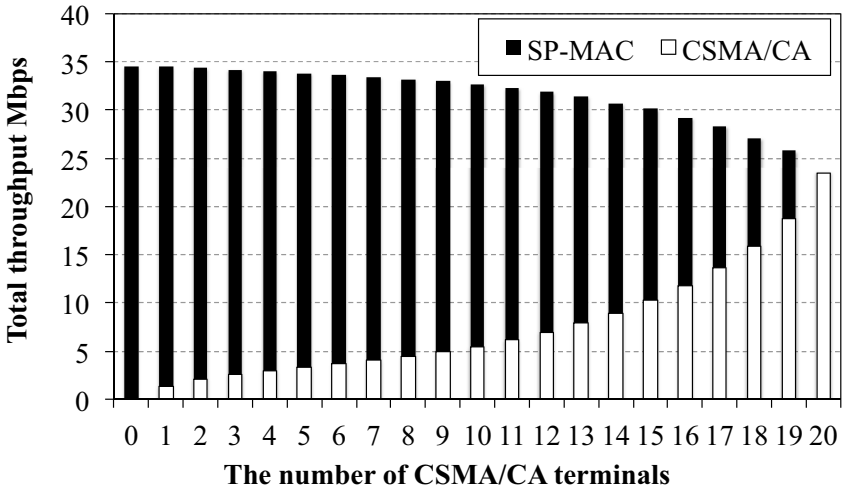

Figure 7.11: The total throughput of UDP when both SP-MAC and CSMA/CA exist.

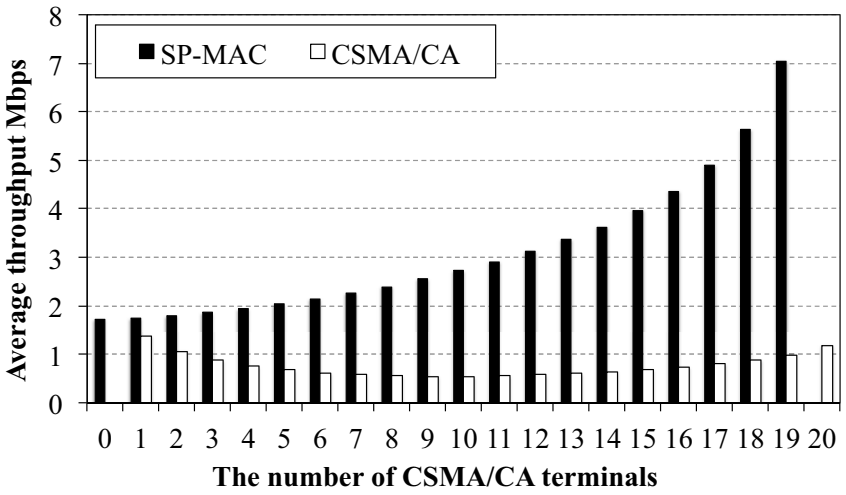

Figure 7.12: The average throughput of UDP when both SP-MAC and CSMA/CA exist.

the case of UDP.

According to the above results, both SP-MAC and CSMA/CA terminals communicate simultaneously. Furthermore, these results show that the total throughput improves as the number of SP-MAC terminals increases because SP-MAC can avoid collisions.

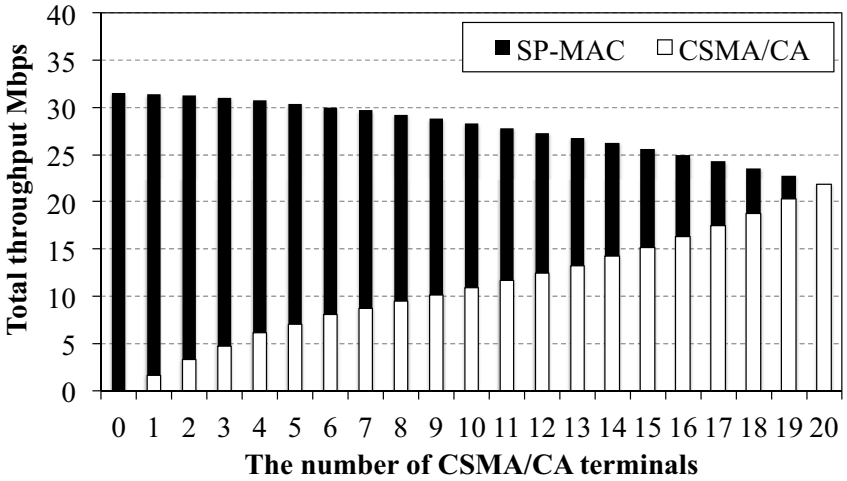

Figure 7.13: The total throughput of CUBIC-TCP when both SP-MAC and CSMA/CA exist.

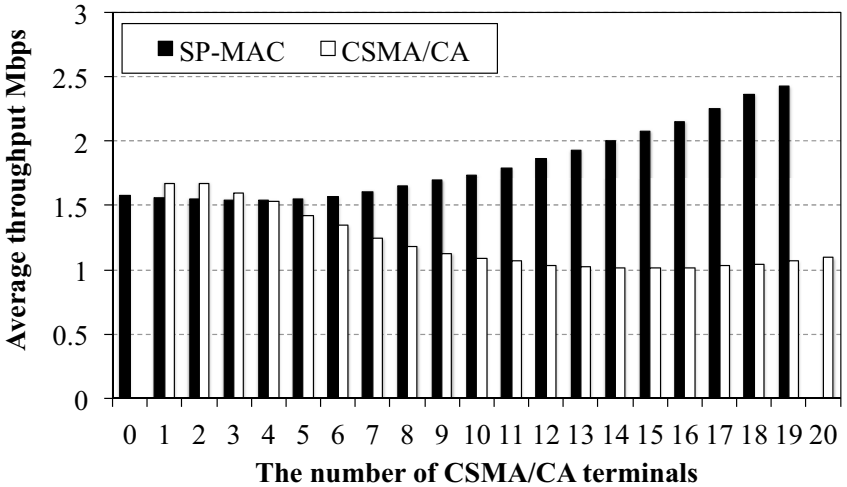

Figure 7.14: The average throughput of CUBIC-TCP when both SP-MAC and CSMA/CA exist.

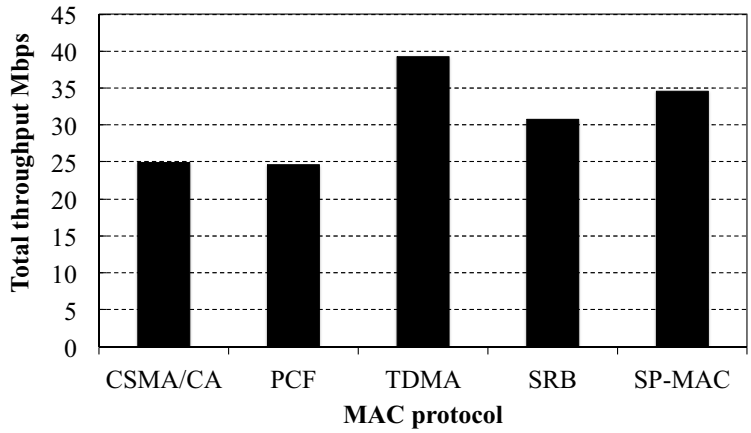

Figure 7.15: The total throughput of UDP when join and leave wireless terminals exist.

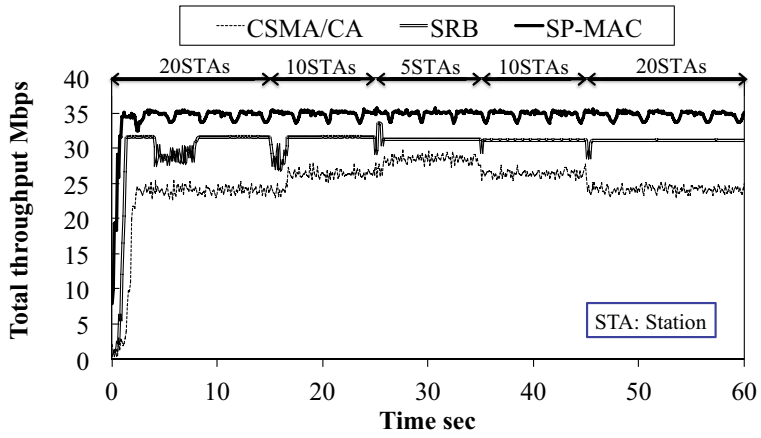

Figure 7.16: The time change of total throughput (UDP) when join and leave wireless terminals exist (SP-MAC, CSMA/CA, and SRB).

7.4.5 Performance evaluation when join and leave wireless terminals exist

Previous evaluations showed the results when the number of wireless terminals is fixed (static condition). However, in the real environment, it is possible that the wireless terminals dynamically join and leave. Therefore, this section shows whether SP-MAC can handle the dynamic condition well when the wireless terminals join and leave. This evaluation considers a following scenario; To begin with, 20 wireless terminals join a network at the begging of simulation. Next, 10 wireless terminals leave from the network at 15s. Then, 5 wireless terminals leave from the network at 25s. After that, 5 wireless terminals join the network at 35s. Finally, 10 wireless terminals join the network at 45s. In this environment, all wireless terminals always have data for transmission while they join the network. Figure 7.15 shows the total throughput of each method when the wireless terminals dynamically join and leave. From Fig.7.15, the trend of total throughput in the dynamic condition is almost same as that of the static condition (see Fig.7.8). Furthermore, the control overhead of the dynamic condition is almost same as that of the static condition in Fig.7.9. Next, Fig.7.16 shows the time

Table 7.5: Estimated total throughput of all terminals when CSMA/CA is used for MAC protocol.

Number of flows	5	10	20
Case 1	20.8 Mbps	30.0 Mbps	38.6 Mbps
Case 2	7.3 Mbps	6.6 Mbps	6.3 Mbps

change of total throughput. In Fig.7.16, the results of CSMA/CA, SRB, and SP-MAC are only shown because these methods are based on the back-off mechanism[3)]. From Fig.7.16, SP-MAC and SRB can obtain the stable throughput because these methods can avoid collisions effectively. Furthermore, SP-MAC can get higher total throughput than CSMA/CA and SRB. In CSMA/CA, the total throughput increases when the number of wireless terminals decreases because the number of collisions decreases. Therefore, SP-MAC can handle the dynamic condition well same as the other methods when the wireless terminals join and leave.

7.4.6 Performance evaluation of SP-MAC over multi-rate wireless LAN environment

Previous evaluations showed that SP-MAC can dramatically decrease the data frame collisions and improve the total throughput of all wireless terminals compared to the one of CSMA/CA in a single-rate environment where all terminals use same transmission rate. Here, the wireless terminals usually use a multi-rate transmission control for effective communication over the environment where each terminal has the different communication environments (see Sect.2.2). This section evaluates the performance of SP-MAC over the multi-rate wireless LAN environment and clarifies whether SP-MAC can get higher total throughput compared to CSMA/CA by avoiding data frame collisions.

This simulation considers the case in which wireless terminals are the senders and generate 60 seconds of traffic (each wireless terminal generated one flow). Next, all wireless terminals generate UDP traffic (30 Mbps). This section evaluates the total throughput determined by receipt data at the receiver terminal, the number of data frame collisions, and the improvement ratio of the SP-MAC's average throughput compared to CSMA/CA. Note that this evaluation assumes that the number of terminals N is stable and none of the terminals were moved. Furthermore, other simulation environments such as parameters of SP-MAC and the number of simulation trials is same as previous evaluations.

This evaluation considers following two multi-rate scenarios; (Case1) $N-1$ terminals send data with 54 Mbps and one terminal sends data with 6 Mbps, (Case2) $N-1$ terminals send data with 6 Mbps and one terminal sends data with 54 Mbps. Note that Case1 and Case2 show the impact of performance anomaly is small or large, respectively. Table 7.5 indicates the estimated total throughput using Eq.(2.2) in case of CSMA/CA.

[3)]The trend of TDMA and PCF are almost same as that of SP-MAC and CSMA/CA, respectively.

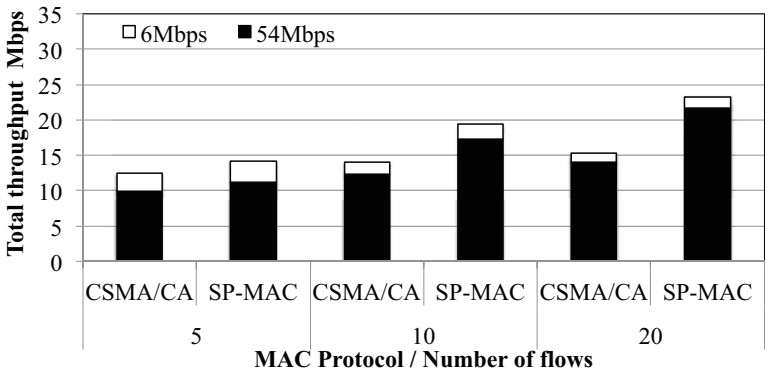

Figure 7.17: The total throughput for each flow (Case1).

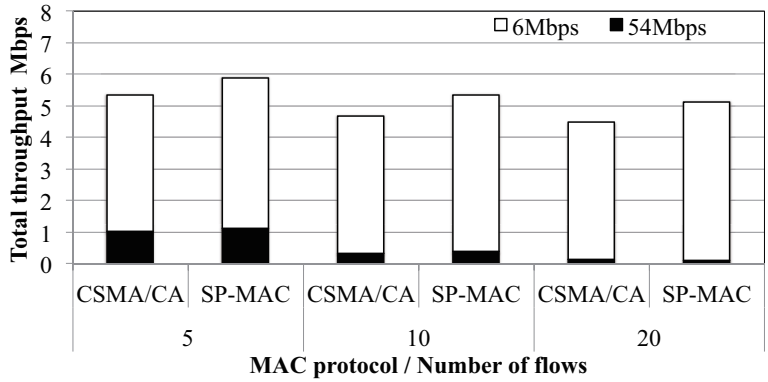

Figure 7.18: The total throughput for each flow (Case2).

Figure 7.17 and Fig.7.18 show the total throughput of all wireless terminals when the number of flows changes from 5 to 20. Fig.7.17 and Fig.7.18 indicate the result of Case1 and Case2, respectively. From Fig.7.17 and Fig.7.18, SP-MAC can get higher total throughput compared to CSMA/CA in both cases. For example, in Case1, when the number of flows is 5, 10, and 20, the differences between CSMA/CA and SP-MAC are 5.8 Mbps, 10.1 Mbps and 13.3 Mbps, respectively. From the above results, SP-MAC improves the total throughput drastically over the multi-rate wireless LAN environment compared to CSMA/CA. Furthermore, the total throughput of SP-MAC is close to the estimated value shown in Table 7.5. From these results, SP-MAC can use the bandwidth effectively in the multi-rate environment than CSMA/CA. Here, Table 7.6 and Table 7.7 show the number of data frame collisions. Table 7.6 and Table 7.7 indicate the results of Case1 and Case2, respectively. From Tables 7.6 and 7.7, the number of data frame collisions increases with the number of flows in each MAC protocol. However, SP-MAC can dramatically reduce the number of data frame collisions compared to CSMA/CA in both cases. As a result, SP-MAC can obtain higher total throughput than CSMA/CA.

Next, Fig.7.19 and Fig.7.20 plot the throughput improvement ratio of SP-MAC compared to CSMA/CA in Case1 and Case2, respectively. From Figs.7.19 and 7.20, SP-MAC increases the throughput improvement ratio as the number of flows increases in both cases. In Case1, when the number of flows is 20, the improvement ratio of SP-MAC terminals with 54 Mbps rate are 1.9 times greater than the one of CSMA/CA

Table 7.6: The number of data frame collisions for each flow (Case1).

Number of flows	CSMA/CA	SP-MAC
5	24129.8	0.5
10	53868.2	2.2
20	95943.2	9.2

Table 7.7: The number of data frame collisions for each flow (Case2).

Number of flows	CSMA/CA	SP-MAC
5	10557.6	0.8
10	16561.8	3.2
20	22928.7	12.2

terminals. Moreover, the SP-MAC terminal with 6 Mbps is 1.2 Mbps greater than the one of CSMA/CA terminal. This is because SP-MAC can use the bandwidth effectively by avoiding data frame collisions compared with CSMA/CA even if the number of flows increases. Furthermore, the throughput of 54 Mbps terminal in Case2 drastically improves comparing with the one in Case1. Especially, if the number of flows is 20, the terminal with 54 Mbps can improve about 3.5 times larger than CSMA/CA. That is, the effect of SP-MAC for the high rate terminal becomes larger in the environment where the impact of performance anomaly is large. On the other hand, the improvement ratio of the terminal with 6 Mbps rate in Case2 is almost same as the one in Case1. This is because the throughput of 6 Mbps terminals is mainly affected by the transmission delay rather than the number of collisions.

From these simulation results, SP-MAC can obtain higher total throughput than CSMA/CA in two multi-rate environments.

7.5 Conclusion

In CSMA/CA of the IEEE802.11 wireless LAN, if the number of wireless terminals connecting to an AP increases, the number of data frame collisions increases. This occurs because the back-off time determined by the initial CW of each flow easily tends to have the same value. Therefore, this chapter proposed a new MAC method, SP-MAC, based on the synchronization phenomena of coupled oscillators. SP-MAC uses the synchronized phase with phase shifting for calculating the back-off time. Moreover, simulation evaluations showed that SP-MAC can avoid collisions and improve the total throughput. In addition, because SP-MAC can drastically avoid collisions, it can effectively use the bandwidth when the number of wireless terminals increases. Therefore, SP-MAC could become a solution for the terrible congestion in future wireless LAN networks.

Finally, the following work could be studied in the future:

- Consideration for overlapping BSS(OBSS)

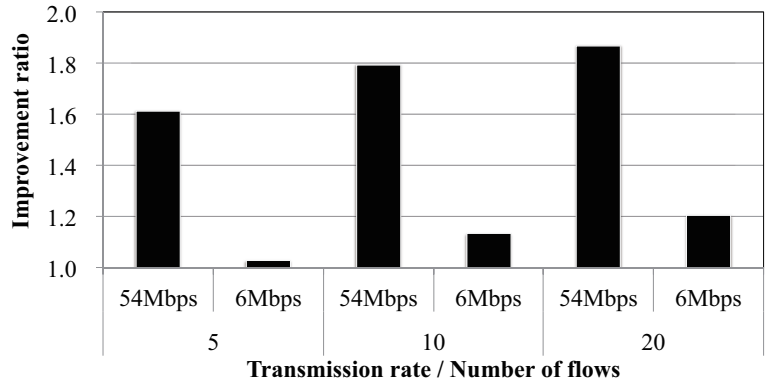

Figure 7.19: Improvement ratio of the SP-MAC's average throughput compared to CSMA/CA (Case1).

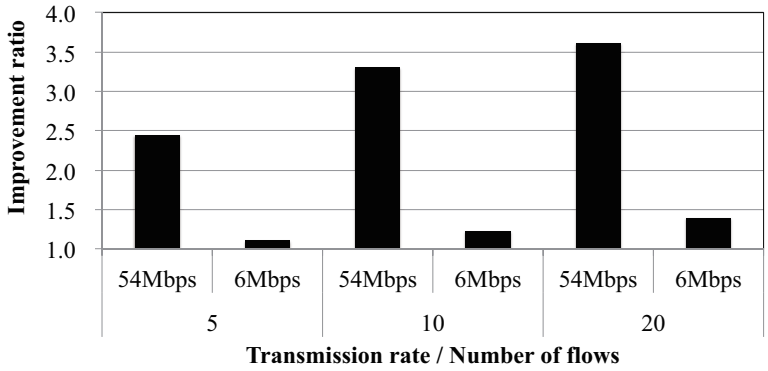

Figure 7.20: Improvement ratio of the SP-MAC's average throughput compared to CSMA/CA (Case2).

- Evaluation when hidden terminals exist
- Detailed evaluation when the uplink flow coexists with the downlink flow [171, 172]
- Extension of SP-MAC to support QoS control method [173, 174]
- Evaluation using SP-MAC implementation in a real environment

Chapter 8

Conclusion

Wireless LANs based on IEEE 802.11 standard have become increasingly popular in recent times, and they are used in various environments such as homes, offices, and schools. However, the wireless LAN technology has various issues. To solve these issues, some technologies are actively studied. An example of the realization for these solutions is to control the entire system by behavior of individual elements constituting a system which is according to the local rule. One of the example of the system which realize the above solution is natural world. By considering the control which imitate the behavior of the natural world, the solution of the issues which is described above can be proposed. However, in order to achieve the purpose, it is necessary to clarify what gimmicks operates in the natural world. To achieve this issue, modeling, which is a method for representing a phenomenon by a formula, is a useful tool. this thesis proposes advanced technologies for wireless LANs which are to control the entire system by behavior of according to the local rule with individual elements constituting a system as the natural world. In particular, this thesis focuses on load balancing, power saving, and improving the reachability of terminals for ad hoc networks. Furthermore, this thesis pays attention to an AP selection method and a media access control method for infrastructure networks. For the power saving and load balancing of ad hoc networks, in particular, this thesis focused on autonomous decentralized clustering based on local interaction (back-diffusion method). Numerical simulations clarified that the back-diffusion method can guarantee the stability of the range of the distributions formed by the proposed method. In addition, by changing the components of the distribution vector, the back-diffusion method cannot set strictly the number of clusters, but can decide the number of clusters to some (large or small) extent. This thesis proposed and evaluated a cluster guaranteeing stability method that maintains the number of clusters. Additionally, this thesis showed the importance of a clustering method that reflects the network condition, with regard to power consumption and data transfer efficiency. Evaluations focused on the temporal change in the percentage of live nodes, the FND time, and the amount of the data received by the sink node. From evaluations, the clusters yielded by the back-diffusion method are superior in all respects to those generated by the bio-inspired method. This means that reflecting the network condition for clusters is effective from the point of view of both power consumption and data transfer efficiency. Moreover, this thesis proposed a design method of a radio transmission range of terminals in order to achieve power saving and communication reachability. This thesis

also clarified the effectiveness of the proposed method using two routing protocols and two MAC protocols. Simulation results demonstrated that setting the communication range using the proposed method can provide significant improvements in goodput and power savings when DSDV and TDMA are used as the routing protocol and the MAC protocol. For infrastructure networks, this thesis also proposed a throughput prediction method for APs based on the estimation method that yields the distribution of the terminals in order to reduce calculation cost. Simulations showed that the proposed method can output almost the same predicted values as the existing method but at low calculation cost of $O(1)$. Moreover, relative error increases when terminals are distributed widely in the system field. Additionally, this thesis compared the calculation cost of the proposed method and the existing method. From evaluations, the number of steps of the proposed method is less than that of the existing method if the number of terminals connected to the AP is greater than 7. Furthermore, this thesis suggested an AP selection method based on coordination between both moving users and moving APs (UACMM) in order to maximize the system throughput. The UACMM can improve system throughput and AP average throughput dramatically compared to the user only cooperation method that only moves a new user because the AP can move to a position where existing users can obtain higher transmission rates. Moreover, this thesis proposed a new MAC method, SP-MAC, based on the synchronization phenomena of coupled oscillators in order to avoid the frame collision. This thesis showed that SP-MAC drastically decreases the data frame collision and improves the total throughput when compared with the original CSMA/CA method and some existing MAC protocols. That is, this thesis showed that SP-MAC can effectively use the bandwidth when the number of wireless terminals increases.

Future works for individual technologies are described in Sect. 3.5, Sect. 4.5, Sect. 5.5, Sect. 6.5, and Sect. 7.5. Common future works for all technologies include:

- Performance evaluation of the proposal when other models of the nature are used
- Evaluation of cooperative operation among each advanced technology
- Evaluation of performance considering real machines

References

[1] IEEE Standard, "Wireless LAN medium access control (MAC) and physical layer (PHY) specifications," *ANSI/IEEE Std 802.11*, 2012.

[2] M.S. Gast, *802.11 Wireless network: The Definitive Guide*, O'REILLY, 2002.

[3] Wi-Fi Alliance, available at `http://www.wi-fi.org/`, 2016.

[4] Y. Morioka, Y. Morihiro, A. Yamada, and Y. Okumura, "Experimental analysis of public wireless LAN quality for moving users," *Proc. 80th IEEE VTC Fall*, pp.1–5, 2014.

[5] N. Fuke, T. Warabino, H. Ishikawa, H. Shinonaga, T. Mizuike, and H. Mori, "Large-scale CFO-SS (high-Speed, long-range 2.4 GHz wireless LAN) network for educational internet access," *Proc. IEEE WCNC 2002*, 2, pp.649–653, 2014.

[6] E.H. Putra, E. Supriyanto, J. Din, and H. Satria, "Cross layer design of IEEE 802.11e enhanced distributed channel access wireless network for telemedicine application," *Proc. CITISIA 2009*, pp.129–133, 2009.

[7] M. Nakamura, S. Kubota, H. Takagi, K. Einaga, M. Yokoyama, K. Mochizuki, M. Takizawa, and S. Murase, "Development of long-range and high-speed wireless LAN for the transmission of telemedicine from disaster areas," *EURASIP Journal on Wireless Communications and Networking*, 2008, 13 pages, 2008.

[8] E.M. Husni, Y. Heryadi, W.T.H. Woon, M.S. Arifianto, D.V. Viswacheda, and L. Barukang, "Mobile ad hoc network and mobile IP for future mobile telemedicine system," *Proc. 3rd IFIP International Conference on WOCN 2006*, p.5, 2006.

[9] H. Suzuki, Y. Kaneko, K. Mase, S. Yamazaki, and H. Makino, "An ad hoc network in the sky, 'SKYMESH,' for large-scale disaster recovery," *Proc. 64th IEEE VTC Fall*, pp.1–5, 2006.

[10] Y. Takahashi, Y. Owada, H. Okada, and K. Mase, "A wireless mesh network testbed in rural mountain areas," *Proc. 2nd ACM International Workshop on WiNTECH 2007*, pp.91–92, 2007.

[11] W. Lu, W.K.G. Seah, E.W.C. Peh, Y. Ge, "Communications support for disaster recovery operations using hybrid mobile ad-hoc networks," *Proc. 32nd IEEE LCN 2007*, pp.763–770, 2007.

[12] K. Shimoda and K. Gyoda, "Analysis of ad hoc network performance for disaster communication models," *Proc. 10th IEEE ISADS 2011*, pp.483–488, 2011.

[13] A. Goncalves, C. Silva, and P. Morreale, "Design of a mobile ad hoc network communication app for disaster recovery," *Proc. 28th International Conference on WAINA 2014*, pp.121–126, 2014.

[14] M. Aida, *Distributed control and hierarchical structure in information networks*, Corona, 2015. (in Japanese)

[15] A.M. Turing, "The chemical basis of morphogenesis," *Phil. Transact. Royal Soc. B, Biological Sciences*, 237, 641, pp.37–72, 1952.

[16] R. FitzHugh, "Impulses and physiological states in theoretical models of nerve membrane," *Biophys. J.*, 1, 6, pp.445–466, 1961.

[17] L.A. Pipes, "A operational analysis of traffic dynamics," *J. Appl. Phys.*, 24, pp.274–281, 1953.

[18] M. Gallegati, A.P. Kirman, and M. Marsili, *The complex dynamics of economic interaction: essays in economics and econophysics*, Springer, 2004.

[19] M. Golshahi, M. Mosleh, and M. Kheyrandish, "Implementing an ACO routing algorithm for ad-hoc networks," *Proc. 1st ICACTE 2008*, pp.143–147, 2008.

[20] T. Murase, R. Shinkuma, G. Hasegawa, K. Yamori, M. Oguchi, C. Ohta, D. Sarkar, and D. Raychaudhuri, "Network control for pareto optimality in future internet, User-centric wired-wireless cognitive technology," *IEICE Technical Report*, CQ2011-38, 2011. (in Japanese)

[21] J. Teramae and N. Wakamiya, "Brain-inspired communication technologies: Information networks with continuing internal dynamics and fluctuation," *IEICE Trans. Commun.*, E98-B, pp.153–159, 2015.

[22] M. Aida, "Concept of chaos-based hierarchical network control and its application to transmission rate control," *IEICE Trans. Commun*, E98-B, 1, pp.135–144, 2015.

[23] C. Takano, M. Aida, M. Murata, and M. Imase, "Proposal for autonomous decentralized structure formation based on local interaction and back-diffusion potential," *IEICE Trans. Commun.*, E95-B, 5, pp.1529-1538, 2012.

[24] R. Hamamoto, C. Takano, K. Ishida, and M. Aida, "Guaranteeing asymptotic stability of clustering by autonomous decentralized structure formation," *Proc. 9th IEEE International Conference on ATC 2012*, pp.408–414, 2012.

[25] R. Hamamoto, C. Takano, K. Ishida, and M. Aida, "Guaranteeing method for the stability of cluster structure formed by autonomous decentralized clustering mechanism," *Proc. 12th IEEE International Workshop on ADSN 2013*, pp.345–350, 2013.

[26] R. Hamamoto, C. Takano, K. Ishida, and M. Aida, "Guaranteeing method of stability for clustering by autonomous decentralized structure formation mechanism based on local interaction," *Journal of Communications*, 10, 8, pp.562–571, 2015.

[27] R. Hamamoto, C. Takano, K. Ishida, and M. Aida, "Power consumption characteristics by autonomous decentralized structure formation technology," *Proc. 9th APSITT 2012*, pp.1–5, 2012.

[28] R. Hamamoto, C. Takano, K. Ishida, and M. Aida, "Characteristics of autonomously configured structure formation based on power consumption and data transfer efficiency," *Proc. 6th International Workshop on ASON 2013*, pp.409–414, 2013.

[29] R. Hamamoto, C. Takano, K. Ishida, and M. Aida, "Power consumption characteristics of autonomous decentralized clustering based on local interaction," *IEICE Trans. Inf. & Syst.*, E97-D, 12, pp.2984–2994, 2014.

[30] R. Hamamoto, C. Takano, H. Obata, M. Aida, and K. Ishida, "Setting radio transmission range using target problem to improve communication reachability and power saving," *Proc. the 7th EAI International Conference on ADHOCNETS 2015 / Lecture Notes of the Institute for Computer Sciences, Social Informatics and Telecommunications Engineering*, 155, pp.15–28, Springer, 2015.

[31] R. Hamamoto, C. Takano, H. Obata, and K. Ishida, "An acceleration of throughput prediction method for access point in multi-rate wireless LAN considering terminal distribution," *IEICE Trans. Fundamentals* (Japanese Edition), J98-A, 2, pp.209–220, 2015. (in Japanese)

[32] R. Hamamoto, C. Takano, H. Obata, K. Ishida, and T. Murase, "An access point selection mechanism based on cooperation of access points and users movement," *Proc. 14th IFIP/IEEE International Symposium on IM 2015*, pp.926–929, 2015.

[33] R. Hamamoto, C. Takano, H. Obata, K. Ishida, and T. Murase, "Characteristics analysis of an AP selection method based on coordination moving both users and APs," *Proc. 7th International Workshop on ASON 2014*, pp.243–248, 2014.

[34] R. Hamamoto, T. Murase, C. Takano, H. Obata, and K. Ishida, "A proposal of access point selection method based on cooperative movement of both access points and users," *IEICE Trans. Inf. & Syst.*, E98-D, 12, pp.2048–2059, 2015.

[35] H. Obata, R. Hamamoto, C. Takano, and K. Ishida, "SP-MAC: A media access control method based on the synchronization phenomena of coupled oscillators over WLAN," *IEICE Trans. Inf. & Syst.*, E98-D, 12, pp.2060–2070, 2015.

[36] H. Obata, R. Hamamoto, C. Takano, and K. Ishida, "Throughput characteristics evaluation of media access control method based on synchronization phenomena of coupled oscillators over WLAN coexisting of CSMA/CA terminals," *Proc. 7th International Workshop on ASON 2014*, pp.254–259, 2014.

[37] R. Hamamoto, H. Obata, Y. Yamamoto, R. Ando, C. Takano, and K. Ishida, "Performance evaluation of media access control method based on synchronization phenomena of coupled oscillators over multi-rate WLAN," *Proc. International Symposium on NOLTA 2015*, pp.415–418, 2015.

[38] R. Hamamoto, H. Obata, C. Takano, and K. Ishida, "A study on applicability of media access control mechanism based on synchronization of coupled oscillators SP-MAC over wireless LAN," *IEICE Trans. Commun.* (Japanese Edition), J99-B, 2, pp.31–44, 2016. (in Japanese)

[39] IEEE 802.11b, "Higher-speed physical layer extension in the 2.4 GHz band," 1999.

[40] IEEE 802.11g, "Further higher data rate extension in the 2.4 GHz band," 2003.

[41] IEEE 802.11n, "Enhancements for higher throughput," 2009.

[42] IEEE 802.11ac, "Enhancements for very high throughput for operation in bands below 6 GHz," 2013.

[43] I.F. Akyildiz, W. Su, Y. Sankarasubramaniam, and E. Cayirc, "A survey on sensor networks," *IEEE Commun. Mag.*, 40, 8, pp.102–114, 2002.

[44] S. Al-Sultan, M.M. Al-Doori, A.H. Al-Bayatti, and H. Zedan, "A comprehensive survey on vehicular ad hoc network," *Journal of Network and Computer Applications*, 37, pp.380–392, 2014.

[45] S. Biaz and S. Wu, "Rate adaptation algorithms for IEEE 802.11 networks: a survey and comparison," *Proc. ISCC 2008*, pp.130–136, 2008.

[46] A. Kamerman and L. Monteban, "WaveLAN-ii: a high-performance wireless LAN for the unlicensed band," *Bell Labs Technical Journal*, 2, 3, pp.118–133, 1997.

[47] M. Heusse, F. Rousseau, G. Berger-Sabbatel, and A. Duda, "Performance anomaly of 802.11b, " *Proc. IEEE INFOCOM 2003*, 2, pp.836–843, 2003.

[48] K. Medepalli and F.A. Tobagi, "Throughput analysis of IEEE 802.11 wireless LANs using a average cycle time approach," *Proc. IEEE GLOBECOM 2005*, pp.3007–3011, 2005.

[49] C.E. Perkins, ed., *AD HOC NETWORKING*, Addition Wesley, 2000.

[50] A. Abbas, J. Bahi, and A. Mostefaoui, "Improving wireless ad hoc networks lifetime," *Proc. IEEE International Conference on SUTC 2006*, 2006.

[51] L. Zhaohua and G. Mingjun, "Survey on network lifetime research for wireless sensor networks," *Proc. 2nd IEEE IC-BNMT 2009*, pp.899–902, 2009.

[52] W. Feng, and J.M.H. Elmirghani, "Lifetime evaluation in energy-efficient rectangular ad hoc wireless networks," *International Journal of Communications Systems*, 23, 12, pp.1500–1520, 2010.

[53] D. Ganesan, A. Cerpa, W. Ye, Y. Yu, J. Zhao, and D. Estrin, "Networking issues in wireless sensor networks," *J. Parallel Distrib. Comput.*, 64, 7, pp.799–814, 2004.

[54] J.Y. Yu and P.H.J. Chong, "A survey of clustering schemes for mobile ad hoc networks," *IEEE Commun. Survey & Tutorial*, 7, 1, pp.32–48, 2005.

[55] T. Nagata, H. Oguma, and K. Yamazaki, "A sensor networking middleware for clustering similar things," *Proc. International Workshop on Smart Object Systems 2005*, 2005.

[56] S. Priyankara, K. Kinoshita, H. Tode, and K. Murakami, "A clustering method for wireless sensor networks with heterogeneous node types," *IEICE Trans. Commun.*, E94-B, 8, pp.2254–2264, 2011.

[57] S. Basagni, "Distributed clustering for ad hoc networks," *Proc. ISPAN 1999*, pp.310–315, 1999.

[58] A.D. Amis, R. Prakash, T.H.P. Vuong, and D. Huynh, "Max-min D-cluster formation in wireless ad hoc networks," *Proc. IEEE INFOCOM 2000*, 1, pp.32–41, 2000.

[59] T. Ohta, S. Inoue, Y. Kakuda, and K. Ishida, "An adaptive multihop clustering scheme for ad hoc networks with high mobility," *IEICE Trans. Fundamentals*, E86-A, 7, pp.1689–1697, 2003.

[60] P. Sasikumar and S. Khara, "*k*-means clustering in wireless sensor networks," *Proc. 4th International Conference on CICN 2012*, pp.140–144, 2012.

[61] S. Thirumurugan and E.G.D.P. Raj, "Ex-PAC: an improved clustering technique for ad hoc network," *Proc. International Conference on RACSS 2012*, pp.196–200, 2012.

[62] I. Tal and G.-M. Muntean, "User-oriented fuzzy logic-based clustering scheme for vehicular ad-hoc networks," *Proc. 77th IEEE VTC Spring*, pp.1–5, 2013.

[63] G. Neglia and G. Reina, "Evaluating activator-inhibitor mechanisms for sensors coordination," *Proc. 2nd IEEE/ACM International Conference on BIONETICS 2007*, pp.129–133, 2007.

[64] K. Hyodo, N. Wakamiya, E. Nakaguchi, M. Murata, Y. Kubo, and K. Yanagihara, "Reaction-diffusion based autonomous control of wireless sensor networks," *International Journal of Sensor Networks*, 7, 4, pp.189–198, 2010.

[65] C. Takano and M. Aida, "Autonomous decentralized flow control mechanism based on diffusion phenomenon as guiding principle: Inspired from local-action theory," *J. IEICE*, 91, 10, pp.875–880, 2008. (in Japanese)

[66] K. Takagi, Y. Sakumoto, C. Takano, and M. Aida, "On convergence rate of autonomous decentralized structure formation technology for clustering in ad hoc networks," *Proc. 11th IEEE International Workshop on ADSN 2012*, pp.356–361, 2012.

[67] S.R. Gandham, M. Dawanda, R. Prakash, and S. Venkatesan, "Energy efficient schemes for wireless sensor networks with multiple mobile base stations," *Proc. IEEE GLOBECOM 2003*, 1, pp.377-381, 2003.

[68] T. Ohta, M. Fujimoto, S. Inoue, and Y. Kakuda, "Hi-TORA: hierarchical routing protocol in ad hoc networks," *Proc. 7th IEEE HASE 2002*, pp.143–148, 2002.

[69] H. Takayama, S. Hatakeyama, and M. Aida, "Self-adjustment mechanism guaranteeing asymptotic stability of clusters formed by autonomous decentralized mechanism," *Journal of Communications*, 9, 2, pp.180–187, 2014.

[70] M.A. Dewar, V. Kadirkamanathan, M. Opper, and G. Sanguinetti, "Parameter estimation and inference for stochastic reaction-diffusion systems: application to morphogenesis in D. melanogaster," *BMC Systems Biology*, 4, 21, pp.1–9, 2010.

[71] K. Masuda, C. Takano, and M. Aida, "Robustness of autonomously formed cluster structure under drastic changes of MANET topology," *IEICE Technical Report*, IN2012-144, 2013. (in Japanese)

[72] K. Takagi, M. Aida, C. Takano, and M. Naruse, 'New autonomous decentralized structure formation based on Huygens' principle and renormalization for mobile ad hoc networks," *International Journal on Advances in Intelligent Systems*, 7, 1&2, pp.64–73, 2014.

[73] B. Liang and Z.J. Haas, "Hybrid routing in ad hoc networks with a dynamic virtual backbone," *IEEE Trans. Wireless Commun.*, 5, 6, pp.1392–1405, 2006.

[74] P. Nain, D. Towsley, B. Liu, and Z. Liu, "Properties of random direction models," *Proc. IEEE INFOCOM 2005*, pp.1897–1907, 2005.

[75] J. Hill, R. Szewczyk, A. Woo, S. Hollar, D. Culler, and K. Pister, "System architecture directions for networked sensors," *Proc. International Conference on ASPLOS-IX*, pp.93–104, 2000.

[76] V.D. Park and M.S. Corson, "A highly adaptive distributed routing algorithm for mobile wireless networks," *Proc. IEEE INFOCOM 1997*, pp.1405–1413, 1997.

[77] T. Ohta, K. Ishida, Y. Kakuda, S. Inoue, and K. Maeda, "Maintenance algorithm for hierarchical structure in large ad hoc networks," *Proc. 1st ICFS 2002*, 2002.

[78] D. Kominami, M. Sugano, M. Murata, and T. Hatauchi, "Robust and resilient data collection protocols for multihop wireless sensor networks," *IEICE Trans. Commun.*, E95-B, 9, pp.2740–2750, 2012.

[79] C. Maihöfer, "A survey of geocast routing protocols," *IEEE Commun. Surveys & Tutorials*, 6, 2, pp.32–42, 2009.

[80] D.G. Reina, S.L. Toral, F. Barrero, N. Bessis, and E. Asimakopoulou, "Evaluation of ad hoc networks in disaster scenarios," *Proc. 3rd International Conference on INCoS 2011*, pp.759–764, 2011.

[81] P. Chen, B. O'Dea, and E. Callaway, "Energy efficient system design with optimum transmission range for wireless ad hoc networks," *Proc. IEEE ICC 2002*, 2, pp.945–952, 2002.

[82] K. Padmanabh, P. Gupta, and R. Roy, "Transmission range management for lifetime maximization in wireless sensor network," *Proc. SPECTS 2008*, pp.138–142, 2008.

[83] J. Deng, Y.S. Han, P.-N. Chen, and P.K. Varshney, "Optimum transmission range for wireless ad hoc networks based on energy efficiency," *IEEE Trans. Commun.*, 55, 9, pp.1772–1782, 2007.

[84] Y. Chen, H. Yang, B. Liu, and J. Cheng, "Transmission power optimization algorithm in wireless ad hoc networks," *Proc. International Conference on CMC 2010*, pp.358–363, 2010.

[85] J. Zhu, "On the power efficiency and optimal transmission range of wireless sensor nodes." *Proc. IEEE International Conference on EIT 2009*, pp.277–281, 2009.

[86] W. Feng, H. Alshaer, and J.M.H. Elmirghani, "Energy efficiency: Optimal transmission range with topology management in rectangular ad-hoc wireless networks," *Proc. International Conference on AINA 2009*, pp.301–306, 2009.

[87] Y. Zou and K. Chakrabarty, "Uncertainty-aware and coverage-oriented deployment for sensor networks," *Journal of Parallel and Distributed Computing*, 64, 7, pp.788–798, 2004.

[88] M. Ishizuka and M. Aida, "The reliability performance of wireless sensor networks configured by power-law and other forms of stochastic node placement," *IEICE Trans. Commun.*, E87-B, 9, pp.2511–2520, 2004.

[89] N.L. Johnson,S. Kotz, and N. Balakrishnan, *Continuous univariate distributions*, 1, Wiley Series in Probability and Statistics, 1994.

[90] N.L. Johnson, S. Kotz, and N. Balakrishnan, *Continuous univariate distributions*, 2, Wiley Series in Probability and Statistics, 1995.

[91] N.L. Johnson, A.W. Kemp, and S. Kotz, *Univariate discrete distributions*, Wiley Series in Probability and Statistics, 2005.

[92] C.E. Perkins and P. Bhagwat, "Highly dynamic destination-sequenced distance-vector routing (DSDV) for mobile computers," *Proc. ACM SIGCOMM 1994*, pp.234–244, 1994.

[93] C.E. Perkins and E.M. Royer, "Ad-hoc on-demand distance vector routing," *Proc. 2nd IEEE WMCSA 1999*, pp.90–100, 1999.

[94] D. D. Falconer, F. Adachi, and B. Gudmundson, "Time division multiple access methods for wireless personal communications," *IEEE Commun. Mag.*, 33, 1, pp.50–57, 1995.

[95] P.M. d'Orey and M. Ferreira, "ITS for sustainable mobility: A survey on applications and impact assessment tools," *IEEE Trans. Intelligent Transportation Systems*, 15, 2, pp.477–493, 2014.

[96] L. Stibor, Y. Zang and H-J. Reumermann, "Evaluation of communication distance of broadcast messages in a vehicular ad-hoc network using IEEE 802.11p," *Proc. IEEE WCNC 2007*, pp.254–257, 2007.

[97] E. Schiller, P. Starzetz, F. Theoleyre, and A. Duda, "Properties of greedy geographical routing in spontaneous wireless mesh networks," *Proc. IEEE GLOBECOM 2007*, pp.4941-4945, 2007.

[98] Network Simulator - ns (version 2), available at `http://www.isi.edu/nsnam/ns/`, 2016.

[99] J. Takada, S. Promwong, and W. Hachitani, "Extension of friis' transmission formula for ultra wideband systems," *IEICE Technical Report*, WBS2003-8, 2003.

[100] R. Endoh, Y. Shiraishi, and O. Takahashi, "Evaluation of the MANET routing protocol in the fixed node environment," *DICOMO symposium 2010*, pp.620–628, 2010. (in Japanese)

[101] C. Thorpe and L. Murphy, "A survey of adaptive carrier sensing mechanisms for IEEE 802.11 wireless networks," *IEEE Commun. Surveys & Tutorials*, 16, 3, pp.1266–1293, 2014.

[102] A. Balachandran, P. Bahl, and G.M. Voelker, "Hot-Spot congestion relief in public-area wireless networks," *Proc. IEEE WMCSA 2002*, pp.70–82, Jun., 2002.

[103] Y. Lin, W. Yu and Y. Lostanlen, "Optimization of wireless access point placement in realistic urban heterogeneous networks," *Proc. IEEE GLOBECOM 2012*, pp.4963–4968, 2012.

[104] D. Plets, N. Machtelinckx, K. Vanhecke, J.V. Ooteghem, K. Casier, M. Pickavet, W. Joseph, and L. Martens, "Calculation tool for optimal wireless design and minimal installation cost of indoor wireless LANs," *Proc. IEEE International Symposium on APS/URSI 2014*, pp.1165–1166, 2014,

[105] W. Zhao, Z. Fadlullah, H. Nishiyama, N. Kato, and K. Hamaguchi, "On joint optimal placement of access points and partially overlapping channel assignment for wireless networks," *Proc. IEEE GLOBECOM 2014*, pp.4922–4927, 2014.

[106] S. Miyata, T. Murase, and K. Yamaoka, "Novel access-point selection for user QoS and system optimization based on user cooperative moving," *IEICE Trans. Commun.*, E95-B, 6, pp.1953-1964, 2012.

[107] F. Miki, D. Nobayashi, Y. Fukuda, and T. Ikenaga, "Performance evaluation of multi-rate communication in wireless LANs," *Proc. 7th IEEE CCNC 2010*, pp.1–3, 2010.

[108] S. Iwaki, T. Murase, and M. Oguchi, "Throughput analysis and measurement on real terminal in multi-rate wireless LAN," *Proc. 6th ACM ICUIMC 2012*, pp.3–12, 2012.

[109] K. Izui, H. Obata, C. Takano, and K. Ishida, "UDP throughput evaluation considering the communication distance between AP and wireless terminals over multi-rate WLAN environment," *Proc. 7th International Workshop on ASON 2014*, pp.249–253, 2014.

[110] S. Fujii, T. Murase, and M. Oguchi, "Performance evaluation on ad-hoc network of IEEE802.11 with considering multi-rate and per-flow scheduling in relay nodes," *Proc. 3rd IEEE GCCE 2014*, pp.95–96, 2014.

[111] NICT 2014 contract research 174B, "Access networks for densely located users," Available at `http://www.nict.go.jp/call-for-app/131206.html`, 2016. (in Japanese)

[112] Y. Imagaki, K. Kashiki, K. Yamazaki, and Akira Yamaguchi, "Novel Wi-Fi throughput estimation method considering CSMA/CA behavior," *Proc. 75th IEEE VTC Spring*, pp.1–5, 2012.

[113] C. Rattaro and P. Belzarena, "Throughput prediction in wireless networks using statistical learning," *Proc. LAWDN 2010*, 4 pages 2010.

[114] R. Hamamoto, C. Takano, H. Obata, and K. Ishida, "An adaptive selection mechanism of prediction formulas for high speed throughput prediction method of access point in multi-rate WLAN environment," *IEICE Technical Report*, IN2014-18, 2014. (in Japanese)

[115] BUFFALO wireless LAN access point: WAPS-APG600H manual, Available at `http://manual.buffalo.jp/buf-doc/35020037-06.pdf`, 2015. (in Japanese)

[116] Ministry of Internal Affairs and Communications, "Report of technical committee on wireless LAN business," Available at `http://www.soumu.go.jp/main_content/000168906.pdf`, 2016. (in Japanese)

[117] H. Yoshida, K. Satoda, and S. Nogaki, "Video streaming control by predicting stochastic diffusion of TCP throughput," *Proc. Internet Conference 2011*, pp.57–66, 2011. (in Japanese)

[118] R. Hamamoto, C. Takano, H. Obata, and K. Ishida, "Improvement of throughput prediction method for access point in multi-rate WLANs considering media access control and frame collision," *Proc. 8th International Workshop on ASON 2015*, pp.227–233, 2015.

[119] T. Ikenaga, F. Miki, D. Nobayashi, and Y. Fukuda, "Performance evaluation of single-channel multi-rate communication in wireless LANs," *International Journal of Research and Reviews in Computer Science*, 2, 1, pp.168–172, 2011.

[120] Y. Fukuda, T. Abe, and Y. Oie, "Decentralized access point selection architecture for wireless LAN," *Proc. WTS 2004*, pp.137–145, 2004.

[121] A.J. Nicholson, Y. Chawathe, M.Y. Chen, B.D. Noble, and D. Wetherall, "Improved access point selection," *Proc. 4th International Conference on MobiSys*, pp.233–245, 2006.

[122] V.A. Siris and D. Evaggelatou, "Access point selection for improving throughput fairness in wireless LANs," *Proc. IFIP/IEEE International Symposium on IM 2007*, pp.469–477, 2007.

[123] L. Du, Y. Bai, and L. Chen, "Access point selection strategy for large-scale wireless local area networks," *Proc. IEEE WCNC 2007*, pp.2161–2166, 2007

[124] A. Fujiwara, Y. Sagara, and M. Nakamura, "Access point selection algorithms for maximizing throughputs in wireless LAN environment," *Proc. 13th ICPADS 2007*, 2, pp.1–8, 2007.

[125] H. Gong, K. Nahm, and J.W. Kim, "Distributed fair access point selection for multi-rate IEEE 802.11 WLAN," *Proc. IEEE CCNC 2008*, pp.528–532, 2008.

[126] X. Wan, X. Wang, U. Heo, and J. Choi, "A new AP-selection strategy for high density IEEE802.11 WLANs," *Proc. International Conference on CyberC*, pp.52–58, 2010.

[127] B. Bojovic, N. Baldo, and P. Dini, "A neural network based cognitive engine for IEEE 802.11 WLAN access point selection," *Proc. IEEE CCNC 2012*, pp.864–868, 2012.

[128] F. Xu, X. Zhu, C.C. Tan, Q.Li, G. Yan, and J. Wu, "SmartAssoc: Decentralized access point selection algorithm to improve throughput," *IEEE Trans. Parallel and Distributed Systems*, 24, 12, pp.2482–2491, 2013.

[129] J.B. Ernst, S. Kremer, and J.J.P.C. Rodrigues, "A utility based access point selection method for IEEE 802.11 wireless networks with enhanced quality of experience," *Proc. IEEE ICC 2014*, pp.2363–2368, 2014.

[130] J. Hwang, H. Lim, S. Oh, and B.-T. Lee, "Association scheme with traffic control for IEEE 802.11 wireless LANs," *IEICE Trans. Commun.*, E98-B, 8, pp.1680–1689, 2015.

[131] S. Kaneda, Y. Akinaga, N. Shinagawa, and A. Miura, "Traffic control by influencing users' behavior in mobile networks," *Proc. 19th ITC 2005*, pp.583–592, 2005.

[132] R. Schoenen, H. Yanikomeroglu, and B. Walke, "User in the loop: Mobility aware users substantially boost spectral efficiency of cellular OFDMA systems," *IEEE Communications letters*, 15, 5, pp.488–490, 2011.

[133] G. Motoyoshi, Y. Sudo,T. Murase, and T. Masuzawa, "Advantages of optimal longcut route for wireless mobile users," *Proc. IEEE ICC 2011*, pp.1–6 2011.

[134] T. Kakehi, R. Shinkuma, T. Murase, G. Motoyoshi, K. Yamori, and T. Takahashi, "Route instruction mechanism for mobile users leveraging distributed wireless resources," *IEICE Trans. Commun.*, E95-B, 6, pp.1965–1973, 2012.

[135] K. Kanai, Y. Akamatsu, J. Katto, and T. Murase, "QoS characteristics on a longcut route with various radio resource models," *Proc. IEEE International Conference on PerCom 2012*, pp.419–422, 2012.

[136] S.D. Hermann, M. Emmelmann, O. Belaifa, and A. Wolisz, "Investigation of IEEE 802.11k-based access point coverage area and neighbor discovery," *Proc. 32nd IEEE LCN*, pp.949–954, 2007.

[137] A. Shawish, X. Jiang, P.-H. Ho, and S. Horiguchi, "Wireless access point voice capacity analysis and enhancement based on clients' spatial distribution," *IEEE Trans. Vehicular Technology*, 58, 5, pp.2597–2603, 2009.

[138] M. Siebert, M. Lott, M. Schinnenburg, and S. Goebbels, "Hybrid information system," *Proc. 59th IEEE VTC Spring*, 5, pp.2982–2986, 2004.

[139] T. Hossfeld, S. Oechsner, K. Tutschku, F.-U. Andersen, and L. Caviglione, "Supporting vertical handover by using a pastry peer-to-peer overlay network," *Proc. IEEE International Conference on PerCom 2006*, pp.163–167, 2006.

[140] M.S. Daskin, *Network and discrete location models, algorithms, and applications*, John Wiley & Sons Inc., 1995.

[141] O. Kariv and L. Hakimi, "An algorithmic approach to network location problems, part ii: The p-medians," *SIAM Journal of Applied Mathematics*, 37, 3, pp.539–560, 1979.

[142] R. Hassin and A. Tamir, "Improved complexity bounds for location problems on the real line," *Operations Research Letters*, 10, 7, pp.395–402, 1991.

[143] H. Tsushima, R. Hamamoto, H. Obata, and K. Ishida, "Performance evaluation of flow QoS guarantee method based on TCP congestion control and MAC frame priority control over multi-rate WLAN environment," *Proc. 7th International Workshop on ASON 2014*, pp.266–271, 2014.

[144] F. Teshima, H. Obata, R. Hamamoto, and K. Ishida, "Redundancy setting method for TCP congestion control based on FEC over wireless LAN," *Proc. 8th International Workshop on ASON 2015*, pp.259–264, 2015.

[145] E. Ziouva and T. Antonakopoulos, "A dynamically adaptable polling scheme for voice support in IEEE802.11 networks," *Computer Communications*, 26, 2, pp.129–142, 2003.

[146] X.J. Dong, "Adaptive polling algorithm for PCF mode of IEEE 802.11 wireless LANs," *Electronics Letters*, 40, 8, pp.482–483, 2004.

[147] B. Anjum, S. Mushtaq, and A. Hussain, "Multiple poll scheme for improved QoS using IEEE 802.11 PCF," *Proc. 9th IEEE INMIC 2005*, pp.1–6, 2005.

[148] J. Zheng and E. Regentova, "I-Poll: Improved polling scheme for augmenting voice support in IEEE 802.11 PCF," *IEICE Trans. Commun.*, E89-B, 6, pp.1964–1967, 2006.

[149] K.-H. Chou and W. Lin, "Performance analysis of packet aggregation for IEEE 802.11 PCF MAC-based wireless networks," *IEEE Trans. Wireless Commun.*, 12, 4, pp.1441–1447, 2013.

[150] C. D. Young, "USAP: A unifying dynamic distributed multichannel TDMA slot assignment protocol," *Proc. IEEE MILCOM 1996*, 1, pp.235–239, 1996.

[151] F. Guo and T. C. Chiueh, "Software TDMA for VoIP applications over IEEE802.11 wireless LAN," *Proc. IEEE INFOCOM 2007*, pp.2370–2366, 2007.

[152] P. Cheng, F. Zhang, J. Chen, Y. Sun, and X. Shen, "A distributed TDMA scheduling algorithm for target tracking in ultrasonic sensor networks," *IEEE Trans. Industrial Electronics*, 60, 9, pp.3836–3845, 2012.

[153] M. F. Tuysuz, H. A. Mantar, G. Celik, and M. R. Celenlioglu, "An uninterrupted collision-free channel access scheme over IEEE 802.11 WLANs," *Proc. IEEE WCNC 2013*, pp.386–391, 2013.

[154] K. Sekiyama, Y. Kubo, S. Fukunaga, and M. Date, "Phase diffusion time division method for wireless communication network," *Proc. IEEE IECON 2004*, 3, pp.2748–2753, 2004.

[155] Y. Kubo and K. Sekiyama, "Communication timing control with interference detection for wireless sensor networks," *EURASIP Journal on Wireless Communication and Networking 2007*, 10 pages, 2007.

[156] M. Ma and Y. Yang, "A novel contention-based MAC protocol with channel reservation for wireless LANs," *IEEE Trans. Wireless Commun.*, 7, 10, pp.3748–3758, 2008.

[157] J. Choi, J. Yoo, S. Choi, and C. Kim, "EBA: An enhancement of the IEEE 802.11 DCF via distributed reservation," *IEEE Trans. Mobile Computing*, 4, 4, pp.378–390, 2005.

[158] S. Ye, T. Korakis, and S. Panwar, "CSMAC: A new centralized scheduling-based MAC protocol for wireless LAN," *Proc. IEEE WCNC 2009*, pp.1–6, 2009.

[159] Y. He, J. Sun, X. Ma, A. Vasilakos, R. Yuan, and W. Gong, "Semi-random backoff: Towards resource reservation for channel access in wireless LAN," *IEEE/ACM Trans. Networking*, 21, 1, pp.204–217, 2013.

[160] X. Yu, P. Navaratnam, and K. Moessner, "Resource reservation schemes for IEEE 802.11-based wireless networks: a survey," *IEEE Commun. Surveys & Tutorials*, 15, 3, pp.1042–1061, 2013.

[161] J.A. Acebrón, L.L. Bonilla, C. J. P. Vicente, F. Ritort, and R. Spigler, "The Kuramoto model: A simple paradigm for synchronization phenomena," *Rev. Mod. Phys.*, 77, pp.137–185, 2005.

[162] J. Buck, "Synchronous rhythmic flashing of fireflies. II.," *Q. Rev. Biol.*, 63, 3, pp.265–289, 1988.

[163] J. Pantaleone, "Synchronization of metronomes," *Am. J. Phys.,* 70, 10, pp.992–1000, 2002.

[164] A. T. Winfree, *The Geometry of biological time*, Springer, 1980.

[165] S.H. Strogatz, "From Kuramoto to crawford: Exploring the onset of synchronization in populations of coupled oscillators," *Physica D*, 143, pp.1–20, 2000.

[166] K. Czolczynski, P. Perlikowski, A. Stefanski, and T. Kapitaniak, "Clustering and synchronization of *n* Huygens' clocks," *Physica A*, 388, pp. 5013–5023, 2009.

[167] T. Mizumoto, T. Otsuka, K. Nakadai, T. Takahashi, K. Komatani, T. Ogata, and H. G. Okuno, "Human-Robot ensemble between robot thereminist and human percussionist using coupled oscillator," *Proc. IEEE/RSJ International Conference on IROS 2010*, pp.1957–1963, 2010.

[168] Y. Kuramoto, *Chemical oscillations, waves, and turbulence*, Springer, 1984.

[169] K. Sekiyama, M. Yamaoka, Y. Kubo, M. Date, J. Takahashi, and T. Fukuda, "Experimental report on distributed communication timing control with phase diffusion time division method," *2007 IEICE General Conference*, BS-2-1, 2007. (in Japanese)

[170] D. J. Leith, P. Clifford, D. Malone, and A. Ng, "TCP fairness in 802.11e WLANs," *IEEE Commun. Letters*, 9, 11, pp.964–966, 2005.

[171] R. Ando, R. Hamamoto, H. Obata, C. Takano, and K. Ishida, "An adaptive control parameter setting method for priority control based on media access control SP-MAC over WLAN," *Proc. 8th International Workshop on ASON 2015*, pp.220–226, 2015.

[172] R. Ando, R. Hamamoto, H. Obata, C. Takano, and K. Ishida, “Characterization of priority control based on media access control method SP-MAC over WLAN,” *Proc. 19th ICIN 2016*, pp.149–156, 2016.

[173] Y. Yamamoto, R. Hamamoto, H. Obata, C. Takano, and K. Ishida, “Performance evaluation of control method to guarantee throughput based on media access control SP-MAC over WLAN,” *Proc. 8th International Workshop on ASON 2015*, pp.265–270, 2015.

[174] Y. Yamamoto, R. Hamamoto, H. Obata, C. Takano, and K. Ishida, “Control method to guarantee throughput based on media access control method SP-MAC over WLAN,” *Proc. IEEE CCNC 2016*, pp.657–662, 2016.